Distance and Time Limit on Quantum Control under Decoherence

February 2021

Kohei Kobayashi

A Thesis for the Degree of Ph.D. in Engineering

Distance and Time Limit on Quantum Control under Decoherence

February 2021

Graduate School of Science and Technology
Keio University

Kohei Kobayashi

Abstract

To realize quantum information technologies, a technique of quantum control for preparing a desired quantum state used for an information resource plays an important role. For example, the measurement-based feedback control is a powerful method and many notable experiments have been demonstrated in superconducting qubit. However, in spite of the large impacts and development of those technologies, decoherence, which is the loss of quantum properties, is the fundamental and biggest obstacle. Due to it, the quantum state collapses to the classical state and the actual control performance is sometimes far away from the ideal one. Therefore, in considering the practical quantum control under decoherence, the following two questions arise: (i) How close the controlled quantum state can be steered to a target state under decoherence? (ii) How long can we preserve the controlled system around at the target state? These questions can be formulated as problems analyzing distance and time respectively; fortunately, these problems are qualitatively evaluated by useful tools; reachability and quantum speed limit (QSL).

Reachability is a measure of the reachable set of quantum state. To clarify and characterize the reachability of the controlled systems under decoherence is essential to evaluate the practical effectiveness of control methods and gives a direct answer to the question (i). However, there has been no general approach for giving an estimate of the reachability under decoherence, and also no research for giving an insight into the further basic questions for quantum engineering; what state should be set to the target, or what the desired structure of open quantum system under given decoherence is.

The question (ii) boils down to the problem analyzing the time for the quantum state maintaining its coherence against decoherence. The QSL, which is defined as a lower bound of the evolution time of a quantum system from an initial state to a final state, is a useful tool for studying this problem. The QSL gives not only a trade-off relation between energy and time but also the shortest time of the state evolution, and thus the investigations of the QSL are significantly important from the viewpoints of fundamentals and engineering.

The goal of this thesis is to give answers to the above fundamental questions. This thesis is organized as follows. Chapter 1 provides some backgrounds and outline of this thesis. Chapter 2 provides some basic topics for describing the framework of quantum mechanics; quantum state, quantum measurement, and quantum dynamics. Chapter 3

presents a limit for the reachability of the controlled states under decoherence and the target state. This limit is applicable for general Markovian open quantum systems and straightforwardly calculated and used as a guide for choosing the target state that is not largely affected by decoherence. Chapter 4 presents a new tractable QSL and exploits new application of the QSL; Hamiltonian engineering for preparing robust states and characterizing the reachability in a given time. Chapter 5 concludes this thesis and discusses future works.

Contents

Chapter 1

Introduction

1.1 Motivation

It is no doubt that the development of quantum mechanics is one of the great achievement in modern physics. Interesting properties of quantum systems, e.g., superposition or entanglement, make it possible to realize the quantum information processing that outperforms the classical one. In recent years, there have been considerable interests in quantum information technologies, e.g., quantum computing, communication, teleportation, metrology, and cryptography. In order to realize these technologies, it is necessary to prepare a desired quantum state for an information resource. Therefore, a technique of quantum control, preparing a desired quantum state, plays an important role in quantum information technology.

Here we give a brief introduction to quantum control scheme; let us consider a quantum state ρ, where ρ is the self-adjoint operator acting on the state space $\mathcal{H}_S$. ρ is dynamical and open to the external control system (modeled by an environment or a reservoir) acting on the another space $\mathcal{H}_E$. The controlled system is characterized by the shorthand $G(u, H, L)$, where u is the scalar function representing the control sequence; also H and L are the operators representing the control energy and the interaction between the system and the environment, respectively. By suitably designing $G(u, H, L)$, we can steer the quantum system towards a target. The concept of quantum control is analogous to ideally controlling the system dynamics. Mathematically, the quantum control problem is modeled in terms of differential equations, e.g., Schrödinger equation, master equation, stochastic master equation, and so on. For example, the quantum dynamics under the continuous measurement and control is described by the stochastic master equation:

$$d\rho = -i[uH, \rho]dt + \mathcal{D}[L]\rho dt + \mathcal{H}[L]\rho dW. \tag{1.1}$$

The meanings of each terms will be explained in Chapter 2. Equation (1.1) is nonlinear and stochastic, and hence in general we cannot obtain its exact solution. Therefore, these tools enable us to develop the techniques of quantum control, although the analysis of the

dynamics under the control is a hard task.

Now let us see several techniques of quantum control: First the open-loop (i.e., non-feedback) control theory [1, 2, 3, 4, 5, 6, 7, 8] offers some powerful means, for example for implementing an efficient quantum gate operation. Second, reservoir engineering techniques including the measurement-based feedback (MBF) [9, 10, 11, 12, 13, 14, 15, 16] and coherent feedback [17, 18, 19, 20, 21, 22, 23] are also well-established methodologies that can be used for generating and protecting a desirable quantum state. Recently, many notable experiments realizing those control techniques have been extensively demonstrated in superconducting qubit system [24, 25, 26, 27, 28, 29].

However, in spite of the large impacts and the development of quantum technologies, there are a lot of problem to be dealt with for their realization; *decoherence* is one of the most fundamental obstacle. Decoherence is the loss of quantum properties induced by the interaction between the quantum system and its environments. Due to this fundamental phenomenon, the quantum state collapses to the classical one and the actual control performance is sometimes far away from the ideal one. For example, the quantum computer must prepare a coherent pure state and preserve it for a long time, in order to realize higher computational performance than classical one. This is why, in considering the practical quantum control under decoherence, the following two questions arise: (i) How close the controlled quantum state can be steered to a target state under decoherence? (ii) How long can we preserve the controlled system around at the target state? These questions can be formulated as problems analyzing distance and time respectively; fortunately these problems can be evaluated by useful tools; *reachability* and *quantum speed limit*.

1.2 Reachability

The question (i) can be rephrased as follows; how much the reachability of the controlled states under decoherence is. Now suppose that the state ρ_t with its initial state ρ_0 evolves to the final state ρ_T. According to the control system, ρ_T can take several states in the Hilbert space. The set of all ρ_T is called the *reachable set* and reachability is a measure of this set. In the literature, the reachability is often defined as the fidelity-based distance [33], the efficiency of coherence transfer [3], or the Lie algebraic structure [36, 37, 38, 39]. The analysis of reachability, which is in our scenario to clarify and characterize the reachability of the controlled quantum systems under decoherence, is essential to evaluate the practical effectiveness of control methods and gives a direct answer to the question (i). The concept of reachability analysis is usually based on numerical simulations that investigate how much the ideal state control is disturbed by decoherence; for example, generation of a nanoresonator superposition state via open-loop control [5, 6], an optical Fock state via MBF [11, 63], and an optomechanical cat state via reservoir

engineering [20, 65]. The optimal control method, which numerically designs a time-dependent control input for steering the state closest to the target one under decoherence [3, 30], is also often used. However, the above computational approaches do not give us deep insight into the further practical questions for quantum engineering; what state should be assigned to the target, and what the desired structure of open quantum system under given decoherence is. A few exceptions are found for specific types of open-loop control [31] and MBF [32, 33], but there has been no general approach. Therefore, the realistic analysis of the reachability under decoherence is one of the most challenging and exciting research area in quantum engineering.

1.3 Quantum speed limit

The question (ii) boils down to the problem analyzing the time for the quantum state maintaining its coherence against decoherence. Time is of course an essential factor that should be carefully treated in quantum engineering, because the change of quantum states often occurs in a very small time interval. Towards this problem, for example, several approaches for finding the time-optimal evolution of quantum states, e.g., quantum brachistochrone, have been proposed [40, 41, 42, 43]. However, it is generally impossible to steer the state to the target state in the presence of decoherence. That is, it is unrealistic to consider the perfect state generation. This is why, in order to treat the question (ii), we focus on the decohering time of quantum states. The quantum speed limit (QSL) is a useful tool for studying this problem.

The QSL is defined as a lower bound of the evolution time T of a quantum system from an initial state to a final state. The general expression of the QSL is given as follows:

$$T \geq T_{\mathrm{QSL}}(D(\rho_0, \rho_T)), \tag{1.2}$$

where $D(\rho_0, \rho_T)$ is a distance function of the initial state ρ_0 and the final state ρ_T. $D(\rho_0, \rho_T)$ is usually given by the relative purity [88, 91], Bures angle [87, 89], or Hilbert-Schmidt norm [94]. The study of the QSL started on closed systems; Mandelstam and Tamm derived the QSL between orthogonal basis, which is given by the variance of the Hamiltonian [75]. Margolus and Levitin derived another QSL depending on the mean energy [76]. Moreover, important generalizations to mixed states [80], nonorthogonal states [81], and time-dependent driven systems [83, 84, 85, 86] were provided later. In recent years, in particular, some types of QSLs for open quantum systems [87, 88, 89, 90, 91, 92, 93, 94, 95, 96, 97, 98, 99] have been extensively investigated. The QSLs give not only a trade-off relation between energy and time but also the shortest time of the state evolution, and thus the investigations of the QSL are significantly important from the viewpoints of fundamentals and engineering. Actually, it has numerous application in quantum computation [66, 67], metrology [68, 69], optimal control [70, 71, 72, 73, 74], and

so on. Note that, in this scenario, the QSL is often used as a tool for characterizing the potential for speeding up the time evolution toward a target state [91, 95, 96, 97, 98, 99]. That is to say, let us consider the problem of transferring an initial state ρ_0 to a target final state ρ_T. If the QSL from ρ_0 to ρ_T under a control system G is smaller than that of another system G', then G is preferable in order to do this task. In this way, the development of an application of the QSL to engineering is an interesting and meaningful field of the QSL.

1.4 Outline

Motivated by the two questions posed above, this thesis explores a fundamental limit for dynamical quantum systems under decoherence in terms of distance and time. The main results of this thesis are given in Chapter 3 and 4. The structure of this thesis is as follows:

Chapter 2 reviews some important topics for describing the framework of quantum mechanics including quantum state, quantum measurement, and quantum dynamics.

Chapter 3 aims to develop a distance limit for the controlled quantum system under decoherence. Section 3.1 demonstrates the performance of the MBF control in the imperfect setting. Section 3.2 presents a theoretical limit for the reachability of any controlled quantum systems. More specifically, we present a lower bound of the fidelity-based distance between a target state and the controlled state in the presence of decoherence. Importantly, it is universally applicable for a Markovian open quantum system driven by the decoherences and any types of control. Also the lower bound can be straightforwardly computed without solving any equation. Moreover, thanks to its generic form, the limit gives a characterization of target states that is largely disturbed by the decoherence. Therefore, it provides a useful guide for choosing the target, as demonstrated in several examples.

Chapter 4 explores the time limit (i.e., QSL) for state evolution of the open quantum system. The main contribution of this chapter is to exploit applications of the QSL. First, we propose a new usage of QSL as a measure of robust quantum states of Markovian open quantum systems. In contrast to the above-mentioned view for speeding up the evolution, we consider an undesired state transition driven by decoherence. Namely, we consider a QSL from ρ_0 to the final state ρ_T such that the distance between ρ_0 and ρ_T is bigger than a certain fixed value. If this QSL is large, the decoherence needs a lot of time to drive the initial state ρ_0 toward ρ_T. In other words, such ρ_0 is less affected by the decoherence, and therefore, in this view, ρ_0 with a larger QSL can be regarded to be robust against the noise process. Based on this idea, in this chapter we establish the following optimization problem; the purpose is to engineer the system Hamiltonian that maximizes the QSL for a given ρ_0 and the decoherence. Here, it is important that the QSL has an explicit form in terms of the parameters characterizing the quantum system

in order to make this optimization problem tractable. Actually, in Section 4.2 we derive a new tractable (i.e., easily computable) QSL, which is applicable to a general Markovian open quantum system and prove that it is tighter than another explicit QSL given in [88], in the setup where the decoherence strength and the distance are both small. Moreover, it is shown that the Hamiltonian engineering problem based on the new explicit QSL is a quadratic convex optimization problem, which is efficiently solvable. Second, we apply the QSL to the characterization of the reachable set of quantum systems in a given time. This approach is based on that the general expression of the QSL (1.2) can be regard as the inequality of $D(\rho_0, \rho_T)$ with respect to the evolution time T. Based on it, we derive the time-dependent distance limit for open quantum systems under decoherence and investigate its performance in the qubit case.

Finally, Chapter 5 concludes this thesis and discusses future works.

Chapter 2

Quantum mechanics

This chapter provides some important topics in quantum mechanics; quantum state, quantum measurement, and quantum dynamics, which are necessary for understanding enough. Section 2.1 reviews a formalism of quantum state describing a quantum system with the introduction of key tools; the density operator and the fidelity. Section 2.2 formulates the concept of quantum measurement from general class to special one. Section 2.3 provides several mathematical tools for describing evolution of quantum systems, e.g., Schrödinger equation, master equation, and stochastic master equation. They play a central role in developing quantum control strategy and deriving the results of this thesis.

2.1 Quantum state

2.1.1 Density operator

Quantum mechanics is largely different from the classical mechanics in many aspects. One of the biggest difference of quantum mechanics from classical one is that a quantum system is probabilistic; that is, in principle, physical properties of quantum systems are not deterministic. In general, a state of a quantum system is composed of a number of states $|\psi_i\rangle$ with probability p_i. Therefore, the quantum state is given by the statistical ensemble described by the self-adjoint operator:

$$\rho = \sum_{i=1}^{N} p_i \left|\psi_i\right\rangle \left\langle\psi_i\right|, \tag{2.1}$$

which is called *density operator* (the notation $|\psi\rangle$ and dual of it $\langle\psi|$ are called *ket* and *bra*, respectively). ρ is defined in the finite-dimensional complex space called *Hilbert space* $\mathcal{H}$, and the set $\{|\psi_i\rangle\}$ is the orthonormal basis of $\mathcal{H}$. Note that ρ has the following properties:

$$\rho^\dagger = \rho, \quad \rho \geq 0, \quad \mathrm{Tr}(\rho) = 1. \tag{2.2}$$

In particular, due to $\mathrm{Tr}(\rho) = 1$, $\sum_{i=1}^{N} p_i = 1$, meaning that the total probability of the measurement on the state is one (we will explain later). When the rank of ρ is one, (i.e.,

$\rho = |\psi\rangle\langle\psi|$), the state is called *pure state*. On the other hand, when the rank of ρ is more than two, the state is called *mixed state*.

2.1.2 Measure of quantum state

How much the state is pure is quantified by *Purity* $P(\rho)$ defined by

$$P(\rho) = \mathrm{Tr}(\rho^2), \tag{2.3}$$

which is bounded as $1/N \leq P(\rho) \leq 1$. This upper bound is achieved if and only if the system is pure, and the lower one is achieved if and only if $\rho = (1/N)I$, which is called *maximally mixed state*.

Proof of the bound for Purity From the definition (2.1),

$$\rho^2 = \sum_{i=1}^{N}\sum_{j=1}^{N} (|\psi_i\rangle\langle\psi_i|)(|\psi_j\rangle\langle\psi_j|) = \sum_{i=1}^{N} p_i^2 |\psi_i\rangle\langle\psi_i|,$$

then we have

$$P(\rho) = \mathrm{Tr}(\rho^2) = \sum_{i=1}^{N} p_i^2.$$

Due to $\sum_{i=1}^{N} p_i = 1$,

$$1 = \left(\sum_{i=1}^{N} p_i\right)^2 \geq \sum_{i=1}^{N} p_i^2 = P(\rho).$$

This bound is achieved if and only if the state is pure $\rho = |\psi\rangle\langle\psi|$. With respect to the lower bound, from inequality of arithmetric-geometric mean $\sum_{i=1}^{N} x_i \geq N(\prod_{i=1}^{N} x_i)^{1/N}$,

$$P(\rho) = \sum_{i=1}^{N} p_i^2 \geq N\left(\prod_{i=1}^{N} p_i^2\right)^{\frac{1}{N}}.$$

The lower bound is achieved if and only if $p_1 = \cdots = p_N = 1/N$, that is $\rho = (1/N)\sum_{i=1}^{N} |\psi_i\rangle\langle\psi_i|$, then

$$P(\rho) = \sum_{i=1}^{N} p_i^2 \geq N\left(\prod_{i=1}^{N} p_i^2\right)^{\frac{1}{N}} = N\left(\frac{1}{N^2}N\right)^{\frac{1}{N}} \geq \frac{1}{N}. \quad \text{(Q.E.D)}$$

When the quantum system ρ is composed of N subsystems $\rho_i \in \mathcal{H}_i$ $(1 \leq i \leq N)$, ρ is described as the tensor product

$$\rho = \rho_1 \otimes \cdots \otimes \rho_N \in \mathcal{H}_1 \otimes \cdots \otimes \mathcal{H}_N, \tag{2.4}$$

If a composite state ρ_{AB} can be represented by $\rho_{AB} = \rho_A \otimes \rho_B$, ρ_{AB} is called *separable state*. Otherwise, if $\rho_{AB} \neq \rho_A \otimes \rho_B$, ρ_{AB} is called *entangled state*.

To evaluate the distance between two quantum states, *Fidelity* is known as a useful measure. For the two quantum states ρ and σ, the fidelity $F(\rho, \sigma)$ is defined as follows:

$$F(\rho, \sigma) = \left(\mathrm{Tr} \left[\sqrt{\rho^{1/2} \sigma \rho^{1/2}} \right] \right)^2, \tag{2.5}$$

where, for any ρ and σ, $0 \leq F(\rho, \sigma) \leq 1$ This upper bound is achieved if and only if $\rho = \sigma$, and the lower one is achieved if and only if ρ and σ are orthogonal. If one of the state is pure, $\sigma = |\psi\rangle \langle\psi|$, the fidelity reduces to $F(\rho, |\psi\rangle \langle\psi|) = \langle\psi|\rho|\psi\rangle$. Moreover, if the another one is also pure $\rho = |\phi\rangle \langle\phi|$, $F(|\phi\rangle, |\psi\rangle) = |\langle\psi|\phi\rangle|^2$.

2.1.3 Qubit

Here we give a simple example explaining the quantum state; a qubit system composed of the excited state $|0\rangle = [1, 0]^\top$ and the ground state $|1\rangle = [0, 1]^\top$, where $|0\rangle$ and $|1\rangle$ represent "spin-up" and "spin-down", respectively. A pure qubit state $|\psi\rangle$ is parametrized as

$$|\psi\rangle = \cos\theta |0\rangle + e^{i\varphi} \sin\theta |1\rangle, \tag{2.6}$$

where $0 \leq \theta \leq \pi/2$ and $0 \leq \varphi \leq \pi$. This special coordination is known as the *Bloch representation*. Thereby, the pure state of the qubit system is defined on the surface of a unit sphere. For instance, when $\theta = \pi/4$, the state is the superposition $|\psi\rangle = (|0\rangle + e^{i\varphi} |1\rangle)/\sqrt{2}$ on the equator of the sphere. On the other hand, a mixed state ρ is parametrized by

$$\rho = \frac{1}{2} \begin{bmatrix} 1+z & x-iy \\ x+iy & 1-z \end{bmatrix}, \tag{2.7}$$

where x, y z are real numbers satisfying $0 \leq x^2 + y^2 + z^2 \leq 1$, which corresponds to $(1/2) \leq P(\rho) \leq 1$. The points on the surface of the sphere correspond to the pure states of the system, whereas the inside points correspond to the mixed states, and especially the origin corresponds to the maximally mixed state. For the qubit system, angular momentum operators of spin 1/2 system along the x, y, z axis are denoted by the *Pauli operators*:

$$\sigma_x = \begin{bmatrix} 0 & 1 \\ 1 & 0 \end{bmatrix} = |1\rangle \langle 0| + |0\rangle \langle 1|,$$

$$\sigma_y = \begin{bmatrix} 0 & -i \\ i & 0 \end{bmatrix} = i |1\rangle \langle 0| - i |0\rangle \langle 1|,$$

$$\sigma_z = \begin{bmatrix} 1 & 0 \\ 0 & -1 \end{bmatrix} = |0\rangle \langle 0| - |1\rangle \langle 1|.$$

These satisfy the canonical commutation relation (CCR):

$$[\sigma_i, \sigma_j] = 2i\epsilon_{i,j,k}\sigma_k,$$

where $\epsilon_{i,j,k}$ denotes the Levi-Civita symbol.

2.2 Quantum measurement

2.2.1 General measurement

Because a quantum system is probabilistic, the measurement outcome varies every time. If the measurement on the quantum system is directly performed, the state collapses to the classical one. Therefore, it is necessary to introduce a special formalism of quantum measurement. Now, we begin with a general measurement modeled by a set of measurement operators $\{M_i\}$ acting on the Hilbert space $\mathcal{H}$ of a quantum system to be measured. The index i refers to the possible outcomes of the measurement. The measurement operators satisfy the completeness relation

$$\sum_i M_i^\dagger M_i = I.$$

For the quantum system ρ, the probability of getting the ith outcome is given by

$$p(i) = \mathrm{Tr}(M_i \rho M_i^\dagger). \tag{2.8}$$

Due to the completeness relation, the probabilities of the outcomes sum to one:

$$\begin{aligned}\sum_i p(i) &= \sum_i \mathrm{Tr}(M_i \rho M_i^\dagger) = \mathrm{Tr}(\rho \sum_i M_i^\dagger M_i) \\ &= \mathrm{Tr}(\rho I) = \mathrm{Tr}(\rho) = 1.\end{aligned}$$

Note that the change of the state $\rho \to \rho'$ is brought about by the measurement. The state after the measurement is given by

$$\rho' = \frac{M_i \rho M_i^\dagger}{\mathrm{Tr}(M_i \rho M_i^\dagger)} = \frac{M_i \rho M_i^\dagger}{p(i)}. \tag{2.9}$$

If the quantum state before measurement is pure, $\rho = |\psi\rangle \langle\psi|$, Eqs. (2.8) and (2.9) are

$$\begin{aligned}p(i) &= \langle\psi| M_i^\dagger M_i |\psi\rangle \,, \\ |\psi\rangle' &= \frac{M_i |\psi\rangle}{\sqrt{\langle\psi| M_i^\dagger M_i |\psi\rangle}} = \frac{M_i |\psi\rangle}{\sqrt{p(i)}}.\end{aligned}$$

Here we give a simple example that the measurement on a qubit system. Let the

measurement operators be $M_1 = |0\rangle\langle 0|$ and $M_2 = |1\rangle\langle 1|$. These satisfy the completeness relation $M_1^\dagger M_1 + M_2^\dagger M_2 = I$. Suppose that the state to be measured is

$$\rho = 0.6\,|0\rangle\langle 0| + 0.4\,|1\rangle\langle 1|\,.$$

Then, the probability of obtaining the result "0" is

$$p(0) = \mathrm{Tr}(M_1 \rho M_1^\dagger) = 60\%,$$

and the probability of obtaining the result "1" is $p(1) = 40\%$. Also, the state after the measurement in two cases are

$$\rho_1' = \frac{M_1 \rho M_1^\dagger}{\mathrm{Tr}(M_1 \rho M_1^\dagger)} = |0\rangle\langle 0|\,,$$
$$\rho_2' = \frac{M_2 \rho M_2^\dagger}{\mathrm{Tr}(M_2 \rho M_2^\dagger)} = |1\rangle\langle 1|\,.$$

2.2.2 Projective measurement

Here we explain a special class of the general measurement. A measurable physical property of the quantum system is called *observable*. It is represented by a self-adjoint operator A acting on the state space $\mathcal{H}_S$. A has a decomposition

$$A = \sum_i a_i\,|a_i\rangle\langle a_i| = \sum_i a_i P_i,$$

where $|a_i\rangle$ is the eigenstate and a_i is the eigenvalue, and the set $\{|a_i\rangle\}$ is an orthonormal basis in $\mathcal{H}_S$. $P_i = |a_i\rangle\langle a_i|$ represents the projector onto $|a_i\rangle$ with a_i; that is, the outcome of the measurement corresponds to a_i. P_i satisfies the following properties:

$$P_i^2 = P_i,\ P \geq 0,\ P_i P_j = P_i \delta_{i,j},\ \sum_i P_i = I.$$

This measurements is known as a *projective measurement*. When the outcome a_i is obtained, the quantum state ρ changes to $\rho_i' = |a_i\rangle\langle a_i|$. Therefore, the rank of the quantum state after the measurement is always one. The probability for getting the outcome a_i is given by

$$p(a_i) = \langle a_i|\rho|a_i\rangle = \mathrm{Tr}(\rho P_i) = \mathrm{Tr}(\rho P_i^\dagger P_i), \tag{2.10}$$

and the state after the measurement is

$$\rho_i' = \frac{P_i \rho P_i^\dagger}{\mathrm{Tr}(\rho P_i^\dagger P_i)} = \frac{P_i \rho P_i^\dagger}{p(a_i)}, \tag{2.11}$$

If the state is pure, $\rho = |\psi\rangle\langle\psi|$, the probability for getting a_i and the post-measurement state are given by

$$p(a_i) = \langle\psi|P_i^\dagger P_i|\psi_i\rangle\,,$$
$$|\psi_i\rangle' = \frac{P_i|\psi\rangle}{\sqrt{\langle\psi|P_i^\dagger P_i|\psi_i\rangle}} = \frac{P_i|\psi\rangle}{\sqrt{p(a_i)}}.$$

2.2.3 Positive operator valued measure

We consider a slightly general case of projective measurement. Consider a operator set $\{E_i\}$, where E_i is a positive operator $E_i \geq 0$ such that $\sum_i E_i = I$, and defines a scalar function

$$p(a_i) = \mathrm{Tr}(\rho E_i). \tag{2.12}$$

$p(a_i)$ is equal to the probabilistic distribution of the measurement outcomes. In this case, the measurement modeled by $\{E_m\}$ is known as a *positive operator valued measure (POVM)*. A difference of POVM from projective measurement is that the measurement operators of a POVM are not necessarily orthogonal. Consequently, the number of the measurement operators of the POVM can be larger than the dimension of the Hilbert space they act on. Conversely, that of the projective measurement is at most the dimension of the Hilbert space.

In reality, it is difficult to directly measure a quantum system without destroying it, and thus actual measurements are done through measurement apparatus indirectly. This physical setting is known as *indirect measurement* and theoretically formulated as follows; let $\mathcal{H}_\mathrm{S}$ and $\mathcal{H}_E$ be a Hilbert space of the quantum system of our interest ρ_S and the measurement apparatus ρ_E. The total system is given by $\rho_S \otimes \rho_E \in \mathcal{H}_S \otimes \mathcal{H}_E$. We first prepare an apparatus in a pure initial state $\rho_E = |\psi_E\rangle\langle\psi_E|$. By performing a unitary transformation U_{SE} on the two systems, we cause the interaction between ρ_S and ρ_E. After that, the local measurement on the apparatus described by $I_S \otimes P_{i,E}$ is performed ($P_{i,E}$ is a projective operator acting on $\mathcal{H}_E$). In this setting, the probability for getting the outcome i is

$$\begin{aligned} p(i) &= \mathrm{Tr}\left[U_{SE}(\rho_S \otimes |\psi_E\rangle\langle\psi_E|)U_{SE}^\dagger(I_S \otimes P_{i,E})\right] \\ &= \mathrm{Tr}\left[(\rho_S \otimes |\psi_E\rangle\langle\psi_E|)U_{SE}^\dagger(I_S \otimes P_{k,E})U_{SE}\right] \\ &= \mathrm{Tr}_S(\rho_S E_{i,S}), \end{aligned}$$

where Tr_S is the trace over $\mathcal{H}_S$. This operation is called *partial trace* and indicates to discard the information on the system ρ_E. An operator $E_{i,S}$ is given by

$$\begin{aligned} E_{i,S} &= \mathrm{Tr}_E \left[(I_S \otimes |\psi_E\rangle \langle\psi_E|) U_{SE}^\dagger (I_S \otimes P_{i,E}) U_{SE} \right] \\ &= \langle\psi_E| U_{SE}^\dagger (I_S \otimes P_{i,E}) U_{SE} |\psi_E\rangle \\ &= \langle\psi_E| U_{SE}^\dagger |i_E\rangle \langle i_E| U_{SE} |\psi_E\rangle , \end{aligned}$$

where we have written $P_{i,E} = |i_E\rangle \langle i_E|$. We find that $E_{i,S}$ satisfies $E_{i,S} \geq 0$ and $\sum_i E_{i,S}^\dagger E_{i,S} = I_S$, and hence $\{E_{i,S}\}$ is a realization of a POVM.

We consider a state transition after the measurement. From (2.11) the post-measurement state becomes

$$\begin{aligned} \rho'_{i,SE} &= \frac{1}{p(i)} \left[(I_S \otimes P_{i,E}) U_{SE} (\rho_S \otimes |\psi_E\rangle \langle\psi_E|) U_{SE}^\dagger (I_S \otimes P_{i,E})^\dagger \right] \\ &= \frac{1}{p(i)} \left[\langle i_E| U_{SE} |\psi_E\rangle \, \rho_S \, \langle\psi_E| U_{SE}^\dagger |i_E\rangle \otimes |\psi_E\rangle \langle\psi_E| \right] , \end{aligned}$$

and writing $K_i := \langle i_E| U_{SE} |\psi_E\rangle$ yields

$$\rho'_{i,SA} = \frac{1}{p(i)} (K_i \rho_S K_i^\dagger) \otimes |i_E\rangle \langle i_E| . \tag{2.13}$$

Therefore after the measurement the system and the environment are separated. Also the post-measurement state is

$$\rho'_{i,S} = \frac{K_i \rho_S K_i^\dagger}{p(i)}. \tag{2.14}$$

By using $K_{i,S} = K_i^\dagger K_i$, the probability for getting the outcome i is

$$p(i) = \mathrm{Tr}[\rho_S K_i^\dagger K_i]. \tag{2.15}$$

We can see that the state transition (2.14) and the probability of measurement (2.15) are generalization of those by (2.10) and (2.11). If the initial state of the quantum system is pure, i.e., $\rho_S = |\psi_S\rangle \langle\psi_S|$, then the post-measurement system's state is given by

$$|\psi_S\rangle' = \frac{K_i |\psi_S\rangle}{\sqrt{p(i)}}. \tag{2.16}$$

2.3 Quantum dynamics

2.3.1 Schrödinger equation

In general, a quantum system evolves in time. In particular, the dynamics of a closed system which does not interact with any environment is governed by the system energy. Let us consider a pure state of the closed system $|\psi_t\rangle$. The change of $|\psi_t\rangle$ is

$$d|\psi_t\rangle = |\psi_{t+dt}\rangle - |\psi_t\rangle,$$

and let $|\psi_{t+dt}\rangle$ be

$$|\psi_{t+dt}\rangle = |\psi_t\rangle + A|\psi_t\rangle\, dt = (I + Adt)|\psi_t\rangle.$$

The state change of the closed system is given as the unitary transformation, and hence

$$(I + Adt)(I + Adt)^\dagger = I \Leftrightarrow (A + A^\dagger)dt + AA^\dagger dt^2 = 0.$$

By ignoring the term of dt^2 and setting $A = -iH$ with self-adjoint operator H, we have

$$\frac{d|\psi_t\rangle}{dt} = -iH|\psi_t\rangle. \tag{2.17}$$

This equation is called *Schrödinger equation* and H is called *Hamiltonian* representing the system energy. The solution of this equation is given by

$$|\psi_t\rangle = e^{-iHt}|\psi_0\rangle = U_t|\psi_0\rangle, \tag{2.18}$$

where $U_t = e^{-iHt}$ is a unitary operator satisfying $U_t^\dagger U_t = U_t U_t^\dagger = I$. This means that the evolution of the closed system is unitary and the rank of the system is preserved. U_t obeys the following equation:

$$\frac{dU_t}{dt} = -iHU_t.$$

When the state is mixed, $\rho_t = \sum_i p_i |\psi_{i,t}\rangle\langle\psi_{i,t}|$, Eq. (2.17) is

$$\begin{aligned}\frac{d\rho_t}{dt} &= \sum_i p_i \left(\frac{d|\psi_{i,t}\rangle}{dt}\langle\psi_{i,t}| + |\psi_{i,t}\rangle\frac{d\langle\psi_{i,t}|}{dt}\right)\\ &= \sum_i p_i \left(-iH|\psi_{i,t}\rangle\langle\psi_{i,t}| + i|\psi_{i,t}\rangle\langle\psi_{i,t}|H\right)\\ &= -i[H, \rho_t],\end{aligned}$$

and the solution of it is given by

$$\rho_t = e^{-iHt}\rho_0 e^{iHt} = U_t\rho_0 U_t^\dagger.$$

2.3.2 Quantum stochastic differential equation

So far, we have considered the time evolution of closed systems. However, in reality quantum systems are never completely isolated from their environments. Quantum systems interacting with their environments are called *open quantum systems*, which are indispensable for modeling various phenomena in quantum field, e.g., the decay of energy of an atom. From now on, we consider the dynamics of open quantum systems.

Let us consider a general open quantum system interacting with a single coherent field. Let a_t and $a_t^\dagger$ be the annihilation and creation operator representing the quantum white noise process satisfying the following CCR:

$$[a_t, a_s^\dagger] = \delta(t-s).$$

Now, we assume that a_t is taken the Markovian approximation, that is, it instantaneously interacts with the system and has no memory of the system. By integrating overall time, the annihilation and creation process operators are defined by

$$A_t = \int_0^t a_s ds,\ A_t^\dagger = \int_0^t a_s^\dagger ds,$$

which satisfy the following Itō rule [44]:

$$\begin{aligned} &dtdA_t = 0,\ dA_t dA_t^\dagger = dt, \\ &dA_t^\dagger dA_t = dA_t dA_t = dA_t^\dagger dA_t^\dagger = 0. \end{aligned}$$

Now, we derive the time evolution of U_t using these mathematical tools; let dU_t be

$$dU_t = (BdA_t + CdA_t^\dagger + Ddt)U_t, \tag{2.19}$$

with $U_0 = I$. From Eq. (2.19), the unitary property $U_t^\dagger U_t = I$, and the Itō product rule

$$d(X_t Y_t) = dX_t Y_t + X_t dY_t + dX_t dY_t,$$

we have

$$\begin{aligned} 0 &= dU_t^\dagger \cdot U_t + U_t^\dagger dU_t + dU_t^\dagger dU_t, \\ &= U_t^\dagger \left(B^\dagger dA_t + C^\dagger dA_t^\dagger + D^\dagger dt\right) U_t + U_t^\dagger \left(BdA_t + CdA_t^\dagger + Ddt\right) U_t \\ &\quad + U_t^\dagger \left(B^\dagger dA_t^\dagger + C^\dagger dA_t + D^\dagger dt\right) \left(BdA_t + CdA_t^\dagger + Ddt\right) U_t. \end{aligned}$$

By using the quantum Itō rule and multiplying from the left by U_t and from the right by $U_t^\dagger$, we have

$$0 = (B + C^\dagger)dA_t + (C + B^\dagger)dA_t^\dagger + (D^\dagger + D + C^\dagger C)dt.$$

Then we obtain the equations

$$B + C^\dagger = 0,$$
$$B^\dagger + C = 0,$$
$$D^\dagger + D + C^\dagger C = 0.$$

In the same way, from $U_t U_t^\dagger = I$, we have

$$B^\dagger + C = 0,$$
$$B + C^\dagger = 0,$$
$$D^\dagger + D + C^\dagger C = 0.$$

Now for satisfying these equations, we set $B = -L^\dagger$, $C = L$, and $D = iH + L^\dagger L/2$. Consequently, we end up with the following equation:

$$dU_t = \left\{ -L^\dagger dA_t + L dA_t^\dagger - \left(iH + \frac{1}{2} L^\dagger L \right) dt \right\} U_t. \tag{2.20}$$

with $U_0 = I$. This equation is called the *quantum stochastic differential equation (QSDE)* [45]. H is the Hamiltonian and L is a system operator representing the coupling with the field. The open quantum system governed by (2.20) is characterized by shorthand $G = (H, L)$.

2.3.3 Markovian master equation

Now, for an arbitrary system operator X, let us derive the time evolution of X_t. Let the unitary evolution of X be $X_t = j_t(X) = U_t^\dagger X U_t$. Using the Itō product rule and the above QSDE,

$$\begin{aligned} dX_t &= U_{t+dt}^\dagger X U_{t+dt} - U_t^\dagger X U_t \\ &= dU_t^\dagger X U_t + U_t^\dagger X dU_t + dU_t^\dagger X dU_t \\ &= j_t \left(i[H, X] + L^\dagger X L - \frac{1}{2} L^\dagger L X - \frac{1}{2} X L^\dagger L \right) dt \\ &\quad + j_t([X, L]) dA^\dagger(t) + j_t([L^\dagger, X]) dA(t). \end{aligned} \tag{2.21}$$

Also, the annihilation process operator A_t changes to $A'_t = U_t^\dagger A_t U_t = j_t(A_t)$ and satisfies the output field

$$dA'_t = j_t(L) dt + dA_t.$$

We assume that the coupling is a coherent field with amplitude α. Then, taking the expectation $\langle X_t \rangle$, due to $\langle dA_t \rangle = \langle dA_t^\dagger \rangle = 0$, we have

$$\frac{d\langle X_t \rangle}{dt} = \left\langle j_t \left(i[H', X_t] + L^\dagger X_t L - \frac{1}{2} L^\dagger L X_t - \frac{1}{2} X_t L^\dagger L \right) \right\rangle,$$

where $H' = H + (\alpha L^\dagger - \alpha^\dagger L)/2i$. In the Schrödinger picture, the expectation $\langle X_t \rangle$ is defined using the time-dependent unconditional state ρ_t as $\langle X_t \rangle = \mathrm{Tr}\,(X\rho_t)$. Then it is easy to find that ρ_t obeys the following equation:

$$\frac{d\rho_t}{dt} = -i[H, \rho_t] + \mathcal{D}[L]\rho_t, \tag{2.22}$$

where H' has been replaced with H. This dynamical equation is called *(Markovian) master equation* and $\mathcal{D}[L]\rho = L\rho L^\dagger - L^\dagger L\rho/2 - \rho L^\dagger L/2$ is the *Lindblad super operator* representing the decohere process. When the system is subjected to multiple Hamiltonians and environments, Eq. (2.22) is generalized to

$$\frac{d\rho_t}{dt} = -i\sum_j [H_j, \rho_t] + \sum_j \mathcal{D}[L_j]\rho_t. \tag{2.23}$$

2.3.4 Stochastic master equation

In the previous subsection, we have focused on the evolution of open quantum systems interacting with a coherent field. We further extend the above discussion to the case where the quantum system is subjected to continuous measurement. We now develop a dynamical equation for open quantum system in a simple setup; the system is coupled to a single probe field L in the vacuum state. Recall that the system dynamics is generated by the following QSDE:

$$dU_t = \left\{ \left(-iH - \frac{1}{2}L^\dagger L \right) dt + L dA_t^\dagger - L^\dagger dA_t \right\} U_t,\ U_0 = I,$$

and the time evolution of the system observable $j_t(X) := U_t^\dagger X U_t$ is given by

$$dj_t(X) = j_t(\mathcal{L}X)dt + j_t([L^\dagger, X])dA_t + j_t([X, L])dA_t^\dagger, \tag{2.24}$$

where

$$\mathcal{L}X := i[H, X] + L^\dagger X L - \frac{1}{2}L^\dagger L X - \frac{1}{2}X L^\dagger L. \tag{2.25}$$

Now the real part of the output field operator is measured by a homodyne detector; we measure the output field operator represented by

$$y_t = Y_t + Y_t^\dagger = U_t^\dagger \left(A_t + A_t^\dagger \right) U_t.$$

By using the quantum Itō rule, the time evolution of y_t can be obtained as

$$dy_t = j_t(L + L^\dagger)dt + dA_t + dA_t^\dagger.$$

Note importantly that the output observable y_t has the *self-non-demolition* property:

$$[y_s, y_t] = 0, \quad \forall s, t.$$

This means that there is sets of measurement result constructed by y_s, which is denoted by $\mathcal{Y}_t = \{y_s | 0 \leq s \leq t\}$. Also, y_t satisfies the *quantum non-demolition (QND)* property,

$$[y_s, j_t(X)] = 0, \quad \forall s \leq t.$$

for all system observables X. From the self-non-demolition property, the observable of the probe system are compatible over all time, and hence the continuous measurement is guaranteed in principle. Further, from the QND property, all probe observables until time t and the system observable $j_t(X)$ are compatible. Therefore, $j_t(X)$ can be conditioned on $\mathcal{Y}_t$, which means that the optimal estimate is given by the quantum conditional expectation $\pi_t(X) := \mathbb{P}\left(j_t(X)|\mathcal{Y}_t\right) = \mathrm{Tr}\left(X\rho_t^c\right)$ defined based on the measurement history.

Let us more deepen this explanation. The goal here is to calculate the best estimate of the system observable $j_t(X)$ based on the history of observations $\mathcal{Y}_t$. In particular, by defining the cost function by the least mean-squared error $\mathbb{P}[(j_t(X) - Z)^2]$, where Z an element of $\mathcal{Y}_t$, we can have an explicit solution; that is, because $\mathcal{Y}_t$ is a commutative algebra and $j_t(X)$ lives in the commutant of $\mathcal{Y}_t$, the mean-squared error is minimized when Z is given by the quantum conditional expectation:

$$\pi_t(X) = \arg\min \mathbb{P}[(j_t(X) - Z)^2] = \mathbb{P}\left(j_t(X)|\mathcal{Y}_t\right),$$

To derive the system dynamics of $\pi_t(X)$, we here consider the following ansatz:

$$d\pi_t(X) = E_t dt + F_t dy_t,$$

where E_t and F_t are functions of $\mathcal{Y}_t$. We wish to derive explicit forms of E_t and F_t. Now we introduce the following function

$$\bar{h}_t = \exp\left(\int_0^t h_s dy_s - \frac{1}{2}\int_0^t h_s^2 ds\right),$$

where $h_t \in \mathcal{Y}_t$ and thus $\bar{h}_t \in \mathcal{Y}_t$ as well. By using the Itō rule, we find that $d\bar{h}_t = \bar{h}_t h_t dy_t$. To determine E_t and F_t, let us calculate $d\mathbb{P}\left(\bar{h}_t j_t(X)\right)$ in two ways as follows.

First, from the Itō product rule we have

$$\begin{aligned}
d\mathbb{P}\left(\bar{h}_t j_t(X)\right) &= \mathbb{P}\left(d\bar{h}_t j_t(X) + \bar{h}_t dj_t(X) + d\bar{h}_t dj_t(X)\right) \\
&= \mathbb{P}\left(\bar{h}_t h_t j_t(L + L^\dagger) j_t(X) + \bar{h}_t j_t(\mathcal{L}X)dt + \bar{h}_t h_t dA_t j_t([X, L]) dA_t^\dagger\right) \\
&= \mathbb{P}\left(\bar{h}_t h_t j_t(LX + L^\dagger X) + \bar{h}_t j_t(\mathcal{L}X) + \bar{h}_t h_t j_t([X, L])\right) dt \\
&= \mathbb{P}\left(\bar{h}_t h_t j_t(XL + L^\dagger X) + \bar{h}_t j_t(\mathcal{L}X)\right) dt,
\end{aligned}$$

where $\mathbb{P}\left(dA_t\right) = \mathbb{P}(dA_t^\dagger) = 0$ and $dA_t dA_t^\dagger = dt$ are used. Now, using the tower property of the quantum conditional expectation, the above equation can be further calculated as

$$\begin{aligned}
\frac{d}{dt}\mathbb{P}\left(\bar{h}_t j_t(X)\right) &= \mathbb{P}\left[\mathbb{P}\left(\bar{h}_t h_t j_t(XL + L^\dagger X) + \bar{h}_t j_t(\mathcal{L}X)|\mathcal{Y}_t\right)\right] \\
&= \mathbb{P}\left[\bar{h}_t h_t \mathbb{P}\left(j_t(XL + L^\dagger X)|\mathcal{Y}_t\right) + \bar{h}_t \mathbb{P}\left(j_t(\mathcal{L}X)|\mathcal{Y}_t\right)\right] \\
&= \mathbb{P}\left(\bar{h}_t h_t \pi_t(XL + L^\dagger X) + \bar{h}_t \pi_t(\mathcal{L}X)\right).
\end{aligned}$$

In the second way,

$$\begin{aligned} d\mathbb{P}\left(\bar{h}_t j_t(X)\right) &= d\mathbb{P}\left[\mathbb{P}\left(\bar{h}_t j_t(X)|\mathcal{Y}_t\right)\right] = d\mathbb{P}\left(\bar{h}_t \mathbb{P}(j_t(X)|\mathcal{Y}_t)\right) \\ &= d\mathbb{P}\left(\bar{h}_t \pi_t(X)\right) = \mathbb{P}\left(d\bar{h}_t \pi_t(X) + \bar{h}_t d\pi_t(X) + d\bar{h}_t d\pi_t(X)\right) \\ &= \mathbb{P}\left[\bar{h}_t h_t \left(\pi_t(L+L^\dagger)\pi_t(X) + F_t\right) + \bar{h}_t \left(E_t + F_t \pi_t(L+L^\dagger)\right)\right] dt. \end{aligned}$$

By comparing the above two equations, we end up with

$$\begin{aligned} &\pi_t(L+L^\dagger)\pi_t(X) + F_t = \pi_t(XL + L^\dagger X), \\ &E_t + F_t \pi_t(L+L^\dagger) = \pi_t(\mathcal{L}X). \end{aligned}$$

Consequently, the dynamics of the conditional expectation $\pi_t(X)$ is given as follows:

$$d\pi_t(X) = \pi_t(\mathcal{L}X)dt + \left\{\pi_t(XL + L^\dagger X) - \pi_t(X)\pi_t(L+L^\dagger)\right\}\left(dy_t - \pi_t(L+L^\dagger)dt\right). \tag{2.26}$$

This is called the *quantum filtering equation*. The last term $dy_t - \pi_t(L+L^\dagger)dt$ is the Wiener increment. In the classical control literature, it is called the *innovation process* representing the update of the estimate based on the output. Here, we turn attention to the Schrödinger picture from the Heisenberg picture to derive the time evolution of the conditional state ρ_t^{c}. By applying the relation $\pi_t(X) = \mathrm{Tr}\left(X\rho_t^{\mathrm{c}}\right)$ to (2.26), we immediately obtain the time evolution of ρ_t^{c} as follows:

$$d\rho_t^{\mathrm{c}} = -i[H, \rho_t^{\mathrm{c}}]dt + \mathcal{D}[L]\rho_t^{\mathrm{c}} + \mathcal{H}[L]\rho_t^{\mathrm{c}} dW_t, \tag{2.27}$$

where $\mathcal{H}[L]\rho = L\rho + \rho L^\dagger - \mathrm{Tr}(L\rho + \rho L^\dagger)\rho$ and $dW_t = dy_t - \mathrm{Tr}(L\rho + \rho L^\dagger)dt$. This equation is called the *stochastic master equation (SME)*. It is the stochastic partial differential equation describing the dynamics of the conditional density operator of a stochastic system. Note that dW_t is the mean-zero Wiener increment, i.e., $\mathbb{E}\left(dW_t\right) = 0$. Now, by averaging the SME, we obtain the dynamics of the ensemble system $\rho_t := \mathbb{E}\left(\rho_t^{\mathrm{c}}\right)$:

$$\frac{d\rho_t}{dt} = -i[H, \rho_t] + \mathcal{D}[L]\rho_t, \tag{2.28}$$

which is analogous to the master equation. Therefore, the master equation describes the unconditional evolution of the quantum system interacting with a coherent field. Furthermore, if $L = 0$, the master equation (2.28) becomes the Schrödinger equation for the mixed state. Therefore, the SME is the most general equation for describing the dynamics of the quantum system. Finally, the SME (2.27) is generalized to the multi-input and multi-probe setup:

$$d\rho_t^{\mathrm{c}} = -i\sum_j [H_j, \rho_t^{\mathrm{c}}]dt + \sum_j \mathcal{D}[L_j]\rho_t^{\mathrm{c}} dt + \sum_j \mathcal{H}[L_j]\rho_t^{\mathrm{c}} dW_t.$$

Chapter 3

Distance limit

In practical situation, the biggest obstacle for quantum control is of course decoherence. The actual performance of quantum control under decoherence is sometimes far away from the ideal one. Therefore, quantifying the reachability, that is how close the controlled quantum system can be steered to a target state under decoherence, is of great importance. Towards this problem, in this chapter we develop a limit for reachability of the controlled system under decoherence; more precisely, we present a lower bound of the fidelity-based distance for open quantum system driven by any types of decohering process and control. Note that this bound is straightforward to calculate and can be used as a guide for choosing the target state. Some examples showing this effectiveness will be given. The topics of this chapter is mainly based on [104].

3.1 Quantum control

3.1.1 Mathematical description of quantum control

In Section 2.3, we have presented several dynamical equations, i.e., Schrödinger equation, master equation, and SME. These are essential to establish control strategies, because the concept of quantum control is to design the controlled dynamics of the quantum system so that the state reaches the target. In this section, we develop a mathematical description of several types of quantum control based on these mathematical tools.

Now, we begin with a simple setting of open-loop control and reservoir engineering; let us assume that the quantum state ρ_t obeys the master equation:

$$\frac{d\rho_t}{dt} = -i[u_t H, \rho_t] + \mathcal{D}[L]\rho_t, \tag{3.1}$$

where u_t is the control sequence. H and L are system operators that can be engineered. The standard open-loop control problem is to design a time-dependent sequence u_t that steers ρ_t towards a target state. Also the aim of the standard reservoir engineering method is to design L, with constant sequense $u_t = u$ so that ρ_t autonomously converges to a

target. In particular, the MBF control setting can also be included in the theory. In this case, the dynamics of the conditional quantum state ρ_t^c based on the measurement result y_t obeys the SME [46, 47, 48]

$$d\rho_t^c = -i[u_t H, \rho_t^c]dt + \mathcal{D}[L]\rho_t^c dt + \mathcal{H}[L]\rho_t^c dW_t. \tag{3.2}$$

The goal of MBF is to design the control input u_t as a function of ρ_t^c, to accomplish a certain goal. Particularly, L represents the probe field for measurement and satisfies $L = L^\dagger$, there are typical types of MBF controls that selectively steer the state to an eigenstate of L.

By focusing on the unconditional state $\rho_t = \mathbb{E}(\rho_t^c)$, which is the ensemble average of ρ_t^c over all the measurement results, Eq. (3.2) becomes the master equation:

$$\frac{d\rho_t}{dt} = -i[H, \mathbb{E}(u_t \rho_t^c)] + \mathcal{D}[L]\rho_t + \mathcal{D}[M]\rho_t. \tag{3.3}$$

Note in particular that u_t is a function of ρ_t^c, and hence Eq. (3.3) is a non-linear equation with respect to ρ_t. In the open-loop control or reservoir engineering setting, u_t is independent of ρ_t^c. Then Eq. (3.3) is reduced to the linear equation due to $\mathbb{E}(u_t \rho_t^c) = u_t \mathbb{E}(\rho_t^c) = u_t \rho_t$:

$$\frac{d\rho_t}{dt} = -i[u_t H, \rho_t] + \mathcal{D}[L]\rho_t + \mathcal{D}[M]\rho_t. \tag{3.4}$$

Therefore, as mentioned above, the SME includes any types of quantum control setting.

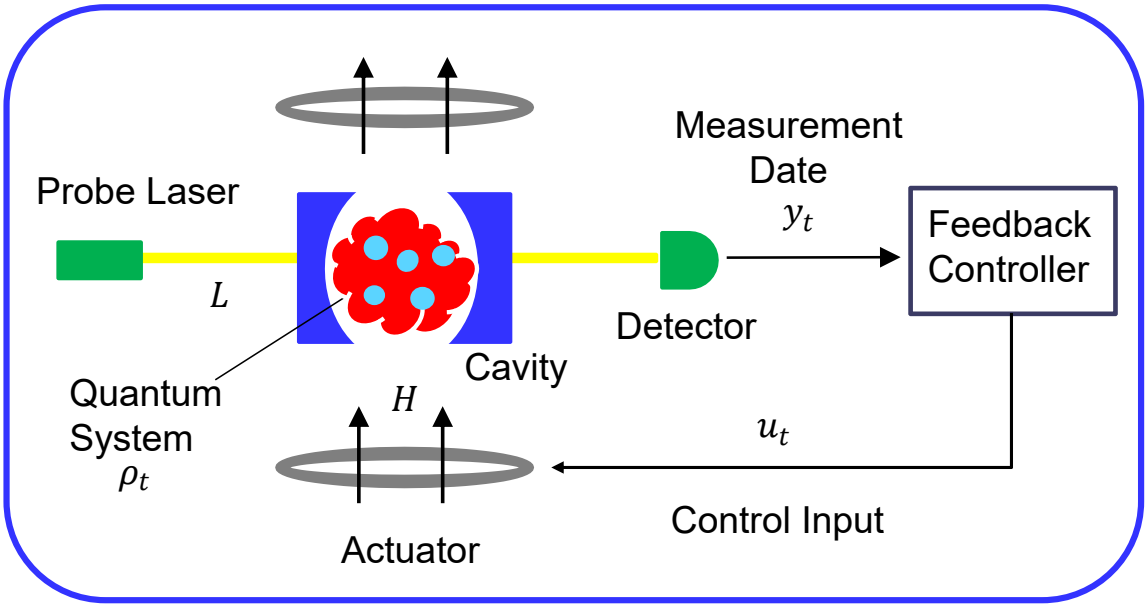

Fig. 3.1: Schematic of MBF.

3.1.2 MBF for ideal case

As an important application of the SME, here we study the MBF control. In fact, the MBF is a versatile and powerful method and some notable experiments have been extensively demonstrated [24, 25, 26, 27, 28, 29]. Here we give a physical implementation of a typical MBF setting (Fig. 3.1). The system of our interest is a cloud of atoms trapped into the optical cavity. Our aim is to control a collective angular momentum of the system. To obtain the information on the system, we scatter a probe laser off the system and cause the interaction between the system and the probe field (the interaction strength can be adjusted by the optical cavity). After the interaction, we measure the output field which carries any information on the system by a photodetector known as a homodyne detector. The information given by the classical output data y_t is processed to continuously update the conditional state, and the state is fed into a controller to calculate the control signal u_t to control the system through actuators implemented by magnetic coils. By repeating this process in continuous time, we end up with a desired quantum state.

We now demonstrate the performance of the MBF in the qubit example; the goal is to stabilize the spin state driven by the SME (3.2) into the excited state, in other words to realize the deterministic convergence $z_t = \mathrm{Tr}\,(\sigma_z \rho_t^{\mathrm{c}}) \to 1$. In this case, the system operators and the feedback control u_t that achieves the goal is given by

$$H = \sigma_y,\ L = \sqrt{\kappa}\sigma_z,\ u_t = -2\kappa x_t, \tag{3.5}$$

where $x_t = \mathrm{Tr}\,(\sigma_x \rho_t^{\mathrm{c}})$.

Proof of the setup (3.5) For the system operators Eq. (3.5), $(H, L) = (\sigma_y, \sqrt{\kappa}\sigma_z)$, the conditional state ρ_t^{c} obeys the SME:

$$d\rho_t^{\mathrm{c}} = -i[u_t\sigma_y, \rho_t^{\mathrm{c}}]dt + \mathcal{D}[\sqrt{\kappa}\sigma_z]\rho_t^{\mathrm{c}}dt + \mathcal{H}[\sqrt{\kappa}\sigma_z]\rho_t^{\mathrm{c}}dW_t, \tag{3.6}$$

which leads to the dynamics

$$dz_t = -2u_t x_t dt + 2\sqrt{\kappa}\left(1 - z_t^2\right) dW_t.$$

Let us consider the cost function

$$\mathcal{V}_t = \mathbb{E}\left[(z_t - 1)^2\right].$$

The infinitesimal change of $\mathcal{V}_t$ is given by

$$\begin{aligned} d\mathcal{V}_t &= \mathbb{E}\left[(z_t + dz_t - 1)^2\right] - \mathbb{E}\left[(z_t - 1)^2\right] \\ &= 2\mathbb{E}\left[(z_t - 1)dz_t\right] + \mathbb{E}\left[(dz_t)^2\right] \\ &= 2\mathbb{E}\left[(z_t - 1)(-2u_t x_t dt + 2\sqrt{\kappa}(1 - z_t^2)dW_t)\right] \\ &\quad + \mathbb{E}\left[\{-u_t x_t dt + 2\sqrt{\kappa}(1 - z_t^2)dW_t\}^2\right] \\ &= 4\mathbb{E}\left[(1 - z_t)u_t x_t\right] dt + 4\mathbb{E}\left[\kappa(1 - z_t^2)^2\right] dt \\ &= 4\mathbb{E}\left[(1 - z_t)\{u_t x_t + \kappa(1 + z_t)x_t^2\}\right] dt, \end{aligned}$$

where we have used the relation $x_t^2 + z_t^2 = 1$. Now choosing $u_t = -2\kappa x_t$, we have

$$\frac{d\mathcal{V}_t}{dt} = -4\kappa\mathbb{E}\left[x_t^2(1 - z_t)^2\right] \leq 0.$$

Hence, the feedback law $u_t = -2\kappa x_t$ makes sure that $\mathcal{V}_t$ monotonically decreases, and thus the deterministic convergence $z_t \to 1$ is accomplished. (Q.E.D)

Figure 3.2 illustrates the sample paths of z_t. If the feedback is not performed, z_t takes ± 1 stochastically. Meanwhile, we can eventually prepare the target $z_t = 1$ by performing the feedback control.

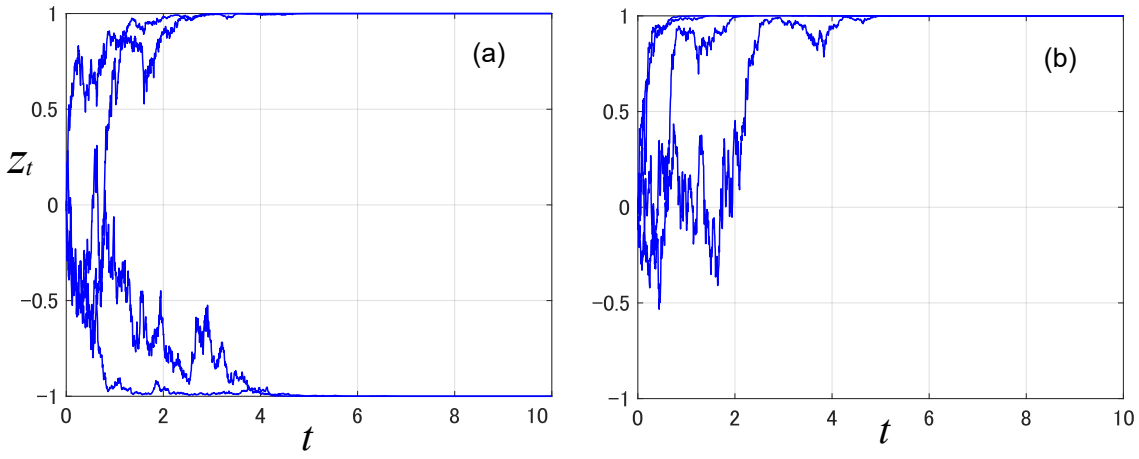

Fig. 3.2: The sample paths of z_t (a) without, (b) with MBF.

3.1.3 MBF in the imperfect setting

Above, we have seen the effectiveness of the MBF in the ideal setup. However, in practical situation, the quantum system is subjected to decoherence process induced by the

environments. Due to it, unfortunately, there is a gap between the target state and the controlled states. Here we add the Lindblad term generated by the decohering operator $\mathcal{D}[M]$ to the SME (3.6):

$$d\rho_t^{\mathrm{c}} = -i[u_t\sigma_y, \rho_t^{\mathrm{c}}]dt + \mathcal{D}[\sqrt{\kappa}\sigma_z]\rho_t^{\mathrm{c}}dt + \mathcal{D}[M]\rho_t^{\mathrm{c}}dt + \mathcal{H}[\sqrt{\kappa}\sigma_z]\rho_t^{\mathrm{c}}dW_t. \tag{3.7}$$

Eq. (3.7) describes the dynamics under the realistic MBF setting. As an example, we consider the energy decay $M = \sqrt{\gamma}\sigma_-$. Figure 3.3 (a) shows the sample path of z_t; clearly the performance of the control severely degrades as the strength of decoherence γ increases. For simplicity, here we focus on the unconditional state $\rho_t = \mathbb{E}\left(\rho_t^{\mathrm{c}}\right)$ obtained by averaging over the measurement results. As shown in Fig. 3.3 (b), for instance, when $\gamma = 0.1$, the reachability of $\mathbb{E}\left(z_t\right)$ is less than 0.7. In this way, taking the ensemble average of the quantum system allows for an analytical approach for finding the reachability of the controlled dynamics.

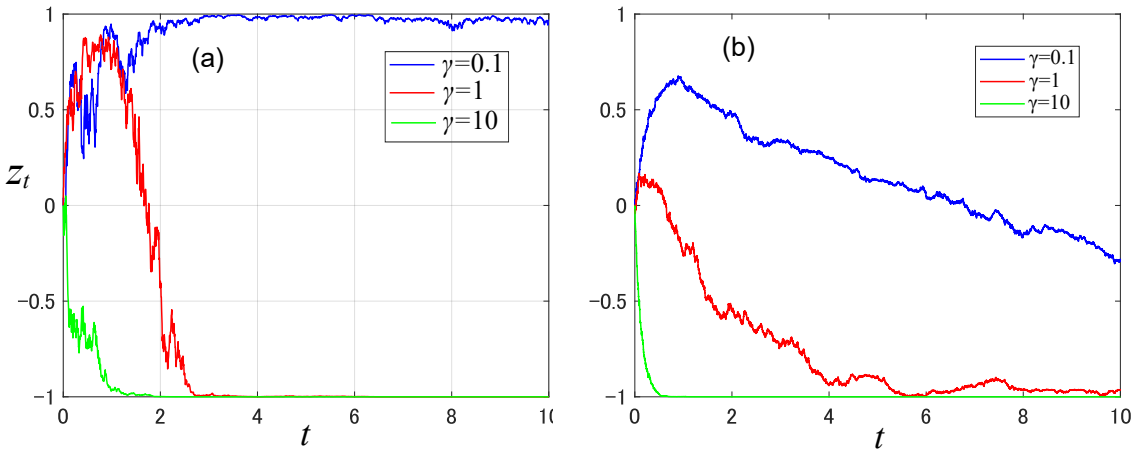

Fig. 3.3: (a) The sample paths of z_t and (b) averaging path $\mathbb{E}\left(z_t\right)$ under decoherence.

3.2 Derivation of the distance limit

Let us consider the master equation for the unconditional state $\rho_t = \mathbb{E}(\rho_t^{\mathrm{c}})$:

$$\frac{d\rho_t}{dt} = -i[H, \mathbb{E}(u_t\rho_t^{\mathrm{c}})] + \mathcal{D}[L]\rho_t + \mathcal{D}[M]\rho_t. \tag{3.8}$$

Now we wish to minimize the cost function

$$J_t = 1 - \mathrm{Tr}\left(Q\rho_t\right), \quad Q = |\psi\rangle\langle\psi| \tag{3.9}$$

where $|\psi\rangle$ is the target pure state and ρ_t is the state driven by Eq. (3.8). J_t represents the fidelity-based distance of ρ_t from the target state. As seen above, in the presence of decoherence term $\mathcal{D}[M]$, in general we cannot deterministically achieve $J_t = 0$ at some time t. The main result of this chapter is to present a lower bound of the cost (3.9) in an explicit form as follows.

Theorem 3.1 *For the conditional quantum state ρ_t^c obeying Eq. (3.8), the cost (3.9) has the lower bound at the steady state*

$$J_\infty \geq J_*(|\psi\rangle) := \left(\frac{\mathcal{E}}{\mathcal{A}+\mathcal{U}}\right)^2, \tag{3.10}$$

where

$$\begin{aligned}
&\mathcal{A} = \sqrt{2}(\|L^\dagger|\psi\rangle\|^2 + \|L^\dagger L|\psi\rangle\| + \|M^\dagger|\psi\rangle\|^2 + \|M^\dagger M|\psi\rangle\|),\\
&\mathcal{U} = 2\bar{u}\sqrt{\langle\psi|H^2|\psi\rangle - \langle\psi|H|\psi\rangle^2}, \quad \bar{u} = \max\{|u_t|\},\\
&\mathcal{E} = \|L|\psi\rangle\|^2 - |\langle\psi|L|\psi\rangle|^2 + \|M|\psi\rangle\|^2 - |\langle\psi|M|\psi\rangle|^2.
\end{aligned}$$

Proof of Theorem 3.1 As a control model, here we take the MBF setting described by the SME, because the open-loop control and reservoir engineering are included by simply setting the control sequence u_t to be independent of the conditional state ρ_t^c. First, we take the infinitesimal change of the random variable

$$j_t = 1 - \mathrm{Tr}\left(Q\rho_t^c\right), \; Q = |\psi\rangle\langle\psi|, \tag{3.11}$$

as follows:

$$\begin{aligned}
dj_t &= -\mathrm{Tr}\left(Qd\rho_t^c\right)\\
&= -\mathrm{Tr}\left\{Q\left(-i[u_tH,\rho_t^c]dt + \mathcal{D}[L]\rho_t^c dt + \mathcal{D}[L]\rho_t^c dt + \mathcal{H}[L]\rho_t^c dW_t\right)\right\}\\
&= \mathrm{Tr}\left(iu_t[Q,H]\rho_t^c\right)dt - \mathrm{Tr}\left(Q\mathcal{D}[L]\rho_t^c\right)dt - \mathrm{Tr}\left(Q\mathcal{D}[M]\rho_t^c\right)dt - \mathrm{Tr}\left(Q\mathcal{H}[L]\rho_t^c\right)dW_t.
\end{aligned} \tag{3.12}$$

The Wiener process (i.e., the classical stochastic process), W_t satisfies the Itō rule $dW_t^2 = dt$ and $\mathbb{E}\left(W_t\right) = 0$. The ensemble average of this dynamics with respect to W_t is given by

$$\frac{d\mathbb{E}(j_t)}{dt} = \mathrm{Tr}\left\{i[Q,H]\mathbb{E}(u_t\rho_t^c)\right\} - \mathrm{Tr}\left\{Q\mathcal{D}[L]\mathbb{E}(\rho_t^c)\right\} - \mathrm{Tr}\left\{Q\mathcal{D}[M]\mathbb{E}\left(\rho_t^c\right)\right\}. \tag{3.13}$$

Note again that u_t is a function of ρ_t^c in the context of MBF control.

To give a proof, we often use the Schwarz inequality for matrices X and Y,

$$\|X\|_{\mathrm{F}}\|Y\|_{\mathrm{F}} \geq \frac{1}{2}|\mathrm{Tr}(X^\dagger Y + Y^\dagger X)|.$$

In particular, $\|X\|_{\mathrm{F}}\|Y\|_{\mathrm{F}} \geq |\mathrm{Tr}(XY)|$ holds if and only if X and Y are self-adjoint. The following inequality is also often used:

$$\begin{aligned}\|\rho_t^{\mathrm{c}} - Q\|_{\mathrm{F}} &= \sqrt{\mathrm{Tr}[(\rho_t^{\mathrm{c}} - Q)^2]} \\ &= \sqrt{\mathrm{Tr}[(\rho_t^{\mathrm{c}})^2 - 2\rho_t^{\mathrm{c}}Q + Q^2]} \\ &\leq \sqrt{2 - 2\mathrm{Tr}(\rho_t^{\mathrm{c}}Q)} \\ &= \sqrt{2j_t},\end{aligned}$$

where $\mathrm{Tr}\left[(\rho_t^{\mathrm{c}})^2\right] \leq 1$ and $\mathrm{Tr}(Q^2) = \mathrm{Tr}(Q) = 1$ are used.

We begin with calculating a lower bound of the first term on the rightmost side of Eq. (3.12) as

$$\begin{aligned}\mathrm{Tr}\left(iu_t[Q,H]\rho_t^{\mathrm{c}}\right) &\geq -\bar{u}|\mathrm{Tr}\left(i[Q,H]\rho_t^{\mathrm{c}}\right)| \\ &= -\bar{u}|\mathrm{Tr}\{i[Q,H](\rho_t^{\mathrm{c}} - Q)\}| \\ &\geq -\bar{u}\|i[H,Q]\|_{\mathrm{F}}\|\rho_t^{\mathrm{c}} - Q\|_{\mathrm{F}} \\ &= -\bar{u}\sqrt{\mathrm{Tr}\{(iHQ - iQH)^2\}}\sqrt{2j_t} \\ &\geq -2\bar{u}\sqrt{\langle\psi|H^2|\psi\rangle - \langle\psi|H|\psi\rangle^2}\sqrt{j_t},\end{aligned}$$

where $\bar{u} := \max\{|u_t|\}$ is the upper bound of the control input. Then, by focusing on the ensemble average of this equation with respect to W_t, we have

$$\begin{aligned}\mathrm{Tr}\{i[Q,H]\mathbb{E}\left(u_t\rho_t^{\mathrm{c}}\right)\} &\geq -2\bar{u}\sqrt{\langle\psi|H^2|\psi\rangle - \langle\psi|H|\psi\rangle^2}\mathbb{E}\left(\sqrt{j_t}\right) \\ &\geq -2\bar{u}\sqrt{\langle\psi|H^2|\psi\rangle - \langle\psi|H|\psi\rangle^2}\sqrt{\mathbb{E}(j_t)},\end{aligned}$$

where $\mathbb{E}\left(\sqrt{j_t}\right) \leq \sqrt{\mathbb{E}\left(j_t\right)}$ is used. Next the second term on the rightmost side of Eq. (3.12) can be bounded as

$$\begin{aligned}-\mathrm{Tr}(Q\mathcal{D}[L]\rho_t^{\mathrm{c}}) &= -\mathrm{Tr}[Q(L\rho_t^{\mathrm{c}}L^\dagger - \frac{1}{2}\rho_t^{\mathrm{c}}L^\dagger L - \frac{1}{2}\rho_t^{\mathrm{c}}LL^\dagger)] \\ &= -\mathrm{Tr}[L^\dagger QL(\rho_t^{\mathrm{c}} - Q)] - \mathrm{Tr}(L^\dagger QLQ) + \mathrm{Tr}(QL^\dagger LQ) \\ &\quad - \frac{1}{2}\mathrm{Tr}[(Q - \rho_t^{\mathrm{c}})L^\dagger LQ + (L^\dagger LQ)(Q - \rho_t^{\mathrm{c}})] \\ &\geq -\|L^\dagger QL\|_{\mathrm{F}}\|\rho_t^{\mathrm{c}} - Q\|_{\mathrm{F}} - \|L^\dagger LQ\|_{\mathrm{F}}\|\rho_t^{\mathrm{c}} - Q\|_{\mathrm{F}} + \mathrm{Tr}(L^\dagger LQ) - \mathrm{Tr}(L^\dagger QLQ) \\ &\geq -\left(\sqrt{\mathrm{Tr}[(L^\dagger QL)^2]} + \sqrt{\mathrm{Tr}[(L^\dagger LQ)^\dagger(L^\dagger LQ)]}\right)\sqrt{2j_t} + \mathrm{Tr}(L^\dagger LQ) - \mathrm{Tr}(L^\dagger QLQ) \\ &= -\sqrt{2}\left(\langle\psi|LL^\dagger|\psi\rangle + \sqrt{\langle\psi|(L^\dagger L)^2|\psi\rangle}\right)\sqrt{j_t} + \langle\psi|L^\dagger L|\psi\rangle - |\,\langle\psi|L|\psi\rangle\,|^2 \\ &= -\sqrt{2}(\|L^\dagger\,|\psi\rangle\,\|^2 + \|L^\dagger L\,|\psi\rangle\,\|)\sqrt{j_t} + \|L\,|\psi\rangle\,\| - |\,\langle\psi|L|\psi\rangle\,|^2.\end{aligned}$$

Hence again it follows from $\mathbb{E}\left(\sqrt{j_t}\right) \leq \sqrt{\mathbb{E}\left(j_t\right)}$ that

$$-\mathrm{Tr}\{Q\mathcal{D}[L]\mathbb{E}\left(\rho_t^{\mathrm{c}}\right)\} \geq -\sqrt{2}\left(\|L^\dagger\,|\psi\rangle\,\|^2 + \|L^\dagger L\,|\psi\rangle\,\|\right)\sqrt{\mathbb{E}(j_t)} + \|L\,|\psi\rangle\,\| - |\,\langle\psi|L|\psi\rangle\,|^2.$$

By replacing L with M, the same inequality as above holds for M. Hence, combining the above inequalities with Eq. (3.12) and using the definition

$$J_t = \mathbb{E}(j_t) = 1 - \mathrm{Tr}\{Q\mathbb{E}\left(\rho_t^{\mathrm{c}}\right)\} = 1 - \mathrm{Tr}\left(Q\rho_t\right),$$

we end up with

$$\frac{dJ_t}{dt} \geq -\mathcal{U}\sqrt{J_t} - \mathcal{A}\sqrt{J_t} + \mathcal{E}, \tag{3.14}$$

where

$$\begin{aligned}
\mathcal{A} &= \sqrt{2}\left(\|L^\dagger|\psi\rangle\|^2 + \|L^\dagger L|\psi\rangle\| + \|M^\dagger|\psi\rangle\|^2 + \|M^\dagger M|\psi\rangle\|\right), \\
\mathcal{U} &= 2\bar{u}\sqrt{\langle\psi|H^2|\psi\rangle - \langle\psi|H|\psi\rangle^2}, \quad \bar{u} := \max\{|u_t|\}, \\
\mathcal{E} &= \|L|\psi\rangle\|^2 - |\langle\psi|L|\psi\rangle|^2 + \|M|\psi\rangle\|^2 - |\langle\psi|M|\psi\rangle|^2.
\end{aligned}$$

To have the lower bound of J_t in the limit $t \to \infty$, let us consider the function

$$f(x) = -\mathcal{U}\sqrt{x} - \mathcal{A}\sqrt{x} + \mathcal{E}$$

for $\forall x \in [0,1]$. Clearly, $f(x)$ is a monotonically decreasing function with respect to x. Also, from the Schwarz inequality $\|L|\psi\rangle\|^2 - |\langle\psi|L|\psi\rangle|^2 \geq 0$, and then we have $f(0) = \mathcal{E} \geq 0$. Moreover, $f(1) = \mathcal{E} - \mathcal{A} - \mathcal{U} \leq 0$ holds because

$$\begin{aligned}
\|L|\psi\rangle\|^2 = \mathrm{Tr}(L^\dagger LQ) &= \frac{1}{2}\{\mathrm{Tr}[(L^\dagger LQ)^\dagger Q] + \mathrm{Tr}[Q^\dagger(L^\dagger LQ)]\} \\
&\leq \|L^\dagger LQ\|_{\mathrm{F}}\|Q\|_{\mathrm{F}} = \|L^\dagger LQ\|_{\mathrm{F}} = \|L^\dagger L|\psi\rangle\|,
\end{aligned}$$

which clearly leads to $\mathcal{E} - \mathcal{A} \leq 0$ and hence $\mathcal{E} - \mathcal{A} - \mathcal{U} \leq 0$. In what follows, we consider the case $\mathcal{E} > 0$. Then, from the above properties of $f(x)$, the equation $f(J_*) = 0$ has a unique solution J_* in (0.1]. Now suppose that $J_\tau < J_*$ at a given driving time τ, and then the inequality (3.14) leads to

$$\begin{aligned}
\left.\frac{dJ_t}{dt}\right|_{t=\tau} &\geq -\mathcal{U}\sqrt{J_t} - \mathcal{A}\sqrt{J_t} + \mathcal{E} \\
&> -\mathcal{U}\sqrt{J_*} - \mathcal{A}\sqrt{J_*} + \mathcal{E} = 0.
\end{aligned}$$

This inequality means that J_t locally increases in time for $t \geq \tau$. Because this argument is true for any τ such that the inequality $J_\tau < J_*$ holds, J_t increases until J_t coincides with J_*, i.e., $\lim_{t\to\infty} J_t = J_*$. On the other hand, for the range such that $J_\tau \geq J_*$, the inequality (3.14) is nothing to do with the local time evolution of J_t for $t \geq \tau$. Consequently, in the long-time limit we have

$$\lim_{t\to\infty} J_t \geq J_* = \left(\frac{\mathcal{E}}{\mathcal{A}+\mathcal{U}}\right)^2.$$

Note that the inequality is valid for the case $\mathcal{E} = 0$ as well.

Next we prove that $J_t \geq J_*$ holds for all $t \in [t_0, \infty)$ if the initial value J_{t_0} is bigger than J_*. For the proof we use the following Lemma; see e.g., [64].

Lemma 3.1: *Consider the real-valued one-dimensional ordinary differential equation*

$$\frac{dx(t)}{dt} = f(x(t)), \quad t \in [t_0, \infty).$$

If $dx_1(t)/dt \leq f(x_1(t))$ *and* $f(x_2(t)) \leq dx_2(t)/dt$ *for* $\forall t \in [t_0, \infty)$ *hold for the initial values satisfying* $x_1(t_0) \leq x_2(t_0)$*, then* $x_1(t) \leq x_2(t)$ *holds for all* $t \in [t_0, \infty)$.

Proof of Lemma 3.1 A contradiction argument will be used. Suppose that there exists $t \in [t_0, \infty)$ such that $x_1(t) > x_2(t)$. Then, because $x_1(t_0) \leq x_2(t_0)$, there exists $T \geq t_0$ satisfying $x_1(T) = x_2(T)$. Moreover, there exists $h > 0$ such that $x_1(T + h) > x_2(T + h)$ holds. Hence,

$$\begin{aligned} \left.\frac{dx_1(t)}{dt}\right|_{T+0} &= \lim_{h \to +0} \frac{x_1(T+h) - x_1(T)}{h} \\ &> \lim_{h \to +0} \frac{x_2(T+h) - x_2(T)}{h} = \left.\frac{dx_2(t)}{dt}\right|_{T+0}. \end{aligned}$$

Then, from the assumption of Lemma 3.1

$$f(x_1(T)) \geq \left.\frac{dx_1(t)}{dt}\right|_{T+0} > \left.\frac{dx_2(t)}{dt}\right|_{T+0} \geq f(x_2(T)).$$

This is a contradiction to $x_1(T) = x_2(T)$. Therefore, $x_1(t) \leq x_2(t)$ holds for all $t \in [t_0, \infty)$. (Q.E.D)

Let us apply Lemma 3.1 to the case $f(x) = -\mathcal{U}\sqrt{x} - \mathcal{A}\sqrt{x} + \mathcal{E}$. Assuming that $x_1(t_0) = J_* = \{\mathcal{E}/(\mathcal{A} + \mathcal{U})\}^2$, we have $dx_1(t)/dt = f(x_1(t)) = 0$ and $x_1(t) = x_1(t_0) = J_*$ for all $t \in [t_0, \infty)$. Also, we take $x_2(t) = J(t)$, which satisfies the inequality (3.12), i.e., $dx_2(t)/dt \geq f(x_2(t))$. Thus, from Lemma 3.1, if $J_* = x_1(t_0) \leq x_2(t_0) = J(t_0)$, then $J_* = x_1(t) \leq x_2(t) = J_t$ for all $t \in [t_0, \infty)$. That is, we obtain

$$J_t \geq J_* = \left(\frac{\mathcal{E}}{\mathcal{A} + \mathcal{U}}\right)^2, \quad \forall t \in [t_0, \infty).$$

This is end of the proof of Theorem 3.1. (Q.E.D)

That is to say, J_* gives a fundamental lower bound on how close the controlled quantum state can be driven to or preserved around a target state under decoherence. Below we list some notable features of J_*.

Remark 3.1: Theorem 3.1 is applicable to a general Markovian open quantum system driven by any types of control method such as the MBF or reservoir engineering.

Remark 3.2: J_* is explicitly conputable, once the system operators and the target state $|\psi\rangle$ are assigned. Thus, there is no need to solve any equation.

Remark 3.3: J_* is monotonically decreasing with respect to the control magnitude $\bar{u}$.

Remark 3.4: If $|\psi\rangle$ is far away from the eigenstate of the operators L and M, then J_* becomes bigger. Conversely, if and only if $|\psi\rangle$ is identical to a common eigenvector of L and M, $J_* = 0$. It is an important fact is that J_* can be used to characterize a target state that is easy (or hard) to approach by some control under decoherence. Namely, a state $|\psi\rangle$ with relatively small value of J_* can be a better candidate as the target, although in general J_* is not achievable. In contrast, we can say that the state $|\psi\rangle$ with a large value of J_* should not be chosen as the target. In the next section, we study several control problems with special notion with respect to this point.

Remark 3.5: Theorem 3.1 can be generalized to the case where the system is driven by multiple environment channels, measurement probes, and control Hamiltonian; If the system dynamics is validity modeled by the SME

$$d\rho_t^{\rm c} = -i\left[\sum_j u_{j,t}H_j, \rho_t^{\rm c}\right]dt + \sum_j \mathcal{D}[L_j]\rho_t^{\rm c}dt + \sum_j \mathcal{D}[M_j]\rho_t^{\rm c}dt + \sum_j \mathcal{H}[L_j]\rho_t^{\rm c}dW_t,$$

we find that the lower bound is given by $J_* = \mathcal{E}^2/(\mathcal{A}+\mathcal{U})^2$ with

$$\begin{aligned}
\mathcal{A} &= \sqrt{2}\sum_j(\|L_j^\dagger|\psi\rangle\|^2 + \|L_j^\dagger L_j|\psi\rangle\|) + \sqrt{2}\sum_j(\|M_j^\dagger|\psi\rangle\|^2 + \|M_j^\dagger M_j|\psi\rangle\|),\\
\mathcal{U} &= 2\sum_j \bar{u}_j\sqrt{\langle\psi|H_j^2|\psi\rangle - \langle\psi|H_j|\psi\rangle^2}, \quad \bar{u}_j = \max\{|u_{j,t}|\},\\
\mathcal{E} &= \sum_j(\|L_j|\psi\rangle\|^2 - |\langle\psi|L_j|\psi\rangle|^2) + \sum_j(\|M_j|\psi\rangle\|^2 - |\langle\psi|M_j|\psi\rangle|^2).
\end{aligned}$$

Remark 3.6: Theorem 3.1 can be extended to the case where the target state is mixed by redefining the cost (3.9) as $j_t' = 1 - {\rm Tr}\left(Q\rho_t^{\rm c}\right)/{\rm Tr}(Q^2)$. Then we obtain the generalized lower bound:

$$J_\infty' \geq J_*'(Q) := \frac{1}{2{\rm Tr}(Q^2)}\left\{2\left(\frac{\mathcal{E}'}{\mathcal{A}'+\mathcal{U}'}\right)^2 + {\rm Tr}(Q^2) - 1\right\}, \tag{3.15}$$

where

$$\mathcal{A}' = \sqrt{2}\left(\sqrt{\mathrm{Tr}[(L^\dagger QL)^2]} + \sqrt{\mathrm{Tr}[(L^\dagger L)^2Q^2]} + \sqrt{\mathrm{Tr}[(M^\dagger QM)^2]} + \sqrt{\mathrm{Tr}[(M^\dagger MQ)^2]}\right),$$
$$\mathcal{U}' = 2\bar{u}\sqrt{\mathrm{Tr}(H^2Q^2) - \mathrm{Tr}[(HQ)^2]}, \quad \bar{u} = \max\{|u_t|\},$$
$$\mathcal{E}' = \mathrm{Tr}(L^\dagger LQ^2) - \mathrm{Tr}(L^\dagger QLQ) + \mathrm{Tr}(M^\dagger MQ^2) - \mathrm{Tr}(M^\dagger QMQ).$$

Proof of Remark 3.6 By replacing j_t in the proof of Theorem 3.1 with j'_t, (3.15) can be proved. The infinitesimal change of j'_t is given by

$$dj'_t = \frac{1}{\mathrm{Tr}(Q^2)}\left(\mathrm{Tr}\left(iu_t[Q,H]\rho_t^{\mathrm{c}}\right)dt - \mathrm{Tr}\left[Q\mathcal{D}[L]\rho_t^{\mathrm{c}}\right]dt - \mathrm{Tr}\left[Q\mathcal{D}[M]\rho_t^{\mathrm{c}}\right]dt - \mathrm{Tr}\left[Q\mathcal{H}[L]\rho_t^{\mathrm{c}}\right]dW_t\right). \tag{3.16}$$

Taking the expectation,

$$\frac{d\mathbb{E}\left(j'_t\right)}{dt} = \frac{1}{\mathrm{Tr}(Q^2)}\left(\mathrm{Tr}\{i[Q,H]\mathbb{E}\left(u_t\rho_t^{\mathrm{c}}\right)\} - \mathrm{Tr}\{Q\mathcal{D}[L]\mathbb{E}\left(\rho_t^{\mathrm{c}}\right)\} - \mathrm{Tr}\{Q\mathcal{D}[M]\mathbb{E}\left(\rho_t^{\mathrm{c}}\right)\}\right). \tag{3.17}$$

To bound the rightmost side of Eq. (3.16), we introduce the distance between ρ_t^{c} and Q:

$$\begin{aligned}
\|\rho_t^{\mathrm{c}} - Q\|_{\mathrm{F}} &= \sqrt{\mathrm{Tr}[\left(\rho_t^{\mathrm{c}} - Q\right)^2]} \\
&= \sqrt{\mathrm{Tr}[(\rho_t^{\mathrm{c}})^2 - 2\rho_t^{\mathrm{c}}Q + Q^2]} \\
&\leq \sqrt{1 - 2\mathrm{Tr}\left(\rho_t^{\mathrm{c}}Q\right) + \mathrm{Tr}(Q^2)} \\
&\leq \sqrt{1 - \mathrm{Tr}(Q^2) + 2\mathrm{Tr}(Q^2)j'_t}.
\end{aligned} \tag{3.18}$$

Setting $\bar{u} := \max\{|u_t|\}$, the first term of the rightmost side of Eq. (3.16) is bounded as

$$\begin{aligned}
\mathrm{Tr}\left(iu_t[Q,H]\rho_t^{\mathrm{c}}\right) &\geq -\bar{u}\|i[H,Q]\|_{\mathrm{F}}\|\rho_t^{\mathrm{c}} - Q\|_{\mathrm{F}} \\
&= -\bar{u}\sqrt{\mathrm{Tr}\{(iHQ - iQH)^2\}}\sqrt{1 - \mathrm{Tr}(Q^2) + 2\mathrm{Tr}(Q^2)j'_t} \\
&= -2\bar{u}\sqrt{\mathrm{Tr}(H^2Q^2) - \mathrm{Tr}[(HQ)^2]}\sqrt{1 - \mathrm{Tr}(Q^2) + 2\mathrm{Tr}(Q^2)j'_t}.
\end{aligned}$$

Then, due to the relation $\mathbb{E}(\sqrt{a + bj_t}) \leq \sqrt{\mathbb{E}(a + bj_t)}$ (a, $b > 0$) we have

$$\mathrm{Tr}\{i[Q,H]\mathbb{E}\left(u_t\rho_t^{\mathrm{c}}\right)\} \geq -2\bar{u}\sqrt{\mathrm{Tr}(H^2Q^2) - \mathrm{Tr}[(HQ)^2]}\sqrt{1 - \mathrm{Tr}(Q^2) + 2\mathrm{Tr}(Q^2)\mathbb{E}(j'_t)}.$$

Next, the second term on the rightmost side of Eq. (3.16) can be bounded as

$$\begin{aligned}
-\mathrm{Tr}\left(Q\mathcal{D}[L]\rho_t^{\mathrm{c}}\right) &\geq -\|L^\dagger QL\|_{\mathrm{F}}\|\rho_t^{\mathrm{c}} - Q\|_{\mathrm{F}} - \|L^\dagger LQ\|_{\mathrm{F}}\|\rho_t^{\mathrm{c}} - Q\|_{\mathrm{F}} + \mathrm{Tr}(L^\dagger LQ^2) - \mathrm{Tr}(L^\dagger QLQ) \\
&\geq -\left(\sqrt{\mathrm{Tr}[(L^\dagger QL)^2]} + \sqrt{\mathrm{Tr}[(L^\dagger LQ)^\dagger(L^\dagger LQ)]}\right)\sqrt{1 - \mathrm{Tr}(Q^2) + 2\mathrm{Tr}(Q^2)j'_t} \\
&\quad + \mathrm{Tr}(L^\dagger LQ^2) - \mathrm{Tr}(L^\dagger QLQ) \\
&\geq -\left(\sqrt{\mathrm{Tr}[(L^\dagger QL)^2]} + \sqrt{\mathrm{Tr}[(L^\dagger L)^2Q^2]}\right)\sqrt{1 - \mathrm{Tr}(Q^2) + 2\mathrm{Tr}(Q^2)j'_t} \\
&\quad + \mathrm{Tr}(L^\dagger LQ^2) - \mathrm{Tr}(L^\dagger QLQ).
\end{aligned}$$

Then,

$$-\mathrm{Tr}\{Q\mathcal{D}[L]\mathbb{E}\left(\rho_t^{\mathrm{c}}\right)\} \geq -\left(\sqrt{\mathrm{Tr}[(L^\dagger QL)^2]}+\sqrt{\mathrm{Tr}[(L^\dagger L)^2Q^2]}\right)\sqrt{1-\mathrm{Tr}(Q^2)+2\mathrm{Tr}(Q^2)\mathbb{E}\left(j_t'\right)} + \mathrm{Tr}(L^\dagger LQ^2)-\mathrm{Tr}(L^\dagger QLQ).$$

The same inequality also holds for M. From the above inequalities, the differential of the cost function $J_t' = \mathbb{E}\left(j_t'\right) = 1-\mathrm{Tr}\{Q\mathbb{E}\left(\rho_t^{\mathrm{c}}\right)\}/\mathrm{Tr}(Q^2)$ with respect to time is bounded from below as

$$\frac{dJ_t'}{dt} \geq \frac{1}{\mathrm{Tr}(Q^2)}\left(-\mathcal{U}'\sqrt{1-\mathrm{Tr}(Q^2)+2\mathrm{Tr}(Q^2)J_t'}-\mathcal{A}'\sqrt{1-\mathrm{Tr}(Q^2)+2\mathrm{Tr}(Q^2)J_t'}+\mathcal{E}'\right), \tag{3.19}$$

where

$$\mathcal{A}' = \sqrt{2}\left(\sqrt{\mathrm{Tr}[(L^\dagger QL)^2]}+\sqrt{\mathrm{Tr}[(L^\dagger L)^2Q^2]}+\sqrt{\mathrm{Tr}[(M^\dagger QM)^2]}+\sqrt{\mathrm{Tr}[(M^\dagger MQ)^2]}\right),$$
$$\mathcal{U}' = 2\bar{u}\sqrt{\mathrm{Tr}(H^2Q^2)-\mathrm{Tr}[(HQ)^2]},\quad \bar{u}=\max\{|u_t|\},$$
$$\mathcal{E}' = \mathrm{Tr}(L^\dagger LQ^2)-\mathrm{Tr}(L^\dagger QLQ)+\mathrm{Tr}(M^\dagger MQ^2)-\mathrm{Tr}(M^\dagger QMQ).$$

The inequality (3.19) has the same form as (3.14), and hence we have

$$\begin{aligned}\frac{dJ_t'}{dt} &\geq \frac{1}{\mathrm{Tr}(Q^2)}\left(-\mathcal{U}'\sqrt{1-\mathrm{Tr}(Q^2)+2\mathrm{Tr}(Q^2)J_t'}-\mathcal{A}'\sqrt{1-\mathrm{Tr}(Q^2)+2\mathrm{Tr}(Q^2)J_t'}+\mathcal{E}'\right)\\ &\geq \frac{1}{\mathrm{Tr}(Q^2)}\left(-\mathcal{U}'\sqrt{1-\mathrm{Tr}(Q^2)+2\mathrm{Tr}(Q^2)J_*'}-\mathcal{A}'\sqrt{1-\mathrm{Tr}(Q^2)+2\mathrm{Tr}(Q^2)J_*'}+\mathcal{E}'\right)\\ &= 0.\end{aligned}$$

Consequently, the derivation of (3.15) is completed. (Q.E.D)

3.3 Examples

3.3.1 Qubit

The first example is a qubit system. Let the target be a Bloch representation

$$|\psi\rangle = [\cos\theta,\ e^{i\varphi}\sin\theta]^\top,\ (0\leq\theta\leq\pi/2,\ 0\leq\varphi\leq 2\pi). \tag{3.20}$$

Here we consider the system operators

$$H=\sigma_y,\ L=\sqrt{\kappa}\sigma_z,\ M=\sqrt{\gamma}\sigma_-. \tag{3.21}$$

This is a typical characterization of MBF control [10, 24, 25, 26, 27]; L represents the controllable dispersive coupling between the qubit and the probe field, which allows for continuous measurement the qubit state by monitoring the output field, and thus performing a MBF control through the Hamiltonian u_tH. In the ideal setting (i.e., $\gamma=0$),

this MBF realizes deterministic and selective steering of the spin state to $|0\rangle$ or $|1\rangle$ for a two-level system. In this setting, the lower bound is given as follows:

$$\begin{aligned}
\mathcal{A} &= \sqrt{2}\left(\|L^\dagger|\psi\rangle\|^2 + \|L^\dagger L|\psi\rangle\| + \|M^\dagger|\psi\rangle\|^2 + \|M^\dagger M|\psi\rangle\|\right) \\
&= \sqrt{2}\left(\kappa + \gamma\sin^2\theta + \gamma\cos\theta\right), \\
\mathcal{U} &= 2\bar{u}\sqrt{\langle\psi|H^2|\psi\rangle - \langle\psi|H|\psi\rangle^2} \\
&= 2\bar{u}\sqrt{1-\sin^2 2\theta\sin^2\varphi}, \\
\mathcal{E} &= \|L|\psi\rangle\|^2 - |\langle\psi|L|\psi\rangle|^2 + \|M|\psi\rangle\|^2 - |\langle\psi|M|\psi\rangle|^2 \\
&= \kappa\sin^2 2\theta + \gamma\cos^4\theta.
\end{aligned}$$

Then we obtain the lower bound

$$J_*(|\psi\rangle) = \frac{1}{2}\left[\frac{\kappa\sin^2 2\theta + \gamma\cos^4\theta}{2\kappa + \gamma(\sin^2\theta + \cos\theta) + \bar{u}\sqrt{2-2\sin^2 2\theta\sin^2 2\varphi}}\right]^2. \tag{3.22}$$

First, we consider the case $\kappa = 0$. In this case, the system obeys the master equation $d\rho_t/dt = -i[u_t\sigma_y, \rho_t] + \mathcal{D}[\sqrt{\gamma}\sigma_-]\rho_t$ driven by the open-loop control input u_t satisfying $|u_t| \leq \bar{u}$ and the energy decay. Figure 3.4 (a) shows the above lower bound J_* when $\gamma = 1$ and $\varphi = 0$. Clearly, J_* takes maximum at $|\psi\rangle = |0\rangle$ and zero at $|\psi\rangle = |1\rangle$. This implies that $|0\rangle$ is the most difficult state to stabilize, while $|1\rangle$ can be stabilized exactly. Actually, these implications are true, as can be analytically verified by solving the above master equation; that is, $|1\rangle$ corresponds to the steady state of the evolution. On the other hand, if $\kappa = 1$, as depicted in Fig. 3.4 (b), J_* at around $\theta = 0$ drastically decreases compared to the case $\kappa = 0$. This result is reasonable because, as demonstrated in Section 3.1, the dispersive coupling represented by $L = \sqrt{\kappa}\sigma_z$ in the ideal setting of MBF makes possible to deterministically stabilize $|0\rangle$. As a result, J_* takes the maximal value at around $\theta = 0.6$, implying that $|+\rangle$ is the most difficult to stabilize.

It is also an interesting problem how the actual tightness of the lower bound J_* is. Here we compare J_* to the actual distance; the steady value J_∞ and the minimal value $J_{\min}$ achieved by a special type of MBF control. We here take the control input $u_t = -2\kappa x_t$ given in Section 3.1 in the numerical simulation. We compute J_∞ and $J_{\min}$ by averaging 300 sample points of conditional state ρ_t^{c} for the case $|\psi\rangle = |0\rangle$ with several value of the ratio γ/κ. Figure 3.4 (c) shows that the gap between J_* and J_∞ is large and hence J_* is not tight in this case. This is maybe because J_* works as a lower bound for $J_{\min}$, as shown in Fig. 3.4 (d). Thereby, a control strategy to reduce the gap and eventually prepare a state close to $|0\rangle$ is a remaining work.

3.3.2 Two-qubits

Here we study a two-qubit system under decoherence. First, we introduce the following Bell states, which are particularly used in the scenario of quantum information science

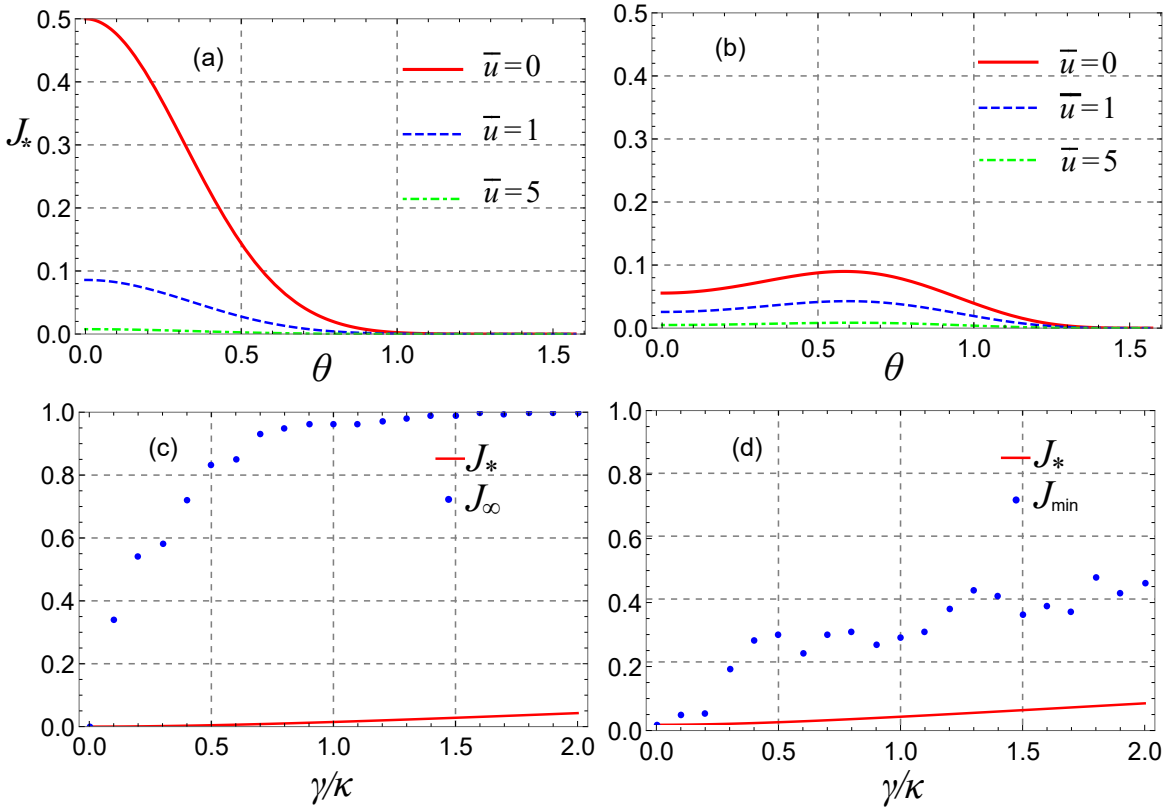

Fig. 3.4: Lower bound J_* as a function of θ for (a) $\kappa = 0$, and (b) $\kappa = 1$ in units of $\gamma = 1$. Plots of (c) J_* and J_∞ and (d) J_* and $J_{\min}$ as a function of γ/κ with u_t a special type of MBF control input. Reprinted figure from [104, DOI: 10.1103/PhysRevA.99.052347]. Creative Commons Attribution 4.0 International license. Copyright 2019 by K. Kobayashi and N. Yamamoto.

[49]:

$$|\Phi^{\pm}\rangle = \frac{1}{\sqrt{2}}(|0\rangle\,|0\rangle \pm |1\rangle\,|1\rangle),$$
$$|\Psi^{\pm}\rangle = \frac{1}{\sqrt{2}}(|1\rangle\,|0\rangle \pm |0\rangle\,|1\rangle).$$

The question here is which states is the best one controllable by any open-loop control unde the assumption that $M = 0$. As discussed in the qubit case, the lower bound J_* gives a rough answer to this question. In particular, we employ the collective decay process modeled by

$$M = \sqrt{\gamma}(\sigma_- \otimes I + I \otimes \sigma_-), \tag{3.23}$$

which globally acts two-atoms. Then, for instance, for the case $|\Phi^+\rangle$,

$$\mathcal{A} = \sqrt{2}(\|L^\dagger |\Phi^+\rangle\|^2 + \|L^\dagger L |\Phi^+\rangle\|) = (2+\sqrt{2})\gamma,$$
$$\mathcal{E} = \|M |\Phi^+\rangle\|^2 - |\langle\Phi^+|M|\Phi^+\rangle|^2 = \gamma.$$

Thereby, together with the other Bell states, the lower bounds are calculated as

$$J_*(|\Phi^\pm\rangle) = \frac{\gamma^2}{[(2+\sqrt{2})\gamma + \mathcal{U}]^2},$$
$$J_*(|\Psi^+\rangle) = \frac{4\gamma^2}{(4\sqrt{2}\gamma + \mathcal{U})^2},$$
$$J_*(|\Psi^-\rangle) = 0.$$

Now, for fair comparison, we assumed that a control Hamiltonian H has the same magnitude of $\mathcal{U}$ appearing in each J_* for each states. Hence, the Bell states have different reachability properties under realistic decoherence, although their amount of entanglement are same. Clearly, $|\Psi^-\rangle$ is the best target state in our case. In fact, $|\Psi^-\rangle$ is identical to the dark state of M and is accessible. Also, for all γ and $\mathcal{U}$, $J_*(|\Phi^\pm\rangle) < J_*(|\Psi^+\rangle)$ holds. This means that $|\Psi^+\rangle$ is the most fragile state against the collective decay process. On the other hand, if each qubit is subjected to a local decay modeled by

$$M_1 = \sqrt{\gamma}\sigma_- \otimes I, \quad M_2 = \sqrt{\gamma} I \otimes \sigma_-, \tag{3.24}$$

we have the same bound for all Bell states as

$$J_* = \left(\frac{\gamma}{(2+\sqrt{2})\gamma + \mathcal{U}}\right)^2.$$

That is, in this case there is no difference between the Bell states, in terms of the reachability property.

Next, we focus on an interesting example of MBF setup; suppose that two qubits are symmetric, which is identical to a qutrit system composed of three distinguishable states

$$|E\rangle = \begin{bmatrix} 1 \\ 0 \\ 0 \end{bmatrix}, \ |S\rangle = \begin{bmatrix} 0 \\ 1 \\ 0 \end{bmatrix}, \ |G\rangle = \begin{bmatrix} 0 \\ 0 \\ 1 \end{bmatrix}, \tag{3.25}$$

where $|S\rangle$ corresponds to the entangled state between two qubits. Here the target state is described by the pure state

$$|\psi\rangle = [\sin(\theta/2)\cos(\varphi/2),\ \cos(\theta/2),\ \sin(\theta/2)\sin(\varphi/2)]^\top,$$

where $0 \le \theta, \varphi \le \pi$. The MBF setup considered here is given by

$$H = \frac{1}{\sqrt{2}} \begin{bmatrix} 0 & -i & 0 \\ i & 0 & -i \\ 0 & i & 0 \end{bmatrix}, \ L = \sqrt{\kappa} \begin{bmatrix} 1 & 0 & 0 \\ 0 & 0 & 0 \\ 0 & 0 & -1 \end{bmatrix}, \ M = \sqrt{\gamma} \begin{bmatrix} 0 & 0 & 0 \\ 1 & 0 & 0 \\ 0 & 1 & 0 \end{bmatrix}.$$

The continuous measurement through the system-probe coupling represented by L ideally induces the probabilistic state change to $|E\rangle$, $|S\rangle$, or $|G\rangle$. The decoherence process M represents the ladder-type decay $|E\rangle \to |S\rangle \to |G\rangle$. In the setting the lower bound $J_*(|\psi\rangle) = \mathcal{E}^2/(\mathcal{A}+\mathcal{U})^2$ can be explicitly given with

$$\mathcal{A} = \sqrt{2}\kappa\left(\sin^2\frac{\theta}{2} + \sin\frac{\theta}{2}\right) + \sqrt{2}\gamma\left(\cos^2\frac{\theta}{2} + \sin^2\frac{\theta}{2}\sin^2\frac{\varphi}{2} + \sqrt{\sin^2\frac{\theta}{2}\cos^2\frac{\varphi}{2} + \cos^2\frac{\theta}{2}}\right),$$
$$\mathcal{U} = \sqrt{2}\bar{u}\sqrt{1+\cos^2\frac{\theta}{2} - \sin^2\frac{\theta}{2}\sin\varphi},$$
$$\mathcal{E} = \kappa\left(\sin^2\frac{\theta}{2} + \sin\frac{\theta}{2}\right) + \gamma\left(\sin^2\frac{\theta}{2}\sin^2\frac{\varphi}{2} + \cos^2\frac{\theta}{2} + \sqrt{\sin^2\frac{\theta}{2}\cos^2\frac{\varphi}{2} + \cos\frac{\theta}{2}}\right).$$

Figure 3.5 illustrates J_* as a function of (θ, φ). As in the qubit case, $J_*(|\psi\rangle)$ takes the maximum at $|E\rangle$ when $\kappa = 0$ [Fig. 3.5 (a)], while $J_*(|E\rangle)$ can be drastically lowered when $\kappa > 0$ [Fig. 3.5 (b)]; that is the measurement allows for combating the decoherence and have a chance to closely approach $|E\rangle$ via MBF. However, this strategy does not work for the case of $|S\rangle$, because $J_*(|\psi\rangle)$ is independent of κ at $\theta = 0$. In general, if the target $|\psi\rangle$ is an eigenstate of $L = L^\dagger$ with a small eigenvalue, then the term related to M takes a small value as well in $\mathcal{A}$ and zero in $\mathcal{E}$. In particular, for the dark state satisfying $M|\psi\rangle = 0$, the lower bound $J_*(|\psi\rangle)$ is independent of M. Hence, the measurement does not at all work for decreasing J_* in this case. In contrast, for an eigenstate of M with a large eigenvalue, i.e., the excited state $|E\rangle$, the term related to L in $\mathcal{A}$ takes a large value and eventually J_* becomes small. This implies that we may closely approach such a state via some MBF control even under decoherence.

3.3.3 N-qubits

Here we study an atomic ensemble composed of N identical qubits. The basic operators for describing this system are the angular momentum operator J_i $(i = x, y, z)$ satisfying the CCR, e.g., $[J_x, J_y] = iJ_z$, the magnitude $J^2 = J_x^2 + J_y^2 + J_z^2$, and the ladder-type operator $J_- = J_x - iJ_y$. Here we focus on the Dicke state $|l, m\rangle$, which are the common eigenstates of J_z and J defined by

$$J_z|l,m\rangle = m|l,m\rangle,$$
$$J^2|l,m\rangle = l(l+1)|l,m\rangle.$$

In quantum physics, m and l are *magnetic quantum number* and *azimuthal quantum number*, respectively, and hence $|m| \le l \le N/2$ holds [57]. Recall, if N is even, that $|N/2, N/2\rangle$ corresponds to the coherent spin state (CSS) $|0\rangle^{\otimes N}$, i.e., the separable state with all the spins pointing along the z axis, while $|N/2, 0\rangle$ is highly entangled. It was proven in [9, 15] that, for the ideal system subjected to the SME (3.2) with $(H, L, M) = (J_y, \sqrt{\kappa}J_z, 0)$, the Dicke state $|N/2, 0\rangle$ for arbitrary $m \in [-N/2, N/2]$ can be deterministically prepared by

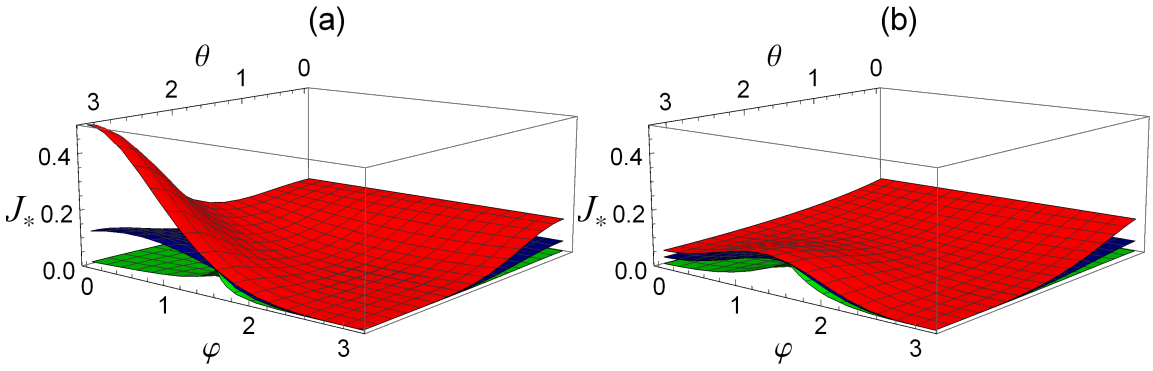

Fig. 3.5: Lower bound $J_*(|\psi\rangle)$ as a function of (θ, φ) for (a) $\kappa = 0$ and (b) $\kappa = 1$, in units of $\gamma = 1$. In both cases the curved surface corresponds to $\bar{u} = 0, 1, 5$ from top to bottom. Reprinted figure from [104, DOI: 10.1103/PhysRevA.99.052347]. Creative Commons Attribution 4.0 International license. Copyright 2019 by K. Kobayashi and N. Yamamoto.

an appropriate MBF control. Now using the lower bound J_*, we can evaluate how much this MBF control could work effectively under decoherence. Let $M = \sqrt{\gamma} J_-$, where

$$J_\pm |l, m\rangle = \sqrt{(l \mp m)(l \pm m + 1)}\, |l, m \pm 1\rangle$$

and

$$\begin{aligned} J_+ J_- &= (J_x + iJ_y)(J_x - iJ_y) \\ &= J_x^2 + J_y^2 - iJ_x J_y + iJ_y J_x \\ &= J^2 - J_z^2 - i[J_x, J_y] \\ &= J^2 - J_z^2 + J_z, \end{aligned}$$

and likewise $J_- J_+ = J^2 - J_z^2 - J_z$. Then we have

$$\begin{aligned} \mathcal{A} &= \sqrt{2}\left(\kappa \| J_z |l, m\rangle \|^2 + \kappa \| J_z^2 |l, m\rangle \| + \gamma \| J_-^\dagger |l, m\rangle \|^2 + \gamma \| J_-^\dagger J_- |l, m\rangle \|\right) \\ &= \sqrt{2}[\kappa m^2 + \kappa m^2 + \gamma\{l(l+1) - m^2 - m\} + \gamma\{l(l+1) - m^2 + m\}] \\ &= \sqrt{2}\{2\kappa m^2 + 2\gamma(l^2 + l - m^2)\}, \\ \mathcal{U} &= \bar{u}\sqrt{\| (J_-^\dagger - J_-) |l, m\rangle \|^2 - |\langle l, m| (J_-^\dagger - J_- |l, m\rangle|^2}, \\ &= \bar{u}\sqrt{\{(l-m)(l+m+1) + (l+m)(l-m+1)\}} \\ &= \sqrt{2}\bar{u}\sqrt{l^2 + l - m^2}, \\ \mathcal{E} &= \kappa \| J_z |l, m\rangle \|^2 - \kappa |\langle l, m| J_z |l, m\rangle|^2 + \gamma \| J_- |l, m\rangle \|^2 - \gamma |\langle l, m| J_- |l, m\rangle|^2 \\ &= \kappa m^2 - \kappa m^2 + \gamma(l+m)(l-m+1) \\ &= \gamma(l^2 + l - m^2 + m). \end{aligned}$$

Then the lower bound for $|\psi\rangle = |l, m\rangle$ is

$$J_*(|l,m\rangle) = \frac{1}{2}\left[\frac{\gamma(l^2+l-m^2+m)}{2\kappa m^2 + 2\gamma(l^2+l-m^2) + \bar{u}\sqrt{l^2+l-m^2}}\right]^2.$$

Figure 3.6 (a) shows the case of $N = 20$ atoms, for the target ideal Dicke state $|\psi\rangle = |10, m\rangle$. As in the above examples, we find that the measurement remarkably decreases J_* especially for the state with large $|m|$, for instance, the CSS $|10, 10\rangle$ is almost unaffected by the measurement. In fact, in general, for a Dicke state with large $|m| \lesssim l = N/2$, such as the CSS, the measurement term proportional to κ is dominant in the denominator of J_*, while for highly entangled Dicke states with $m \sim 0$ the decoherence term proportional to γ becomes dominant. Note in particular that

$$J_*(|N/2, N/2\rangle) = \left[\frac{\sqrt{2}\gamma N}{\kappa N^2 + 2\gamma N + \bar{u}\sqrt{2N}}\right]^2,$$
$$J_*(|N/2, 0\rangle) = \frac{1}{2}\left[\frac{\gamma(N^2+2N)}{2\gamma N^2 + 4\gamma N + 2\bar{u}\sqrt{N^2+2N}}\right]^2.$$

Hence, if an ensemble is sufficiently large $N \to \infty$, we have $J_*(|N/2, N/2\rangle) \to 0$ and $J_*(|N/2, 0\rangle) \to 1/8$. Here we emphasize that this fundamental bound $J_* = 1/8$ is applied to all highly entangled Dicke states satisfying $m \sim 0$ and $l \lesssim N/2 \gg 1$. That is, while no limitation appears for the case of the CSS due to the measurement effect, preparing those highly entangled Dicke states is severely prohibited, without respect to the use of measurement and control. This result means that, in practice, there exists a strict limitation in quantum magnetmetry that utilizes a highly entangled Dicke states [52].

Another important subject in quantum metrology is the frequency standard, where as a resource the Greenberger-Horne-Zeilinger (GHZ) state

$$|\mathrm{GHZ}\rangle = \frac{|0\rangle^{\otimes N} + |1\rangle^{\otimes N}}{\sqrt{2}} \tag{3.26}$$

is used for estimating the atomic frequency, over the standard quantum limit attained by employing the product state [58]

$$|+\rangle^{\otimes N} = \left(\frac{|0\rangle + |1\rangle}{\sqrt{2}}\right)^{\otimes N}. \tag{3.27}$$

The essential issue of this technique is that the estimation performance is severely limited due to the dephasing noise [59, 60], which affects both the state preparation process and the free-precession process. Now, using the lower bound J_*, we can characterize the performance degradation occurring in the former process. In the usual setup where no continuous monitoring is performed, the actual system is driven by the master equation

$d\rho_t/dt = -i[H, \rho_t] + \mathcal{D}[M]\rho_t$, where the dephasing noise M is represented by

$$\begin{aligned} M &= \sqrt{\gamma} J_z = \sqrt{\gamma} \sum_{j=1}^{N} \sigma_z^{(j)} \\ &= \sqrt{\gamma} \left(\sigma_z^{(1)} \otimes I \otimes I \cdots I + \cdots + I \otimes I \otimes \cdots \sigma_z^{(N)} \right). \end{aligned}$$

H is a system Hamiltonian representing an appropriate open-loop control. Now, as for the product state

$$M \left|+\right\rangle^{\otimes N} = \sqrt{\gamma} \sum_{j=1}^{N} \left|+\right\rangle \cdots \left|+\right\rangle \left|-\right\rangle \left|+\right\rangle \cdots \left|+\right\rangle$$

holds, where $\left|-\right\rangle = (\left|0\right\rangle - \left|1\right\rangle)/\sqrt{2}$ appears in the jth component. This leads to $\langle+|^{\otimes N} M |+\rangle^{\otimes N} = 0$ and thus

$$\mathcal{E} = \| M \left|+\right\rangle^{\otimes N} \|^2 - |\langle+|^{\otimes N} M |+\rangle^{\otimes N}|^2 = \gamma N.$$

Also, we have

$$M^\dagger M \left|+\right\rangle^{\otimes N} = \gamma \left(N \left|+\right\rangle^{\otimes N} + 2 \sum_{i \neq j} \left|+\right\rangle \cdots \left|-\right\rangle \cdots \left|-\right\rangle \cdots \left|+\right\rangle \right),$$

where $\left|-\right\rangle$ appears only in the ith and jth components ($i \neq j$). Therefore

$$\begin{aligned} \mathcal{A} &= \sqrt{2} \left(\| M^\dagger \left|+\right\rangle^{\otimes N} \|^2 + \| M^\dagger M \left|+\right\rangle^{\otimes N} \| \right) \\ &= \sqrt{2}\gamma N + \sqrt{6N^2 - 4N}\gamma. \end{aligned}$$

On the other hand, with respect to the GHZ state,

$$\begin{aligned} M \left|\mathrm{GHZ}\right\rangle &= M^\dagger \left|\mathrm{GHZ}\right\rangle = \frac{\gamma N (\left|0\right\rangle^{\otimes N} - \left|1\right\rangle^{\otimes N})}{\sqrt{2}}, \\ M^\dagger M \left|\mathrm{GHZ}\right\rangle &= \gamma N \left|\mathrm{GHZ}\right\rangle, \end{aligned}$$

and $\langle \mathrm{GHZ}|M|\mathrm{GHZ}\rangle = 0$, and thus

$$\begin{aligned} \mathcal{A} &= \sqrt{2} \left(\| M^\dagger \left|\mathrm{GHZ}\right\rangle \|^2 + \| L^\dagger M \left|\mathrm{GHZ}\right\rangle \| \right) \\ &= \sqrt{2} \left(\gamma N^2 + \gamma N^2 \right) = 2\sqrt{2}\gamma N^2, \\ \mathcal{E} &= \| M \left|\mathrm{GHZ}\right\rangle \|^2 - | \left\langle \mathrm{GHZ}|M|\mathrm{GHZ}\right\rangle |^2 \\ &= \frac{\gamma}{2} N^2 \| \left|0\right\rangle^{\otimes N} - \left|1\right\rangle^{\otimes N} \|^2 - 0 = \gamma N^2. \end{aligned}$$

Consequently, we end up with

$$\begin{aligned} J_*(\left|+\right\rangle^{\otimes N}) &= \left(\frac{\gamma N}{\sqrt{2}\gamma N + \gamma\sqrt{6N^2 - 4N} + \mathcal{U}} \right)^2, \\ J_*(\left|\mathrm{GHZ}\right\rangle) &= \left(\frac{\gamma N^2}{2\sqrt{2}\gamma N^2 + \mathcal{U}} \right)^2. \end{aligned}$$

Hence, under the assumption that $\mathcal{U}$ is of the order at most $\sqrt{N}$ and N, $J_*(|+\rangle^{\otimes N}) \to 1/(8+4\sqrt{3})$ and $J_*(|\mathrm{GHZ}\rangle) \to 1/8$ in the limit $N \to \infty$, respectively, regardless of the control techniques. From this, it is more difficult to prepare the GHZ state than the product state, and this gap would erase the quantum advantage realized by employing the GHZ state in the ideal setting. In both cases, the estimation performance must be severely limited under decoherence, if the total time taken for state preparation and free-precession process becomes longer; this is why these two processes have to be conducted in as short a time as possible.

3.3.4 Fock state

The last example in this section is the problem of generating an arbitrarily Fock state in an optical cavity. In the setup, in [11, 12, 14], the conditional cavity state obeys the master equation Eq. (3.8) with

$$H = i(a^\dagger - a),\ L = \sqrt{\kappa}a^\dagger a,\ M = \sqrt{\gamma}a,$$

where a and $a^\dagger$ are the annihilation and creation operator, respectively. H is known as a displacement operator moving the state. L is known as the cross Kerr coupling between the cavity field and the probe field. This coupling induces a phase shift on the output probe field that is proportional to the number of photons in the cavity. Hence, by measuring the output probe field, we can obtain the information on the number of photons and get one of the eigenstates of L, that is, a conditional Fock state. In fact, it was proven in the ideal case (i.e., $M = 0$) that one can deterministically steer the state to a target Fock state $|n\rangle$ by choosing a suitable MBF input u_t. M is a typical dissipative process representing the photon leakage caused by the interaction between the probe field and the optical cavity.

Now the lower bound J_* can be used to evaluate the performance of this MBF control under decoherence. Using the relation $a|n\rangle = \sqrt{n}|n-1\rangle$ and $a^\dagger|n\rangle = \sqrt{n+1}|n+1\rangle$, we have

$$\begin{aligned}
\mathcal{A} &= \sqrt{2}\left(\kappa\|a^\dagger a|n\rangle\|^2 + \kappa\|a^\dagger a a^\dagger a|n\rangle\| + \gamma\|a^\dagger|n\rangle\|^2 + \|a^\dagger a|n\rangle\|\right) \\
&= 2\sqrt{2}\kappa n^2 + \sqrt{2}\gamma(2n+1), \\
\mathcal{U} &= 2\bar{u}\sqrt{\|i(a^\dagger - a)|n\rangle\|^2 - \langle n|i(a^\dagger - a)|n\rangle^2} \\
&= 2\bar{u}\sqrt{2n+1}, \\
\mathcal{E} &= \kappa\|a^\dagger a|n\rangle\|^2 - \kappa|\langle n|a^\dagger a|n\rangle|^2 + \gamma\|a|n\rangle\|^2 - \gamma|\langle n|a|n\rangle|^2 \\
&= \gamma n.
\end{aligned}$$

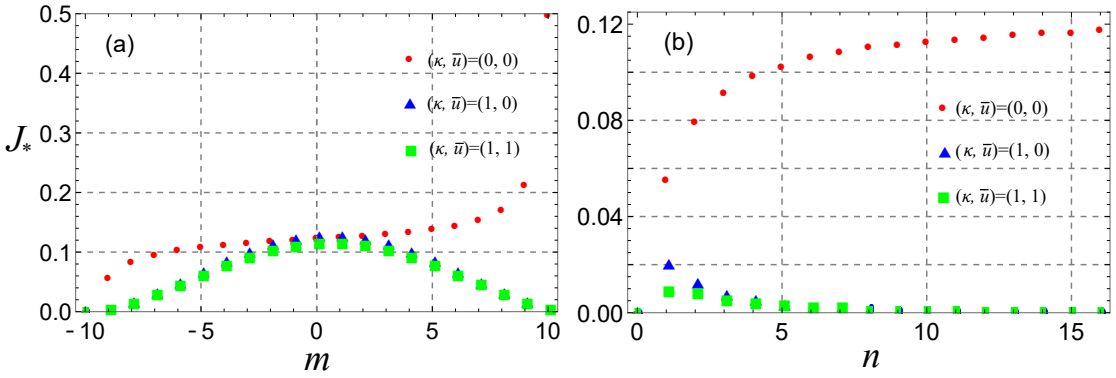

Fig. 3.6: Lower bound J_* for (a) the atomic Dicke state as a function of m and (b) the optical Fock states, in unit of $\gamma = 1$. Reprinted figure from [104, DOI: 10.1103/PhysRevA.99.052347]. Creative Commons Attribution 4.0 International license. Copyright 2019 by K. Kobayashi and N. Yamamoto.

Therefore, J_* is calculated as

$$J_*(|n\rangle) = \frac{1}{2}\left(\frac{\gamma n}{2\kappa^2 + \gamma(2n+1) + \bar{u}\sqrt{4n+2}}\right)^2.$$

Figure 3.6 (b) plots J_* when $\gamma = 1$. As seen in the previous studies, the measurement effect notably decreases J_*. However, in this case $J_* \sim 0$ for large Fock states $|n\rangle$ ($n \gtrsim 5$) does not necessarily mean that these states can be exactly stabilized via MBF, because it is known that a large Fock state might be harder to prepare than a small one such as a single-photon state $|1\rangle$. Thus, the lower bound only for small Fock states $|n\rangle$ ($n \lesssim 4$) has a practical meaning.

3.4 Summary

Quantum control offers a powerful means for generating a desired quantum state, although the actual performance of quantum control severely degrades in the presence of decoherence. Therefore, to clarify the reachability, which in our scenario the distance between the controlled state in the presence of decoherence and the target state, is of significant importance to evaluate the actual performance of those technologies. In this chapter, we have presented the fundamental lower bound J_* of the distance between the controlled quantum state under decoherence and an arbitrary target state. The notable points of J_* is the following two; (i) J_* is applicable to a general Markovian open quantum system; it is not necessary for specifying the control setup. (ii) J_* is directly computable and used as a useful guide for engineering open quantum systems; that is, for example, the system operators should be configured so that J_* takes the minimum for a given target state in the reservoir engineering scenario. In particular, from the practical viewpoint, it

is noted that the lower bound is used to derive a theoretical limit in quantum metrology; for a typical large-size atomic ensemble under control and decoherence, the fidelity to the target GHZ state must be less than 0.875, irrespective to the control strategy.

Chapter 4

Quantum speed limit

In the previous chapter, we have presented the distance limit to the target state. In this chapter, we turn our attention to time, which is a dual concept of distance. Actually, the time is an important factor to be delicately dealt with in the quantum mechanics, because the change of quantum states occurs in very small time interval. In particular, in the presence of decoherence, quantum states loss its coherence immediately. Towards the problem of evaluating the decohering time, *Quantum speed limit (QSL)* offers a powerful mean.

The QSL is defined as a lower bound on the evolution time of a quantum system evolving from the initial state to the final state. The QSL gives not only a trade-off relation between energy and time but also the shortest time for the state change. Thus, the investigation of the QSL is of great importance from both fundamental and practical sides. The purpose of this chapter is to exploit applications of the QSL. The first is to propose a new use of QSL as a measure of robust states, viewing a state with a bigger QSL to be more robust. From this perspective, we can formulate an engineering problem of the Hamiltonian that makes a target state robust against a decoherence. In order to efficiently solve this problem, we present a general and explicitly computable QSL. The second is the use for characterization of the reachable set. This approach is based on that evolution time and distance are correlated by the QSL. As a consequence, we present a time-dependent limit for the distance of the controlled quantum system under decoherence with some notable examples. The topics provided in Section 4,2, 4.3, and 4.4 are based on [105].

4.1 Quantum speed limit for closed system

4.1.1 Mandelstam-Tamm bound and Margolus-Levitin bound

We begin with a brief overview of the field of QSL. The first treatment of QSLs was given by Mandelstam and Tamm [75]; suppose that a pure state in a closed system $|\psi_t\rangle$ is driven by the time-independent Hamiltonian H. In this case, the evolution time T needed for evolving to its orthogonal state is bounded as follows:

$$T \geq T_{\mathrm{MT}} := \frac{\pi\hbar}{2\Delta E}, \tag{4.1}$$

where $\Delta E := \sqrt{\langle\psi_t|H^2|\psi_t\rangle - \langle\psi_t|H|\psi_t\rangle^2}$ is the energy variance. T_{MT} is called *Mandelstam-Tamm bound*. This inequality implies that quantum mechanics sets a fundamental limit on the evolution time characterized by the energy variance and $\hbar$.

Here we introduce another famous result in the same assumption; the Margolus-Levitin bound [76]:

$$T \geq T_{\mathrm{ML}} := \frac{\pi\hbar}{2E}, \tag{4.2}$$

where $E := \langle\psi_t|H|\psi_t\rangle$ (we set $\hbar = 1$ in the following).

Proof of Mandelstam-Tamm bound and Margolus-Levitin bound There are several approach to deriving the Mandelstam-Tamm bound and Margolus-Levitin bound [75, 76, 77, 78, 79, 82]. Here we employ the technique provided in [81] including the general case that the initial state and the final state are not orthogonal. We first derive the Mandelstam-Tamm bound. Let a given initial state $|\psi_0\rangle$ be expanded with the energy eigenbasis,

$$|\psi_0\rangle = \sum_n c_n |n\rangle ,$$

and $|n\rangle$ satisfies the eigenequation

$$H|n\rangle = E_n |n\rangle ,$$

where E_n is the energy eigenvalue. The solution of the Schrödinger equation is given by

$$|\psi_t\rangle = \sum_n c_n e^{-iE_n t} |n\rangle .$$

Now the fidelity between $|\psi_0\rangle$ and $|\psi_t\rangle$ is

$$F_t = |\langle\psi_0|\psi_t\rangle|^2 = \left|\sum_n |c_n|^2 e^{-iE_n t}\right|^2 .$$

The derivative of F_t with respect to t is calculated as follows:

$$\begin{aligned}\frac{dF_t}{dt} &= \sum_m \sum_n |c_m|^2|c_n|^2(-iE_n + iE_m)e^{iE_m t - iE_n t} \\ &= \sum_m \sum_n |c_m|^2|c_n|^2(-iE_n)(e^{iE_m t - iE_n t} - e^{-iE_m t + iE_n t}) \\ &= 2\sum_m \sum_n |c_m|^2|c_n|^2 E_n \sin(E_m t - E_n t) \\ &= 2\sum_m \sum_n |c_m|^2|c_n|^2 (E_n - E)\sin(E_m t - E_n t). \end{aligned} \tag{4.3}$$

Then, taking the absolute value of the both-side of (4.3), we have

$$\begin{aligned}\left|\frac{dF_t}{dt}\right| &= 2\left|\sum_m \sum_n |c_m|^2|c_n|^2(E_n - E)\sin(E_m t - E_n t)\right| \\ &\leq 2\left|\sum_m \sum_n |c_m|^2|c_n|^2(E_n - E)e^{-iE_n t - iE_m t}\right| \\ &\leq 2\left|\sum_n c_n^*(E_n - E)\left\{c_n\left(\sum_m |c_m|^2 e^{-iE_n t - iE_m t} - F_t\right)\right\}\right| \\ &\leq 2\sqrt{\sum_n |c_n^*(E_n - E)|^2}\sqrt{\sum_n \left|c_n\left(\sum_m |c_m|^2 e^{-iE_n t + iE_m t} - F_t\right)\right|^2} \\ &= 2\Delta E\sqrt{F_t\,(1 - F_t)}, \end{aligned} \tag{4.4}$$

where we have used the Schwarz inequality. Finally, due to the relation

$$\frac{d}{dt}\arccos(\sqrt{x}) = \frac{1}{2\sqrt{x(1-x)}},$$

the inequality (4.4) is

$$\frac{d}{dt}\arccos(\sqrt{F_t}) = \Delta E. \tag{4.5}$$

Therefore, we end up with

$$T \geq \frac{\arccos(\sqrt{F_T})}{\Delta E}. \tag{4.6}$$

When $F_T = 0$, the rightmost side of (4.6) becomes Mandelstam-Tamm bound.

Next, we derive the Margolus-Levitin bound. Setting the fidelity $F_t = |\langle\psi_0|\psi_t\rangle|^2 = \epsilon$ with the positive constant ϵ, the overlap $|\langle\psi_0|\psi_t\rangle|$ is

$$|\langle\psi_0|\psi_t\rangle| = \sqrt{\epsilon}e^{i\theta} = \sum_n |c_n|^2 e^{-iE_n t}, \tag{4.7}$$

where $0 \leq \theta \leq \pi/2$. By comparing the real and imaginary part of (4.7), we have

$$\mathrm{Re}\left[|\left\langle\psi_0|\psi_t\right\rangle|\right] = \sum_n |c_n|^2 \cos(E_n t) = \sqrt{\epsilon}\cos\theta,$$
$$\mathrm{Im}\left[|\left\langle\psi_0|\psi_t\right\rangle|\right] = \sum_n |c_n|^2 \sin(E_n t) = -\sqrt{\epsilon}\sin\theta.$$

Now we consider the following inequality

$$\cos x + q\sin x \geq 1 - ax \quad (x, q \geq 0), \tag{4.8}$$

where a and q are implicitly related as follows:

$$a = \frac{y + \sqrt{y^2(1+q^2)+q^2}}{1+y^2},$$
$$\sin y = \frac{a(1-qy)+q}{1+q^2},$$

where $y \in [\pi - \arctan(1/q), \pi + \arctan(q)]$. With respect to (4.8), setting $x = E_n t$ and multiplying $|c_n|^2$ and summing over n, we have

$$\sqrt{\epsilon}\cos\theta - q\sqrt{\epsilon}\sin\theta \geq 1 - aEt,$$

where the mean energy $E = \langle\psi|H|\psi\rangle = \sum_n |c_n|^2 E_n$. Then

$$t \geq \frac{1 - \sqrt{\epsilon}(\cos\theta - q\sin\theta)}{aE} = \frac{\alpha(\epsilon)}{aE}.$$

This is the Margolus-Levitin bound including the case that the two states are not orthogonal. Then, the inequality means that the minimal time $T_{\mathrm{QSL}}(\epsilon)$ needed for ϵ is limited

$$T_{\mathrm{QSL}}(\epsilon) = \frac{\alpha(\epsilon)}{E},$$
$$\alpha(\epsilon) = \min_\theta \left\{ \max_q \left\{ 1 - \sqrt{\epsilon}(\cos\theta - q\sin\theta)\frac{1}{a} \right\} \right\}.$$

When $\epsilon = 0$, the Margolus-Levitin bound is obtained. (Q.E.D)

4.1.2 Quantum speed limit for open quantum system

A recent interest in the field of QSL is the generalization to open quantum systems [87, 88, 89]. In particular, Del Campo has derived an explicit QSL for Markovian open quantum systems based on the angle between two states

$$\Theta_t := \arccos\left\{\mathrm{Tr}\left(\rho_0\rho_t\right)\right\}.$$

Suppose that ρ_t is driven by the master equation

$$\frac{d\rho_t}{dt} = -i[H, \rho_t] + \mathcal{D}[M]\rho_t.$$

Under the assumption that H and M are time-independent, the evolution time is bounded as follows:

$$T \geq T_{\mathrm{DC}} := \frac{1 - \cos \Theta_T}{\|i[H, \rho_0] + \mathcal{D}^\dagger[M]\rho_0\|_{\mathrm{F}}}. \tag{4.9}$$

In this thesis we call T_{DC} the Del Campo's bound.

Proof of the Del Campo's bound The time evolution of Θ_t is given as follows:

$$\begin{aligned}
\frac{d\Theta_t}{dt} &= \frac{-1}{\sqrt{1 - \mathrm{Tr}\left(\rho_0 \rho_t\right)^2}} \mathrm{Tr}\left(\rho_0 \cdot \frac{d\rho_t}{dt}\right) \\
&= \frac{-1}{\sin \Theta_t} \mathrm{Tr}\left\{\rho_0 \left(-i[H, \rho_t] + \mathcal{D}[M]\rho_t\right)\right\} \\
&= \frac{1}{\sin \Theta_t} \mathrm{Tr}\left\{\left(i[H, \rho_0] + \mathcal{D}^\dagger[M]\rho_0\right)\rho_t\right\} \\
&\leq \frac{1}{\sin \Theta_t} \|i[H, \rho_0] + \mathcal{D}^\dagger[M]\rho_0\|_{\mathrm{F}} \|\rho_t\|_{\mathrm{F}} \\
&\leq \frac{1}{\sin \Theta_t} \|i[H, \rho_0] + \mathcal{D}^\dagger[M]\rho_0\|_{\mathrm{F}}.
\end{aligned}$$

Then, integrating the above inequality from $t = 0$ to T yields T_{DC}. (Q.E.D)

When the system is closed, $M = 0$, the denominator of T_{DC} is given

$$\|i[H, \rho_0]\|_{\mathrm{F}} = \sqrt{2}\sqrt{\langle\psi_0|H^2|\psi_0\rangle - \langle\psi_0|H|\psi_0\rangle^2},$$

which is the energy variance in the initial state. Thereby, we can say that T_{DC} is a certain kind of a form of the Mandelstam-Tamm bound. In the next section, we will analytically compare T_{DC} with our bound that will be presented in the next section.

4.2 New explicit QSL

4.2.1 Setup and derivation

In Chapter 3, we have employed the SME for deriving the lower bound J_*. However, in general it is difficult to treat the stochastic term dW_t for analyzing the time of state evolution. Hence, in this chapter we consider the master equation:

$$\frac{d\rho_t}{dt} = -i[H, \rho_t] + \mathcal{D}[M]\rho_t. \tag{4.10}$$

Now for simplicity suppose that the Hamiltonian H and decoherence M are time-independent, and the initial state is pure $\rho_0 = |\psi_0\rangle\langle\psi_0|$. Next, we employ the fidelity-based distance from the initial state as a cost function:

$$V_t = 1 - \mathrm{Tr}\left(\rho_0 \rho_t\right). \tag{4.11}$$

This takes the maximum when ρ_t is orthogonal to ρ_0, and the minimum is achieved only when $\rho_t = \rho_0$. This is why, a new lower bound, that is, the minimum time of the time T needed for the cost (4.11) to evolve from $V_0 = 0$ to a given $V_T \in [0, 1]$, is given by the following:

Theorem 4.1 *For the quantum state ρ_t obeying the master equation (4.10), the cost (4.11) has the lower bound:*

$$T \geq T_* := \frac{2\lambda}{\mathcal{K}} + \frac{2\mathcal{C}}{\mathcal{K}^2} \ln \left[\frac{\mathcal{C}}{\mathcal{C} + \mathcal{K}\lambda} \right], \tag{4.12}$$

with

$$\begin{aligned} \mathcal{K} &= \sqrt{2} \| i[H, \rho_0] + \mathcal{D}^\dagger[M]\rho_0 \|_{\mathrm{F}}, \\ \mathcal{C} &= \| M \left| \psi_0 \right\rangle \|^2 - | \left\langle \psi_0 \right| M \left| \psi_0 \right\rangle |^2, \\ \lambda &= \sqrt{V_T}. \end{aligned}$$

Proof of Theorem 4.1 The dynamics of V_t is given by

$$\begin{aligned} \frac{dV_t}{dt} &= -\mathrm{Tr} \left(\rho_0 \frac{d\rho_t}{dt} \right) \\ &= -\mathrm{Tr} \left\{ \rho_0 \left(-i[H, \rho_t] + \mathcal{D}[M]\rho_t \right) \right\} \\ &= \mathrm{Tr} \left\{ \left(i[\rho_0, H] - \mathcal{D}^\dagger[M]\rho_0 \right) \rho_t \right\}. \end{aligned} \tag{4.13}$$

To derive an upper bound of the rightmost side of Eq. (4.13), we use two inequalities; the Schwarz inequality $\|X\|_{\mathrm{F}} \|Y\|_{\mathrm{F}} \geq |\mathrm{Tr}(XY)|$ and

$$\begin{aligned} \| \rho_t - \rho_0 \|_{\mathrm{F}} &= \sqrt{\mathrm{Tr} \left[\left(\rho_t - \rho_0 \right)^2 \right]} \\ &= \sqrt{\mathrm{Tr} \left[\rho_t^2 - 2\rho_t \rho_0 + \rho_0^2 \right]} \\ &\leq \sqrt{2 - 2\mathrm{Tr} \left(\rho_t \rho_0 \right)} \\ &= \sqrt{2V_t}. \end{aligned}$$

Using these, the rightmost side of Eq. (4.13) is upper bounded as follows:

$$\begin{aligned} &\mathrm{Tr} \left\{ \left(i[\rho_0, H] - \mathcal{D}^\dagger[M]\rho_0 \right) \rho_t \right\} \\ &= \mathrm{Tr} \left\{ \left(i[\rho_0, H] - \mathcal{D}^\dagger[M]\rho_0 \right) (\rho_t - \rho_0) \right\} - \mathrm{Tr} \left(\rho_0 \mathcal{D}^\dagger[M]\rho_0 \right) \\ &= \mathrm{Tr} \{ \left(i[H, \rho_0] + \mathcal{D}^\dagger[M]\rho_0 \right) (\rho_0 - \rho_t) \} + \mathrm{Tr} \left(M^\dagger M \rho_0 \right) - \mathrm{Tr} \left(M^\dagger \rho_0 M \rho_0 \right) \\ &\leq \| i[H, \rho_0] + \mathcal{D}^\dagger[M]\rho_0 \|_{\mathrm{F}} \cdot \| \rho_t - \rho_0 \|_{\mathrm{F}} + \| M \left| \psi_0 \right\rangle \|^2 - | \left\langle \psi_0 \right| M \left| \psi_0 \right\rangle |^2 \\ &\leq \sqrt{2} \| i[H, \rho_0] + \mathcal{D}^\dagger[M]\rho_0 \|_{\mathrm{F}} \sqrt{V_t} + \| M \left| \psi_0 \right\rangle \|^2 - | \left\langle \psi_0 \right| M \left| \psi_0 \right\rangle |^2, \end{aligned}$$

Combining these with (4.13), we have

$$\frac{dV_t}{dt} \leq \mathcal{K}\sqrt{V_t} + \mathcal{C}, \tag{4.14}$$

where

$$\mathcal{K} = \sqrt{2}\|i[H,\rho_0] + \mathcal{D}^\dagger[M]\rho_0\|_{\mathrm{F}},$$
$$\mathcal{C} = \|M\,|\psi_0\rangle\,\|^2 - |\,\langle\psi_0|\,M\,|\psi_0\rangle\,|^2.$$

Then by integrating the inequality (4.14), from 0 to T, we end up with Theorem 4.1. (Q.E.D)

Likewise the distance limit J_*, T_* also gives a fundamental lower bound on the evolution time. Here we list some notable points of T_*.

Remark 4.1: T_* has an explicit form in terms of (ρ_0, H, M, λ). Thanks to this, T_* is straightforwardly calculated once those parameters are given, and thus it is not necessary for solving any equation.

Remark 4.2: T_* is monotonically decreasing with respect to the magnitude of the decoherence M. This means that, the state evolution can become faster as the decoherence becomes bigger.

Proof of Remark 4.2 Let us show that T_* is monotonically decreasing with respect to the strength of the decoherence, γ, which is defined by setting $M = \sqrt{\gamma}M'$ with fixed M'. In terms of γ, we can express $\mathcal{K}$ and $\mathcal{C}$ as $\mathcal{K} = \sqrt{a\gamma^2 + b\gamma + c}$ and $\mathcal{C} = d\gamma$, where (a, c, d) are non-negative constants and b is a constant. Then T_* can be expressed as

$$T_* = \frac{2\lambda}{\sqrt{a\gamma^2 + b\gamma + c}} + \frac{d\gamma}{a\gamma^2 + b\gamma + c}\ln\left[\frac{d\gamma}{d\gamma + \lambda\sqrt{a\gamma^2 + b\gamma + c}}\right],$$

and $\partial T_*/\partial\gamma$ is calculated as

$$\frac{\partial T_*}{\partial\gamma} = -\frac{(2a\gamma + b)\lambda}{\mathcal{K}^3} + \frac{2d(a\gamma^2 - c)}{\mathcal{K}^4}\ln\left[1 + \frac{\mathcal{K}\lambda}{\mathcal{C}}\right] + \frac{d(b\gamma + 2c)\lambda}{\mathcal{K}^3(\mathcal{C} + \mathcal{K}\lambda)}.$$

The goal here is to show $\partial T_*/\partial\gamma \leq 0$. The proof is divided into three cases: $a\gamma^2 > c$, $a\gamma^2 = c$, and $a\gamma^2 < c$. First, for the case $a\gamma^2 > c$ we have

$$\begin{aligned}\frac{\partial T_*}{\partial\gamma} &\leq -\frac{(2a\gamma + b)\lambda}{\mathcal{K}^3} + \frac{2d(a\gamma^2 - c)}{\mathcal{K}^4}\frac{\mathcal{K}\lambda(\mathcal{K}\lambda + 2\mathcal{C})}{2\mathcal{C}(\mathcal{K}\lambda + \mathcal{C})} + \frac{d(b\gamma + 2c)\lambda}{\mathcal{K}^3(\mathcal{C} + \mathcal{K}\lambda)} \\ &= \frac{-\lambda^2}{\gamma(\mathcal{C} + \mathcal{K}\lambda)} \leq 0,\end{aligned}$$

where the inequality $\ln(1+x) \leq x(x+2)/\{2(x+1)\}$ for $x \geq 0$ is used. Next, for the case $a\gamma^2 = c$,

$$\frac{\partial T_*}{\partial \gamma} = -\frac{\lambda^2}{\gamma(\mathcal{C}+\mathcal{K}\lambda)} \leq 0.$$

Lastly, for the case $a\gamma^2 < c$, we have

$$\begin{aligned}\frac{\partial T_*}{\partial \gamma} &= -\frac{(2a\gamma+b)\lambda}{\mathcal{K}^3} + \frac{2d(a\gamma^2-c)}{\mathcal{K}^5\lambda}\mathcal{K}\lambda \ln\left(\frac{\mathcal{C}+\mathcal{K}\lambda}{\mathcal{C}}\right) + \frac{d(b\gamma+2c)\lambda}{\mathcal{K}^3(\mathcal{C}+\mathcal{K}\lambda)} \\ &\leq -\frac{(2a\gamma+b)\lambda}{\mathcal{K}^3} + \frac{2d(a\gamma^2-c)}{\mathcal{K}^5\lambda}\frac{2\mathcal{K}^2\lambda^2}{2\mathcal{C}+\mathcal{K}\lambda} + \frac{d(b\gamma+2c)\lambda}{\mathcal{K}^3(\mathcal{C}+\mathcal{K}\lambda)} \\ &= \frac{-\lambda^2}{\mathcal{K}^2(\mathcal{C}+\mathcal{K}\lambda)}\left(2a\gamma+b+\frac{2d(c-a\gamma^2)}{2\mathcal{C}+\mathcal{K}\lambda}\right),\end{aligned}$$

where the inequality $2(\alpha-\beta)^2/(\alpha+\beta) \leq (\alpha-\beta)\ln(\alpha/\beta)$ for $\alpha, \beta \geq 0$ is used. Now, $2a\gamma + b > 0$ immediately leads to $\partial T_*/\partial\gamma \leq 0$. If $2a\gamma + b \leq 0$, the above inequality can be further calculated as

$$\begin{aligned}\frac{\partial T_*}{\partial \gamma} &\leq \frac{-\lambda^2(2a\gamma^2+b\gamma)(2\mathcal{C}+\mathcal{K}\lambda)}{\gamma\mathcal{K}^2(\mathcal{C}+\mathcal{K}\lambda)(2\mathcal{C}+\mathcal{K}\lambda)} + \frac{2\lambda^2(a\gamma^2-c)}{\gamma\mathcal{K}^2(\mathcal{C}+\mathcal{K}\lambda)(2\mathcal{C}+\mathcal{K}\lambda)} \\ &= \frac{-\lambda^2\{2\mathcal{C}\mathcal{K}^2-(4\mathcal{C}+\mathcal{K}\lambda)(2a\gamma^2+b\gamma)\}}{\gamma\mathcal{K}^2(\mathcal{C}+\mathcal{K}\lambda)(2\mathcal{C}+\mathcal{K}\lambda)} \leq 0. \quad \text{(Q.E.D)}\end{aligned}$$

Remark 4.3: T_* is monotonically decreasing with respect to $\mathcal{K}$ for a fixed $\mathcal{C}$.

Proof of Remark 4.3 Let us calculate $\partial T_*/\partial\mathcal{K}$:

$$\begin{aligned}\frac{\partial T_*}{\partial \mathcal{K}} &= -\frac{2}{\mathcal{K}^2}\left\{\lambda + \frac{\mathcal{C}}{\mathcal{K}}\ln\left[\frac{\mathcal{C}}{\mathcal{C}+\mathcal{K}\lambda}\right]\right\} - \frac{2\mathcal{C}}{\mathcal{K}^2}\left\{\frac{1}{\mathcal{K}}\ln\left[\frac{\mathcal{C}}{\mathcal{C}+\mathcal{K}\lambda}\right] + \frac{\lambda}{\mathcal{C}+\mathcal{K}\lambda}\right\} \\ &= -\frac{2}{\mathcal{K}^2}\left\{\lambda + \frac{k\lambda}{k+\lambda} - 2k\ln\left[1+\frac{\lambda}{k}\right]\right\},\end{aligned}$$

where $k = \mathcal{C}/\mathcal{K}$. Then from the inequality $\ln(1+x) \leq x(2+x)/2(1+x)$ for $x \geq 0$, we have

$$\frac{\partial T_*}{\partial \mathcal{K}} \leq -\frac{2}{\mathcal{K}^2}\left\{\lambda + \frac{k\lambda}{k+\lambda} - 2k\frac{(\lambda/k)(2+\lambda/k)}{2(1+\lambda/k)}\right\} = 0. \quad \text{(Q.E.D)}$$

In general, a closed system with bigger Hamiltonian H evolves faster, although this dynamics can be changed by the decoherence effect M in the case of open quantum systems. Intuitively, $\mathcal{K}$ corresponds to the amplitude of such an effective Hamiltonian. In Section 4.4, we will see that the monotonically decreasing property of T_* with respect to $\mathcal{K}$ is the key point for formulating the Hamiltonian engineering problem for robust state preparation.

Remark 4.4: T_* can be straightforwardly generalized to the case where the system is subjected to multiple decoherence channels and Hamiltonians. In this case T_* is given by (4.12) with

$$\mathcal{K} = \sqrt{2}\left\| \sum_j i[H_j, \rho_0] + \sum_j \mathcal{D}^\dagger[M_j]\rho_0 \right\|_{\mathrm{F}},$$
$$\mathcal{C} = \sum_j \left(\| M_j |\psi_0\rangle \|^2 - |\langle\psi_0| M_j |\psi_0\rangle|^2 \right).$$

Remark 4.5: T_* can be extended to the case where the initial state ρ_0 is mixed. By redefining the cost (4.11) as $V_t' = 1 - \mathrm{Tr}\left(\rho_0\rho_t\right)/\mathrm{Tr}\left(\rho_0^2\right)$, we can derive the generalized QSL:

$$T \geq T_*' := \frac{2(\lambda_T' - \lambda_0')}{\mathcal{K}'} + \frac{2\mathcal{C}'}{\mathcal{K}'^2} \ln\left[\frac{\mathcal{C}' + \mathcal{K}'\lambda_0'}{\mathcal{C}' + \mathcal{K}'\lambda_T'}\right], \tag{4.15}$$

where

$$\mathcal{K}' = \sqrt{2}\|i[H, \rho_0] + \mathcal{D}^\dagger[M]\rho_0\|_{\mathrm{F}},$$
$$\mathcal{C}' = \mathrm{Tr}\left(M^\dagger\rho_0 M\rho_0\right) - \mathrm{Tr}\left(M^\dagger M\rho_0^2\right),$$
$$\lambda_t' = \sqrt{1 - \mathrm{Tr}\left(\rho_0^2\right) + 2\mathrm{Tr}\left(\rho_0^2\right) V_t}/\sqrt{2}.$$

Note that if ρ_0 is pure, the lower bound (4.15) is equivalent to (4.12).

Proof of Remark 4.5 By replacing V_t with V_t', T_*' can be derived in the same manner as the derivation of T_*. The distance between ρ_0 and ρ_t is

$$\begin{aligned}
\|\rho_t - \rho_0\|_{\mathrm{F}} &= \sqrt{\mathrm{Tr}\left[(\rho_t - \rho_0)^2\right]} \\
&= \sqrt{\mathrm{Tr}\left[\rho_t^2 - 2\rho_t\rho_0 + \rho_0^2\right]} \\
&\leq \sqrt{\mathrm{Tr}\left(\rho_t^2\right) - 2\mathrm{Tr}\left(\rho_t\rho_0\right) + \mathrm{Tr}\left(\rho_0^2\right)} \\
&\leq \sqrt{1 - \mathrm{Tr}(\rho_0^2) + 2\mathrm{Tr}(\rho_0^2)V_t'}.
\end{aligned}$$

Also, the upper bound of dV_t'/dt is given as

$$\begin{aligned}
\frac{dV_t'}{dt} &= \frac{-1}{\mathrm{Tr}(\rho_0^2)}\mathrm{Tr}\left(\rho_0\frac{d\rho_t}{dt}\right) \\
&= \frac{1}{\mathrm{Tr}(\rho_0^2)}\mathrm{Tr}\left[\rho_0\left(-i[H, \rho_t] + \mathcal{D}[M]\rho_t\right)\right] \\
&= \frac{1}{\mathrm{Tr}(\rho_0^2)}\left(\mathrm{Tr}\left[\left(i[H, \rho_0] + \mathcal{D}^\dagger[M]\rho_0\right)(\rho_t - \rho_0)\right] - \mathrm{Tr}\left(M^\dagger M\rho_0^2\right) + \mathrm{Tr}\left(M^\dagger\rho_0 M\rho_0\right)\right) \\
&\leq \frac{1}{\mathrm{Tr}(\rho_0^2)}\left(\|i[H, \rho_0] + \mathcal{D}^\dagger[M]\rho_0\|_{\mathrm{F}}\|\rho_t - \rho_0\|_{\mathrm{F}} + \mathcal{C}'\right) \\
&\leq \frac{1}{\mathrm{Tr}(\rho_0^2)}\left(\mathcal{K}'\lambda' + \mathcal{C}'\right),
\end{aligned} \tag{4.16}$$

where

$$\mathcal{K}' = \sqrt{2}\|i[H,\rho_0] + \mathcal{D}^\dagger[M]\rho_0\|_{\mathrm{F}},$$
$$\mathcal{C}' = \mathrm{Tr}\left(M^\dagger\rho_0 M\rho_0\right) - \mathrm{Tr}\left(M^\dagger M\rho_0^2\right),$$
$$\lambda' = \sqrt{1-\mathrm{Tr}(\rho_0^2)+2\mathrm{Tr}(\rho_0^2)V_t'}/\sqrt{2}.$$

By integrating the above inequality (4.16), we end up with the speed limit extended to the mixed state:

$$T \geq T_* := \frac{2}{\mathcal{K}'}\left(\lambda_T' - \lambda_0' + \frac{\mathcal{C}'}{\mathcal{K}'}\ln\left[\frac{\mathcal{C}'+\mathcal{K}'\lambda_0'}{\mathcal{C}'+\mathcal{K}'\lambda_T'}\right]\right), \tag{4.17}$$

with

$$\mathcal{K}' = \sqrt{2}\|i[H,\rho_0] + \mathcal{D}^\dagger[M]\rho_0\|_{\mathrm{F}},$$
$$\mathcal{C}' = \mathrm{Tr}\left(M^\dagger\rho_0 M\rho_0\right) - \mathrm{Tr}\left(M^\dagger M\rho_0^2\right). \quad \text{(Q.E.D)}$$

4.2.2 Comparison to the previous QSL

Recall the Del Campo's bound provided in Section 4.1:

$$T \geq T_{\mathrm{DC}} := \frac{1-\mathrm{Tr}\left(\rho_0\rho_T\right)}{\|i[H,\rho_0]+\mathcal{D}^\dagger[M]\rho_0\|_{\mathrm{F}}} = \frac{\sqrt{2}\lambda^2}{\mathcal{K}} \tag{4.18}$$

Likewise T_*, T_{DC} is also explicitly expressed once the parameters (ρ_0, H, M, λ) are given. This fact is indeed the key point for engineering a system having a robust initial state ρ_0 in terms of QSL. Note that, to our best knowledge, no explicit expression of QSL for open quantum systems has been developed, except for T_* and T_{DC}. Thereby, it has an important meaning to compare the tightness of T_* and T_{DC}. Let us examine the following ratio:

$$\begin{aligned}\frac{T_*}{T_{\mathrm{DC}}} &= \left\{\frac{2\lambda}{\mathcal{K}} + \frac{2\mathcal{C}}{\mathcal{K}^2}\ln\left[\frac{\mathcal{C}}{\mathcal{C}+\mathcal{K}\lambda}\right]\right\}\frac{\mathcal{K}}{\sqrt{2}\lambda^2} \\ &= \frac{\sqrt{2}}{\lambda} + \frac{\sqrt{2}k}{\lambda^2}\ln\left[\frac{k}{k+\lambda}\right],\end{aligned}$$

where $k = \mathcal{C}/\mathcal{K}$. Note that from Schwarz inequality we have

$$\begin{aligned}\mathcal{K} &= \sqrt{2}\|i[H,\rho_0]+\mathcal{D}^\dagger[M]\rho_0\|_{\mathrm{F}}\cdot\|\rho_0\|_{\mathrm{F}} \\ &\geq \sqrt{2}|\mathrm{Tr}\left\{\left(i[H,\rho_0]+\mathcal{D}^\dagger[M]\rho_0\right)\rho_0\right\}| = \sqrt{2}\mathcal{C},\end{aligned}$$

hence $0 \leq k \leq 1/\sqrt{2}$. First, T_*/T_{DC} is a monotonically decreasing function with respect to k, because

$$\begin{aligned}\frac{\partial}{\partial k}\left(\frac{T_*}{T_{\mathrm{DC}}}\right) &= \frac{\sqrt{2}}{\lambda}\left\{-\frac{1}{\lambda}\ln\left[1+\frac{\lambda}{k}\right] + \frac{1}{k+\lambda}\right\} \\ &\leq \frac{\sqrt{2}}{\lambda}\left(-\frac{1}{\lambda}\frac{\lambda}{k+\lambda} + \frac{1}{k+\lambda}\right) = 0,\end{aligned}$$

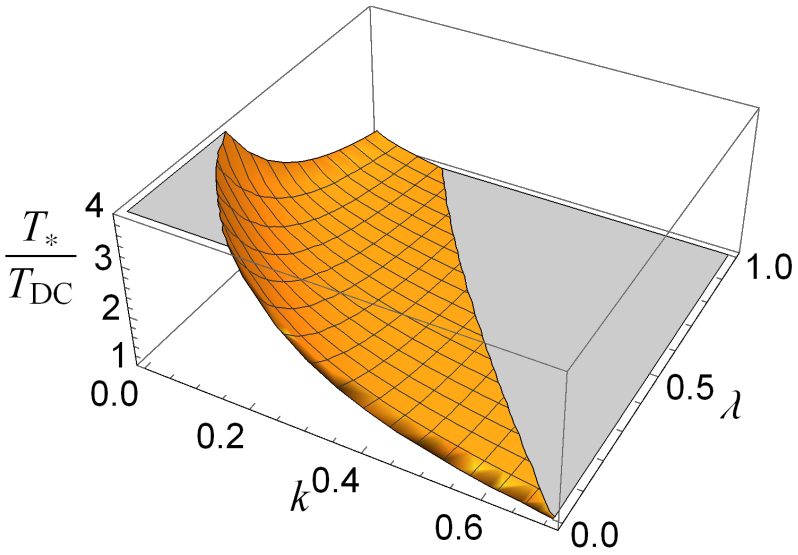

Fig. 4.1: The 3-dimensional plot of the ratio of bounds, $T_*/T_{\rm DC}$, as a function of $k \in [0, 1/\sqrt{2}]$ and $\lambda \in [0, 1]$. Reprinted figure from [105, DOI: 10.1103/PhysRevA.102.042606]. Creative Commons Attribution 4.0 International license. Copyright 2020 by K. Kobayashi and N. Yamamoto.

where we used $\ln(1+x) \geq x/(1+x)$ for $x \geq 0$. Now, when $k = 0$ or equivalently when the system is closed (i.e., $\mathcal{C} = 0$), then $T_*/T_{\rm DC} \geq \sqrt{2}/\lambda > 1$. Together with the above monotonically decreasing property of $T_*/T_{\rm DC}$ with respect to k, hence, T_* is tighter than $T_{\rm DC}$ if the decoherence is small. Next, $T_*/T_{\rm DC}$ decreases with respect to λ, because

$$\begin{aligned}\frac{\partial}{\partial\lambda}\left(\frac{T_*}{T_{\rm DC}}\right) &= -\frac{\sqrt{2}}{\lambda^2} + \frac{2\sqrt{2}k}{\lambda^3}\ln\left[1+\frac{\lambda}{k}\right] - \frac{\sqrt{2}k}{\lambda^2}\frac{1}{k+\lambda} \\ &\leq \frac{\sqrt{2}}{\lambda^2}\left\{-1 + \frac{2k+\lambda}{k+\lambda} - \frac{k}{k+\lambda}\right\} = 0,\end{aligned}$$

where we used $\ln(1+x) \leq x(2+x)/\{2(1+x)\}$ for $x \geq 0$. From this inequality, T_* works as a tighter bound than $T_{\rm DC}$, in the region $\mathcal{R}_\lambda(\rho_0)$ with small radius λ, which can be quantitatively seen in Fig. 4.1, which plots $T_*/T_{\rm DC}$ as a function of $k \in [0, 1/\sqrt{2}]$ and $\lambda \in [0, 1]$. The yellow-colored region shows the set of parameters (λ, k) such that $T_* > T_{\rm DC}$. Note that, when the decoherence is weak (i.e., k is small) and $\mathcal{R}_\lambda(\rho_0)$ is small (i.e., λ is small), then T_* works as a much bigger lower bound for the escape time T, than $T_{\rm DC}$.

4.3 Examples

4.3.1 Qubit

The first example is a qubit system consisting of the excited state $|0\rangle = [1,0]^\top$ and the ground state $|1\rangle = [0,1]^\top$. Let the initial state $\rho_0 = |\psi_0\rangle\langle\psi_0|$ be

$$|\psi_0\rangle = [\cos\theta, e^{i\varphi}\sin\theta]^\top,\ (0 \le \theta < \pi/2,\ 0 \le \varphi < 2\pi).$$

Here we assign the system operators

$$H = \omega\sigma_z,\ M = \sqrt{\gamma}\sigma_x.$$

H rotates the state vector along the z axis with driving frequency $\omega > 0$. M represents the dephasing noise with decay rate $\gamma > 0$. In this setup, the QSL is given by (4.12) with

$$\begin{aligned}\mathcal{K} &= \sqrt{2}\|i\omega[\sigma_z,\rho_0] + \gamma\mathcal{D}^\dagger[\sigma_x]\rho_0\|_{\mathrm{F}} \\ &= 2\sqrt{\gamma^2(\cos^2 2\theta + \sin^2 2\theta\sin^2\varphi) + 4\omega^2\sin^2 2\theta + 4\omega\gamma\sin^2 2\theta\sin 2\varphi}, \\ \mathcal{C} &= \gamma\|\sigma_x|\rho_0\rangle\|^2 - \gamma|\langle\psi_0|\sigma_x|\psi_0\rangle|^2 \\ &= \gamma - \gamma\sin^2 2\theta\cos^2\varphi.\end{aligned}$$

Figure 4.2 (a) shows T_* for the initial state satisfying $\varphi = 0$, as a function of θ, for a fixed value $\lambda = 0.1$. That is, this figure shows the lower bound of the escape time when the state starting from $|\psi_0\rangle = [\cos\theta, \sin\theta]^\top$ first exits from the region $\mathcal{R}_\lambda(\rho_0)$. If $\gamma = 0$, $T_* = \lambda/(\omega|\sin 2\theta|)$, which is plotted with the red solid line; in this case the state simply rotates along the z axis, and thus the state near $|0\rangle$ or $|1\rangle$ remains inside $\mathcal{R}_\lambda(\rho_0)$ for all time, then $T_* \to \infty$ holds. Also T_* takes the minimum at $\theta = \pi/4$, simply because the state on the equator of the Bloch sphere, i.e., $|+\rangle := (|0\rangle + |1\rangle)/\sqrt{2}$, changes the most. Thus, in our definition, $|+\rangle$ is the most fragile state. If $\gamma > 0$, the dependence of T_* on θ remarkably changes, as depicted with the blue dashed and green dotted lines. Again, $\lambda = 0.1$ is chosen. When $(\omega,\gamma) = (0,1)$, $T_* \to \infty$ at $\theta = \pi/4$; that is, $|+\rangle$ is the most robust, because in this case $|+\rangle$ is a steady state of the master equation $d\rho_t/dt = \mathcal{D}[M]\rho_t$. This means that $|+\rangle$ does not change under the influence of this decoherence and the state around $|+\rangle$ remains in $\mathcal{R}_\lambda(\rho_0)$ for all time. On the other hand, when $(\omega,\gamma) = (1,1)$, T_* takes a finite time for all θ, meaning that the state may escape from $\mathcal{R}_\lambda(\rho_0)$ at a certain time for any ρ_0.

Now, recall that T_* is a lower bound of the exact escape time T. Hence, it is worth comparing these quantities to evaluate the actual tightness of T_*. For this purpose, here we set $\omega = 0$ and choose the initial state $|\psi_0\rangle = |0\rangle$. In this case the master equation $d\rho_t/dt = \mathcal{D}[M]\rho_t$ yields a simple solution $\mathrm{Tr}\,(\rho_0\rho_T) = (1 + e^{-2\gamma T})/2$. As a consequence,

we obtain T and T_* as follows:

$$T = -\frac{1}{2\gamma}\ln[1-2\lambda^2],$$
$$T_* = \frac{\lambda}{\gamma} - \frac{1}{2\gamma}\ln[2\lambda+1].$$

Figure 4.2 (b) shows the plots of T and T_* in unit of $\gamma = 1$, as a function of λ; in particular, the gap between T and T_* are close to zero when λ is small, which is reasonable because the state will take a short time to escape from a small region $\mathcal{R}_\lambda(\rho_0)$. However, this gap becomes bigger, as λ becomes large. This fact suggests us to use T_*, especially when λ is small.

Next, let us see the ratio T_*/T_{DC} discussed above, especially for the following setup:

$$H = \omega\sigma_z,\ M = \sqrt{\gamma}\sigma_-.$$

The initial state is set to the superposition $|\psi_0\rangle = |+\rangle$. In fact, this example demonstrates the difference of the two lower bounds more drastically than the above setup. We now have $\mathcal{K} = \sqrt{48\omega^2+11\gamma^2}/4$ and $\mathcal{C} = \gamma/16$, and thus

$$T_* = \frac{8}{\sqrt{48\omega^2+11\gamma^2}}\left(\lambda + \frac{\gamma}{4\sqrt{48\omega^2+11\gamma^2}}\ln\left[\frac{\gamma}{\gamma+4\sqrt{48\omega^2+11\gamma^2}}\right]\right),$$
$$T_{\mathrm{DC}} = \frac{4\sqrt{2}\lambda^2}{\sqrt{48\omega^2+11\gamma^2}}.$$

Then T_*/T_{DC} depends on only γ/ω and $\lambda = \sqrt{V_T}$. Figure 4.2 (c) shows the plot of T_*/T_{DC}, as a function of γ/ω, for each values of λ. As expected from the discussion in Subsection 4.2.2, T_*/T_{DC} increases as γ/ω becomes small for all λ, and also it becomes bigger for smaller λ. That is, T_* is a tighter bound than T_{DC}, if the decoherence is relatively small and the region $\mathcal{R}_\lambda(\rho_0)$ is small.

Lastly, we examine the QSL for the mixed initial state. Let the initial state be

$$\rho_0 = p\,|0\rangle\langle 0| + (1-p)\,|1\rangle\langle 1|,$$

where $0 \le p \le 1/2$. When $p = 0$ or 1 the state is pure, whereas when $p = 1/2$ the state is maximally mixed. The system operators is assigned as

$$H = \omega\sigma_x,\ M = \sqrt{\gamma}\sigma_-.$$

Then the extended QSL T_*' is given with

$$\mathcal{K}' = \sqrt{2}(1-2p)\sqrt{\gamma^2+2\omega^2},$$
$$\mathcal{C}' = \gamma p(1-2p),$$
$$\lambda_T' = \sqrt{p-p^2+\mathrm{Tr}\,(\rho_0\rho_T)},$$
$$\lambda_0' = \sqrt{p-p^2}.$$

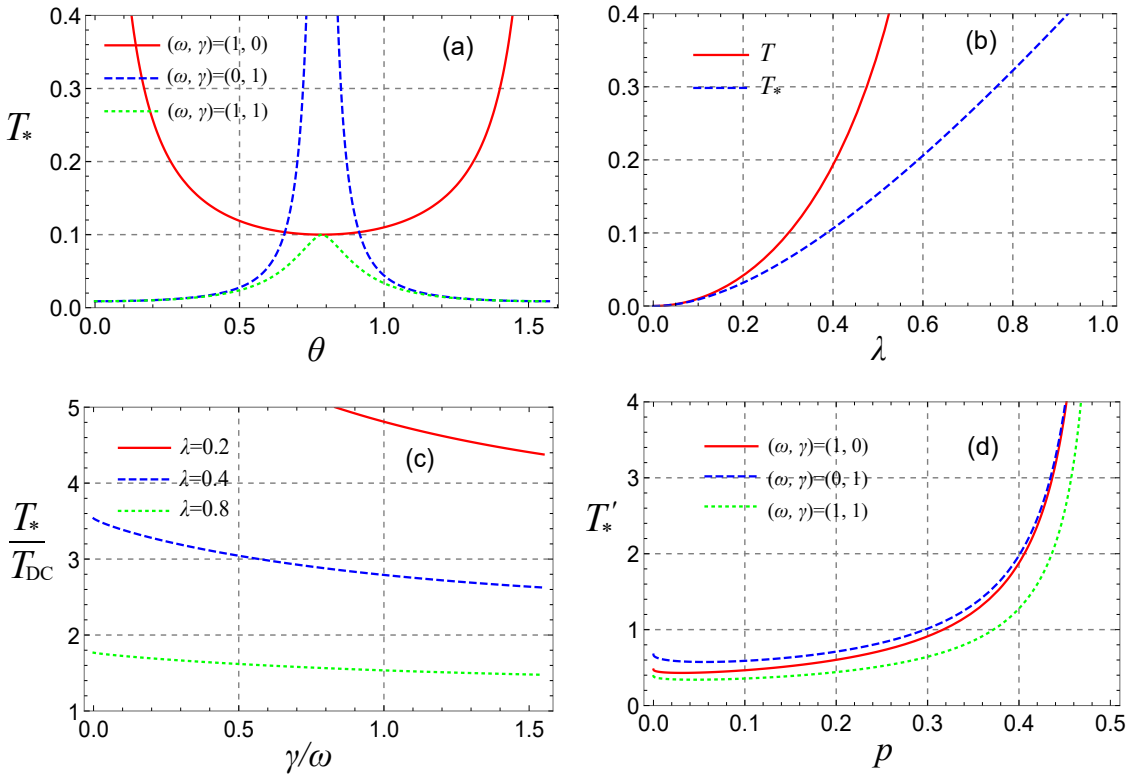

Fig. 4.2: (a) The lower bound T_* as a function of θ, for several values of (ω, γ). For all cases, $\lambda = 0.1$. (b) Comparison of the exact escape time T and its lower bound T_* as a function of λ, where $\gamma = 1$ is fixed. (c) The ratio $T_*/T_{\rm DC}$, as a function of γ/ω, for several values of λ. (d) The extended bound T_*' as a function of p, for several values of (ω, γ) and $\mathrm{Tr}\,(\rho_0\rho_T) = 0.9$. Reprinted figure from [105, DOI: 10.1103/PhysRevA.102.042606]. Creative Commons Attribution 4.0 International license. Copyright 2020 by K. Kobayashi and N. Yamamoto.

Figure 4.2 (d) illustrates T_*' as a function of p (T_*' has a symmetric form with respect to $p = 1/2$). In the limit $p \to 1/2$, i.e., $\rho_0 \to (1/2)I$, $T_*' \to \infty$. Indeed, the initial state $\rho_0 = (1/2)I$ never changes by any Hamiltonian and decoherence. This means that the maximally mixed state (i.e., the most classical state) is most robust against the state change, although it has no advantage in quantum mechanics.

4.3.2 Two-qubits

Next we study a two-qubits system. Let us reconsider the Bell states defined in Section 3.3 again:

$$|\Phi^{\pm}\rangle = \frac{1}{\sqrt{2}}(|0\rangle|0\rangle \pm |1\rangle|1\rangle),$$
$$|\Psi^{\pm}\rangle = \frac{1}{\sqrt{2}}(|1\rangle|0\rangle \pm |0\rangle|1\rangle).$$

In Section 3.3, we have discussed their reachability properties under a specific decoherence. Now, our interest is which state is the most robust under a given decoherence. As seen in the above example, comparing T_* of these states gives a rough answer to this question. Here we assume that the system is subjected to the collective noise $M = \sqrt{\gamma}(\sigma_- \otimes I + I \otimes \sigma_-)$ and $H = 0$. For the state $|\Phi^{\pm}\rangle = (|0\rangle|0\rangle \pm |1\rangle|1\rangle)/\sqrt{2}$, $\mathcal{K} = \sqrt{5}\gamma$ and $\mathcal{C} = \gamma$. Then, for the same λ, the QSLs are calculated as

$$T_*(|\Phi^{\pm}\rangle) = \frac{2\lambda}{\sqrt{5}\gamma} - \frac{2}{5\gamma}\ln[1+\lambda],$$
$$T_*(|\Psi^{+}\rangle) = \frac{\lambda}{2\gamma} - \frac{1}{4\gamma}\ln[1+2\lambda].$$

Also $T_*(|\Psi^-\rangle) \to \infty$ due to $\mathcal{K} = 0$, which is equivalent to that $|\Psi^-\rangle$ is identical to an eigenstate of M. Hence, $|\Psi^-\rangle$ is the most robust Bell state in our definition. Moreover, $T_*(|\Phi^{\pm}\rangle) > T_*(|\Psi^+\rangle)$ always holds, and thus $|\Psi^+\rangle$ is the most fragile state to this M. Together with the result given in Subsection 3.3.2, we can conclude that $|\Psi^-\rangle$ is the best state in terms of reachability and robustness. Note that, for the case of the non-collective (local) decoherence modeled by $M_1 = \sqrt{\gamma}\sigma_- \otimes I$ and $M_2 = \sqrt{\gamma} I \otimes \sigma_-$, we have

$$T_* = \frac{2\lambda}{\sqrt{5}\gamma} - \frac{2}{5\gamma}\ln[1+\lambda]$$

for all Bell states. That is, in this case there is no difference of states in robustness, and especially for $|\Phi^{\pm}\rangle$, the robustness against the collective or non-collective decay does not change in terms of QSL.

4.3.3 N-qubits

Next we consider an ensemble composed of N identical qubits. Recall the product state of the superposition $|+\rangle^{\otimes N} = (|0\rangle/\sqrt{2} + |1\rangle/\sqrt{2})^{\otimes N}$ and the GHZ state $|\mathrm{GHZ}\rangle = (|0\rangle^{\otimes N} + |1\rangle^{\otimes N})/\sqrt{2}$. As mentioned in Chapter 3, $|\mathrm{GHZ}\rangle$ is a powerful resource in quantum metrology such as the frequency standard and enables us to estimate the atomic frequency with error of the order $1/N$, while $1/\sqrt{N}$ is the best order in the case of $|+\rangle^{\otimes N}$ [58]. However, in a realistic situation, the system is always subjected to decoherence such as the dephasing noise $M = \sqrt{\gamma}\sum_{j=1}^{N}\sigma_z^{(j)}$, which erases the advantage of using $|\mathrm{GHZ}\rangle$ [59]. In Chapter 3, we have concluded that the GHZ state is harder to prepare than the

product state by comparing of J_* for two states. To evaluate the undesired effect caused by the dephasing noise in the language of QSL, here we examine T_* of those two states. Now, for simplicity, suppose that the magnitude of the system Hamiltonian H is much smaller than the decoherence strength γ. Using the relation given in Subsection 3.3.3

$$
\begin{aligned}
&M\left|+\right\rangle^{\otimes N} = M^\dagger\left|+\right\rangle^{\otimes N} = \sqrt{\gamma}\sum_{j=1}^{N}\left|+\right\rangle\cdots\left|+\right\rangle\left|-\right\rangle\left|+\right\rangle\cdots\left|+\right\rangle,\\
&M^\dagger M\left|+\right\rangle^{\otimes N} = \gamma\left(N\left|+\right\rangle^{\otimes N} + 2\sum_{i\neq j}\left|+\right\rangle\cdots\left|-\right\rangle\cdots\left|-\right\rangle\cdots\left|+\right\rangle\right),\\
&M\left|\mathrm{GHZ}\right\rangle = M^\dagger\left|\mathrm{GHZ}\right\rangle = \frac{\gamma N(\left|0\right\rangle^{\otimes N} - \left|1\right\rangle^{\otimes N})}{\sqrt{2}},\\
&M^\dagger M\left|\mathrm{GHZ}\right\rangle = \gamma N\left|\mathrm{GHZ}\right\rangle,
\end{aligned}
$$

we can obtain the pairs of $(\mathcal{K},\mathcal{C})$ as

$$
\begin{aligned}
&(\mathcal{K},\mathcal{C})(\left|+\right\rangle^{\otimes N}) \approx \left(\gamma\sqrt{6N^2-2N},\ \gamma N\right),\\
&(\mathcal{K},\mathcal{C})(\left|\mathrm{GHZ}\right\rangle) \approx \left(2\gamma N^2,\ \gamma N^2\right).
\end{aligned}
$$

These expressions lead to $T_*(\left|+\right\rangle^{\otimes N}) \sim O(1/N)$ and $T_*(\left|\mathrm{GHZ}\right\rangle) \sim O(1/N^2)$, for fixed λ and γ. Therefore, although $\left|\mathrm{GHZ}\right\rangle$ can ideally improve the estimation accuracy, it is harder to prepare and more fragile than $\left|+\right\rangle^{\otimes N}$.

4.3.4 Fock state

Finally, we see the behavior of T_* in the case of ideal Fock state with n photons under the photon leakage modeled by $M = \sqrt{\gamma}a$. Following the example in Chapter 3, we set the initial state to be $\rho_0 = \left|n\right\rangle\left\langle n\right|$ and the system Hamiltonian to be $H = i\omega(a^\dagger - a)$. Then,

$$
\begin{aligned}
&\mathcal{K} = \sqrt{2}\|-\omega[a^\dagger - a,\rho_0] + \gamma\mathcal{D}^\dagger[a]\rho_0\|_{\mathrm{F}} = \sqrt{\omega^2(8n+4)+\gamma^2(4n^2+4n+2)},\\
&\mathcal{C} = \gamma\|a\left|n\right\rangle\|^2 - \gamma|\left\langle n|a|n\right\rangle|^2 = \gamma n,
\end{aligned}
$$

and thus we obtain the QSL

$$
\begin{aligned}
T_*(\left|n\right\rangle) = &\frac{\lambda}{\sqrt{\omega^2(2n+1)+\gamma^2(n^2+n+1/2)}}\\
&+\frac{\gamma n}{\omega^2(4n+2)+\gamma^2(2n^2+2n+1)}\ln\left[\frac{\gamma n}{\gamma n+\sqrt{\omega^2(8n+4)+\gamma^2(4n^2+4n+2)}\lambda}\right].
\end{aligned}
$$

Figure 4.3 shows $T_*(\left|n\right\rangle)$ for each pair of (ω,γ). As the initial photon number n increasing, T_* decreases, implying the natural fact that a large Fock state is fragile to the photon leakage. When $n = 0$, i.e., the vacuum state, each lower bounds takes 0.1, because there is no photon to be leaked.

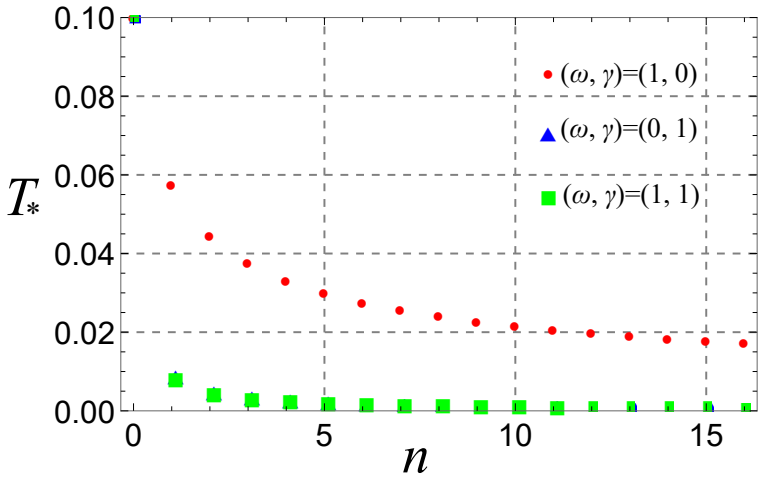

Fig. 4.3: T_* as a function of n for each (ω, γ) when $\lambda = 0.1$.

4.4 Robust state preparation based on quantum speed limit

4.4.1 Quantum speed limit as a measure of robustness

Let us consider the situation that a pure initial state $\rho_0 = |\psi_0\rangle \langle\psi_0|$ and a value of radius $\lambda = \sqrt{V_T}$ are specified. This means that we are specified a region $\mathcal{R}_\lambda(\rho_0)$, which is the set of all states whose distance from ρ_0 is less than λ. That is, as depicted in Fig. 4.4, λ can be interpreted as the radius of a circle region $\mathcal{R}_\lambda(\rho_0)$. Then the evolution time T of the cost V_t for evolving from $V_0 = 0$ to V_T has the meaning of the time that the state first exits from $\mathcal{R}_\lambda(\rho_0)$. Thus, if T is large for a given λ, the state ρ_t starting from the initial state ρ_0 takes a long time to exit from $\mathcal{R}_\lambda(\rho_0)$. In this case, we can say that ρ_0 is robust against the decoherence M. Conversely, if we choose another initial state ρ_0' and find that the evolution time T' is smaller than T for the same value of λ, this means that the state faster escapes from $\mathcal{R}_\lambda(\rho_0')$ (Fig. 4.4). In this case, the initial state ρ_0' is largely affected by the decoherence and can be easily changed; that is, ρ_0' is fragile. From this idea, it is natural that the QSL $T_*(\rho_0)$ can be used to characterize a robust initial state ρ_0 against a decoherence M. More precisely, for a certain λ, the state ρ_0 with a large value of T_* is guaranteed to take a longer time T than T_* to escape from $\mathcal{R}_\lambda(\rho_0)$. Also, in this thesis we define that ρ_0 is more robust than ρ_0' when $T_*(\rho_0) > T_*(\rho_0')$, although this does not always lead to $T(\rho_0) > T(\rho_0')$. Moreover, for a given ρ_0 and a relatively small value of λ, it has an important meaning to suitably design the system operators such that $T_*(\rho_0)$ becomes larger, to protect ρ_0 against the decoherence M. In this section, we discuss this

engineering problem, especially in the case where H is the design object.

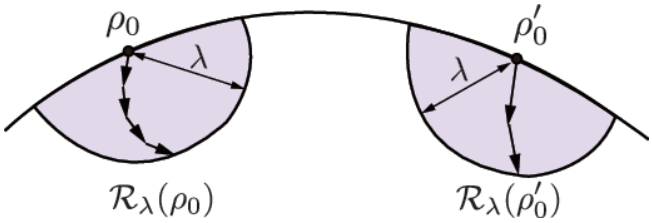

Fig. 4.4: Robustness of the quantum state. (Left) If $T_*(\rho_0)$ is large, the quantum state ρ_t must take a long time to exit from the region $R_\lambda(\rho_0)$ with fixed radius λ. This means that ρ_0 is robust. (Right) If $T_*(\rho_0')$ is small for the same λ, then ρ_t may quickly exit from $R_\lambda(\rho_0')$. This means that ρ_0' fragile compared to ρ_0. Reprinted figure from [105, DOI: 10.1103/PhysRevA.102.042606]. Creative Commons Attribution 4.0 International license. Copyright 2020 by K. Kobayashi and N. Yamamoto.

4.4.2 Hamiltonian engineering for robust state preparation

In the examples given in Section 4.3, we identified a robust state $\rho_0 = |\psi_0\rangle\langle\psi_0|$, under given decoherence and system Hamiltonian by comparing the QSL T_*. In this section, as an application of this idea, we discuss designing an optimal Hamiltonian that maximizes T_*, given a fixed initial state ρ_0 and decoherence M. More specifically, our purpose is to find H that protects ρ_0 against a given decoherence M by maximizing the lower bound of the escape time of the state from a region initialized at ρ_0.

Here we give a mathematical explanation of this problem; maximizing T_* with respect to H is equivalent to minimizing $\mathcal{K}$, because, as verified above, T_* is a monotonically decreasing function with respect to $\mathcal{K}$. Now we see the function:

$$\begin{aligned}\mathcal{K}^2/2 &= \mathrm{Tr}[\left(i[H,\rho_0] + \mathcal{D}[M]^\dagger\rho_0\right)^2] \\ &= \mathrm{Tr}\left(-[H,\rho_0]^2\right) + 2\mathrm{Tr}\left(i[H,\rho_0]\mathcal{D}[M]^\dagger\rho_0\right) + \mathrm{Tr}\left[(\mathcal{D}[M]^\dagger\rho_0)^2\right] \\ &= 2\left(\mathrm{Tr}\left(H^2\rho_0\right) - \mathrm{Tr}\left(H\rho_0 H\rho_0\right)\right) + 2\mathrm{Tr}\left(i[H,\rho_0]\mathcal{D}^\dagger[M]\rho_0\right) + \mathrm{Tr}[\left(\mathcal{D}^\dagger[M]\rho_0\right)^2]\end{aligned}$$

Then, we consider the following cost function:

$$F(H) = \mathrm{Tr}\left(H^2\rho_0\right) - \mathrm{Tr}\left(H\rho_0 H\rho_0\right) + \mathrm{Tr}\left(i[\rho_0, \mathcal{D}^\dagger[M]\rho_0]H\right),$$

which is equivalent to $\mathcal{K}^2/4 - \mathrm{Tr}[\left(\mathcal{D}^\dagger[M]\rho_0\right)^2]/2$. Here it is clear that $F(H)$ is a convex quadratic function with respect to H, and thus the optimal Hamiltonian H_{opt} can be systematically determined. Note that this tractable problem can be formulated due to

the explicit form of the QSL; recall that this was indeed the motivation to derive T_* and compare it to $T_{\rm DC}$.

In order to have $H_{\rm opt} = \mathrm{argmin}_H F(H)$, we calculate the matrix derivative of $F(H)$ with respect to H:

$$\frac{\partial F(H)}{\partial H} = (H\rho_0 + \rho_0 H)^\top - 2\left(\rho_0 H \rho_0\right)^\top + i\left([\rho_0, \mathcal{D}^\dagger[M]\rho_0]\right)^\top,$$

where we have used the following matrix formulae [100]:

$$\begin{aligned}
&\frac{\partial}{\partial X}\mathrm{Tr}(XA) = A^\top, \\
&\frac{\partial}{\partial X}\mathrm{Tr}(X^2 A) = (XA + AX)^\top, \\
&\frac{\partial}{\partial X}\mathrm{Tr}(AXAX) = 2(AXA)^\top.
\end{aligned}$$

Hence, $H_{\rm opt}$ satisfies

$$H_{\rm opt}\rho_0 + \rho_0 H_{\rm opt} - 2\rho_0 H_{\rm opt}\rho_0 + i[\rho_0, \mathcal{D}^\dagger[M]\rho_0] = 0. \tag{4.19}$$

This is a simple linear equation with respect to H, for a given ρ_0 and M. Thus, $H_{\rm opt}$ can be efficiently computed by solving Eq. (4.19).

4.4.3 Example

Let us again consider the dissipative qubit system. We choose the decoherence as $M = \sqrt{\gamma}\sigma_-$, and the initial state to be protected as $|\psi_0\rangle = [1/2, \sqrt{3}/2]$. Also, we parametrize $H_{\rm opt}$ as

$$H_{\rm opt} = u_1\sigma_x + u_2\sigma_y + u_3\sigma_z,$$

where (u_1, u_2, u_3) are real-constant parameters to be determined. Then by solving the linear equation (4.19) we have

$$\begin{aligned}
u_2 &= -\frac{\sqrt{3}}{16}\gamma, \\
u_1 &= -\sqrt{3}u_3.
\end{aligned}$$

The term $u_1\sigma_x + u_3\sigma_z$ always commutes with $\rho_0 = |\psi_0\rangle\langle\psi_0|$ when $u_1 = -\sqrt{3}u_3$. Thus, only the term of $u_2\sigma_y$ has an effect on the dynamics of V_t given in Eq. (4.11). Figure 4.5 (a) shows the evolution of V_t, in the following three cases: $H = H_{\rm opt}$, $H = 0$ (i.e., the system is simply decohered), and $H = \sigma_z$. The decoherence strength is chosen as $\gamma = 1$. It is clear that $H_{\rm opt}$ makes longer the time for the state escaping from $\mathcal{R}_\lambda(\rho_0)$ for any $\lambda = \sqrt{V_T}$, than the other two cases. In particular, when $H_{\rm opt}$ is applied, the state remains in the region $\mathcal{R}_\lambda(\rho_0)$ with radius $\lambda = \sqrt{1 - 0.9}$, for all time. From a physical viewpoint, this result is attributed the fact that the anticlockwise rotation around the y axis with the

driving frequency $\sqrt{3}\gamma/16$ combats the undesired dynamics caused by the decoherence.

Next, we study a qutrit system. We adopt the decoherence as the ladder-type decay

$$M = \sqrt{\gamma}\begin{bmatrix} 0 & 0 & 0 \\ 1 & 0 & 0 \\ 0 & 1 & 0 \end{bmatrix},$$

and the initial state as $|\psi_0\rangle = \left[1/2,\ 1/\sqrt{2},\ 1/2\right]$, which corresponds to the vector of the qutrit with $\theta = \varphi = \pi/4$. The control Hamiltonian to be determined can be fully parametrized as

$$H_{\text{opt}} = \sum_{i=1}^{8} u_i \Lambda_i, \tag{4.20}$$

where $\{\Lambda_i\}_{i=1}^{8}$ are the Gell-Mann matrices defined as

$$\Lambda_1 = \begin{bmatrix} 0 & 1 & 0 \\ 1 & 0 & 0 \\ 0 & 0 & 0 \end{bmatrix},\ \Lambda_2 = \begin{bmatrix} 0 & -i & 0 \\ i & 0 & 0 \\ 0 & 0 & 0 \end{bmatrix},\ \Lambda_3 = \begin{bmatrix} 1 & 0 & 0 \\ 0 & -1 & 0 \\ 0 & 0 & 0 \end{bmatrix},$$

$$\Lambda_4 = \begin{bmatrix} 0 & 0 & 1 \\ 0 & 0 & 0 \\ 1 & 0 & 0 \end{bmatrix},\ \Lambda_5 = \begin{bmatrix} 0 & 0 & -i \\ 0 & 0 & 0 \\ i & 0 & 0 \end{bmatrix},\ \Lambda_6 = \begin{bmatrix} 0 & 0 & 0 \\ 0 & 0 & 1 \\ 0 & 1 & 0 \end{bmatrix},$$

$$\Lambda_7 = \begin{bmatrix} 0 & 0 & 0 \\ 0 & 0 & -i \\ 0 & i & 0 \end{bmatrix},\ \Lambda_8 = \frac{1}{\sqrt{3}}\begin{bmatrix} 1 & 0 & 0 \\ 0 & 1 & 0 \\ 0 & 0 & -2 \end{bmatrix}.$$

Note that these matrices form an orthonormal basis set in SU(3). In this setting, using (4.19), we obtain the condition

$$\begin{cases} 2\sqrt{2}u_1 + 5u_3 + 2u_4 - 2\sqrt{2}u_6 + \sqrt{3}u_8 = 0, \\ 3u_3 + 2u_4 - \sqrt{3}u_8 = 0, \\ 3\sqrt{2}u_2 + 2u_5 - \sqrt{2}u_7 = -\gamma, \\ 8u_5 + 8\sqrt{2}u_7 = -\gamma. \end{cases}$$

Under this parametrization, the terms with coefficients $(u_1, u_3, u_4, u_6, u_8)$ in H_{opt} always commute with ρ_0, hence they do not affect on the dynamics of V_t as well as $\mathcal{K}$. Figure 4.5 (b) shows the time evolution of V_t, in the cases of $H = H_{\text{opt}}$ with the parameters

$$(u_2, u_5, u_7) = (-3\sqrt{2}\gamma/16,\ 0,\ -\sqrt{2}\gamma/16)$$

and compares it to the cases $H = 0$ and $S_z = |E\rangle\langle E| - |G\rangle\langle G|$. We can find that certainly $H = H_{\text{opt}}$ makes the escaping time longer, though the advantage over the other two cases

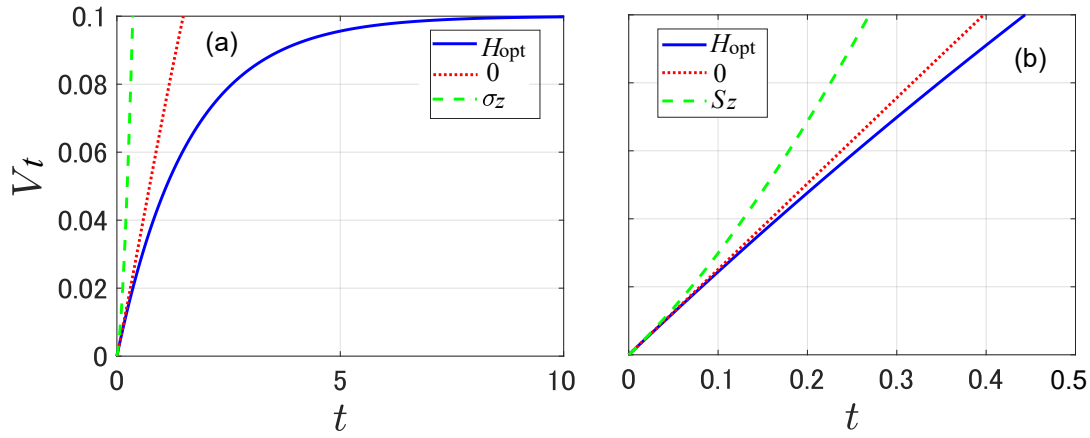

Fig. 4.5: Time evolution of V_t in the case of (a) qubit driven by $H = H_{\rm opt}$ (blue solid line), 0, (red dotted line), and σ_z (green dashed line). Also the case of (b) qutrit driven by $H = H_{\rm opt}$ (blue solid line), 0, (red dotted line), and S_z (green dashed line). Reprinted figure from [105, DOI: 10.1103/PhysRevA.102.042606]. Creative Commons Attribution 4.0 International license. Copyright 2020 by K. Kobayashi and N. Yamamoto.

is not so big compared to the previous qubit case. It is assumed that, as the dimension of the system becomes higher, the effect of $H_{\rm opt}$ against the noise becomes small, although we cannot say for certain.

4.5 Time-dependent limit for reachability

In Chapter 3, we have discussed the reachability problem under decoherence and presented the distance limit for a general open quantum systems. However, the limit works only for the steady state of the controlled system and the transition time has not been considered. In general, the reachable set usually depends on the transition time, hence it is natural to take time constraints into account for rigorously analyzing the reachability problem.

Let us show the QSL T_* again:

$$T \geq T_* := \frac{2\lambda}{\mathcal{K}} + \frac{2\mathcal{C}}{\mathcal{K}^2} \ln\left[\frac{\mathcal{C}}{\mathcal{C}+\mathcal{K}\lambda}\right],$$

where

$$\mathcal{K} = \sqrt{2}\|i[H,\rho_0] + \mathcal{D}^\dagger[M]\rho_0\|_{\mathrm{F}},$$
$$\mathcal{C} = \|M|\psi_0\rangle\|^2 - |\langle\psi_0|M|\psi_0\rangle|^2.$$

This inequality means that the evolution time T and the fidelity-based distance $\lambda = \sqrt{1-\mathrm{Tr}(\rho_0\rho_T)}$ implicitly correlated. Furthermore, T_* is monotonically increasing with respect to λ as

$$\frac{\partial T_*}{\partial \lambda} = \frac{2}{\mathcal{K}}\left(1 - \frac{\mathcal{C}}{\mathcal{K}}\frac{\mathcal{K}}{\mathcal{C}+\mathcal{K}\lambda}\right) = \frac{2\lambda}{\mathcal{C}+\mathcal{K}\lambda} \geq 0.$$

From the above facts, if the parameters characterizing the system's evolution (ρ_0, H, M, T) are specified, λ has a time-dependent limit;

When the system is closed, the explicit upper bound λ^* is easily obtained:

$$\lambda \leq \lambda^* := \frac{\mathcal{K}T}{2}.$$

On the other hand, when the system is open, it is impossible to obtain the explicit expression of λ^*. Then, we further bound T_* from below:

$$T \geq \frac{2\lambda}{\mathcal{K}} - \frac{2\mathcal{C}}{\mathcal{K}^2}\ln\left[1+\frac{\mathcal{K}\lambda}{\mathcal{C}}\right] \geq \frac{2\lambda}{\mathcal{K}} - \frac{2\mathcal{C}}{\mathcal{K}^2}\frac{(\mathcal{K}\lambda/\mathcal{C})(2+\mathcal{K}\lambda/\mathcal{C})}{2(1+\mathcal{K}\lambda/\mathcal{C})}$$
$$= \frac{\lambda^2}{\mathcal{C}+\mathcal{K}\lambda},$$

where the inequality $\ln(1+x) \leq x(2+x)/\{2(1+x)\}$ $(x \geq 0)$ has been used. As a result, λ^* for open quantum systems is as follows:

$$\lambda \leq \lambda^* := \frac{\mathcal{K}T + \sqrt{(\mathcal{K}T)^2 + 4\mathcal{C}T}}{2}.$$

4.5.1 Example

We first consider the dynamics of the open qubit system characterized by the following setting:

$$|\psi_0\rangle = [\cos\theta,\ \sin\theta]^\top,\ H = \omega\sigma_z,\ M = \sqrt{\gamma}\sigma_-,$$

which leads to

$$\mathcal{K} = \sqrt{2\gamma^2 \cos^2 2\theta + (4\omega^2 + \gamma^2/4)\sin^2 2\theta},$$
$$\mathcal{C} = \gamma \cos^4 \theta.$$

Figure 4.6 (a) shows λ^* when $\gamma = 0$; in this case $\lambda^* = \omega|\sin 2\theta|T$ takes zero at $|\psi_0\rangle = |0\rangle$ or $|1\rangle$ for each T. This means that $|0\rangle$ or $|1\rangle$ does not change because those are the steady state of the equation $d\rho_t/dt = -i[H, \rho_t]$. Meanwhile, λ^* takes maximum at $|\psi_0\rangle = |+\rangle$, corresponding to that T_* takes minimum at $|\psi_0\rangle = |+\rangle$ when $(\omega, \gamma) = (1, 0)$ as shown in Fig. 4.3 (a). Importantly, in a given evolution time $T = 0.5$, λ can only take at most 0.5, i.e., the final fidelity $F_T = 0.5$. Figure 4.6 (b) shows λ^* when $\gamma > 0$; λ^* takes the maximum at $|\psi_0\rangle = |0\rangle$, implying that $|0\rangle$ is mostly driven by the decoherence. In particular, it is noted that the state cannot reach its orthogonal state for $T = 0.1$, 0.3, while the initial state with $\theta \leq 57.3^\circ$ may reach its orthogonal state for the sufficient time $T = 0.5$.

Next, we study a unitary gate implementation of the qubit system. Let a target 2×2 unitary gate be followed by

$$U(\alpha, \beta) = \begin{bmatrix} e^{i\frac{\alpha}{2}} \cos\frac{\beta}{2} & e^{i\frac{\alpha}{2}} \sin\frac{\beta}{2} \\ -e^{-i\frac{\alpha}{2}} \sin\frac{\beta}{2} & e^{-i\frac{\alpha}{2}} \cos\frac{\beta}{2} \end{bmatrix}, \tag{4.21}$$

where $0 \leq \alpha \leq 2\pi$, $0 \leq \beta \leq \pi$. The control Hamiltonian is chosen as

$$H = u_1\sigma_x + u_2\sigma_z.$$

Note that $U(\alpha, \beta)$ can be implemented by suitably choosing u_1 and u_2 for sufficient time. Also, let the initial state be $= [\cos\theta, \sin\theta]^\top$ and the final state be $|\psi_T\rangle = U(\alpha, \beta)|\psi_0\rangle$. Now the lower bound $T_*(|\psi_0\rangle)$ is calculated as follows:

$$\begin{aligned} T_*(|\psi_0\rangle) &= \frac{2\sqrt{1 - |\langle\psi_0|\psi_T\rangle|^2}}{\mathcal{K}} \\ &= \frac{\sqrt{1 - |\langle\psi_0|U|\psi_0\rangle|^2}}{\sqrt{\langle\psi_0|H^2|\psi_0\rangle - \langle\psi_0|H|\psi_0\rangle^2}} \\ &= \frac{\sqrt{1 - \cos^2(\alpha/2)\cos^2(\beta/2) - \sin^2(\alpha/2)\cos^2(2\theta + \beta/2)}}{|u_1 \cos 2\theta - u_2 \sin 2\theta|}. \end{aligned} \tag{4.22}$$

Figure 4.6 (c) shows $T_*(\alpha, \beta)$ in case of $\theta = 0$ for each driving times $T = 0.3$, 0.5, and 0.8, and fixed values $u_1 = 1$. The colored area is the all sets satisfying (4.22) and the white area is the one that does not satisfy (4.22). For instance, when $T = 0.5$, the inequality $T \geq T_*(|\psi_0\rangle)$ is saturated at $\beta = \pi/3$. In this case, the unitary operator (4.21) is

$$U(\alpha, \beta) = \frac{1}{2}\begin{bmatrix} \sqrt{3}e^{i\frac{\alpha}{2}} & e^{i\frac{\alpha}{2}} \\ -e^{i\frac{\alpha}{2}} & \sqrt{3}e^{-i\frac{\alpha}{2}} \end{bmatrix},$$

which leads to the final fidelity $F_T = |\langle\psi_0|\psi_T\rangle|^2 = 0.75$. This means that we can only steer the state to that with fidelity 0.75 at most in $T = 0.5$. Next, if $\theta = \pi/4$, the lower bound is

$$T_*(\alpha, \beta) = \frac{|\sin\{(\alpha - \beta)/2\}|}{|u_2|}.$$

As depicted in Fig. 4.6 (d), the reachable set is remarkably changed from Fig. 4.6 (c). Note that $T_*(\alpha, \beta)$ takes zero at $U(0, 0) = U(2\pi, 0) = I$ and $U(\pi, \pi) = i\sigma_x$. In this case, the final fidelity is $F_T = |\langle\psi_0|\psi_T\rangle|^2 = |\langle\psi_0|U|\psi_0\rangle|^2 = 1$, hence there is no difference between the initial state and the final state in terms of the distance. On the other hand, $T_*(\alpha, \beta)$ is maximized at $U(0, \pi) = U(2\pi, \pi) = -i\sigma_y$ and $U(\pi, 0) = i\sigma_z$, and in fact those gates cannot be prepared even if $T = 0.8$. Indeed, this result is reasonable because the final states for each gates are $|\psi_T\rangle = -i\sigma_y |\psi_0\rangle = [1, -1]/\sqrt{2}$ and $|\psi_T\rangle = i\sigma_z |\psi_0\rangle = [i, -i]/\sqrt{2}$, which are identical to the orthogonal states to $|\psi_0\rangle$; that is, those gates are the one that generates the state that is far from the initial state. In this way, by means of the QSL T_*, we can characterize the implementable gate in a certain control time.

4.6 Summary

The main contribution of this chapter is to exploit the usage of QSLs. The first is to propose an idea to use the QSL to characterize robust quantum states of a given open quantum system. Based on this view, we have formulated the engineering problem of a Hamiltonian that makes a target states robust against a decoherence. In this engineering problem, it is important for the QSL to be explicitly computable. In order that, the QSL derived in Section 4.2 indeed satisfies this requirement and further it is tighter than another known QSL in a setup where the decoherence is small and the region $\mathcal{R}_\lambda(\rho_0)$ is small. In addition, the Hamiltonian engineering problem is proven to be a convex quadratic optimization problem, which is efficiently solvable. Several examples have been studied, in particular showing another view of the fragility of the GHZ state in quantum metrology. The second is the application to characterization of reachability. This approach is based on that the fidelity-based distance λ and evolution time T are related by the inequality $T \geq T_*(\lambda)$. As a result, we have obtained the explicit upper bound λ^* depending on T. Compared to the control limit J_* given in Chapter 3, the advantage of λ^* is that λ^* can take a meaningful value except even if the system is closed. Due to this, λ^* can be used for characterizing the implementable gate in a given control time, as illustrated in Subsection 4.5.2.

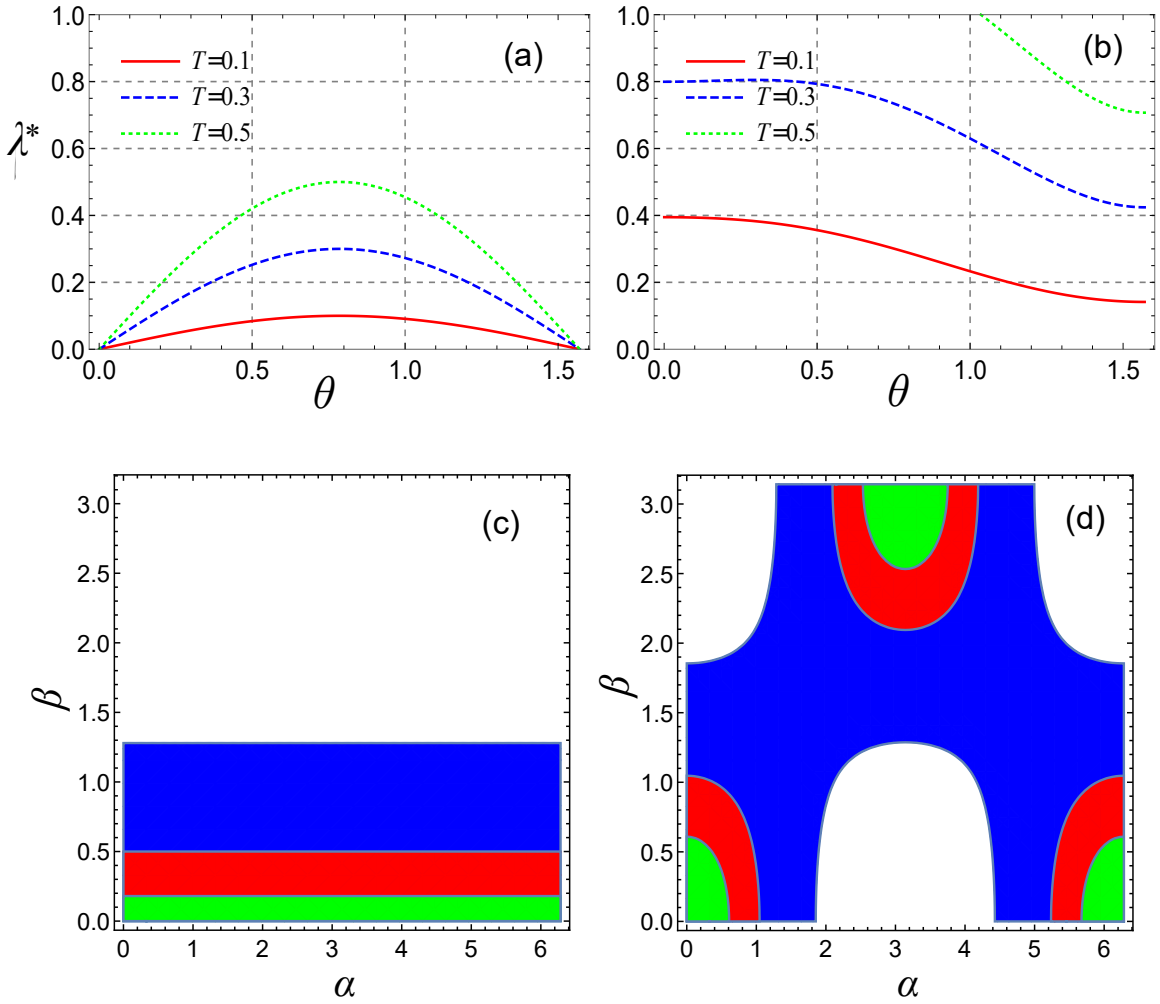

Fig. 4.6: λ^* as a function of θ for each evolution time T when (a) $\gamma = 0$ and (b) $\gamma = 1$, in unit of $\omega = 1$. Reachable set of the unitary dynamics of the qubit when (c) $\theta = 0$ and (d) $\theta = \pi/4$ for $T = 0.3$ (green area), $T = 0.5$ (red area), and $T = 0.8$ (blue area).

Chapter 5

Conclusion

5.1 Conclusion

This thesis is motivated by the two questions posed in Chapter 1: (i) How close the controlled quantum state can be steered to a target state under decoherence? (ii) How long can we preserve the controlled system around at the target state? Aiming to give answers to these fundamental questions, we have provided the distance and time limits for a dynamical quantum system under decoherence by means of reachability and QSL.

Chapter 3 has studied the distance limit for a controlled open quantum system under decoherence. First, Section 3.1 has shown the performance of the quantum control (i.e., MBF) for the imperfect case under the decoherence and presented the idea of analyzing the problem. Based on it, Section 3.2 has derived a fundamental limit for the reachability under decoherence; more specifically, we present a lower bound of the fidelity-based distance between the controlled quantum state under decoherence and the target state. This lower bound has advantages in generality and computability; that is, it can not only be applied for a general open Markovian quantum system driven by the decoherence process and some types of control method, e.g., the open-loop and MBF controls and reservoir engineering, but also is straightforward to calculate without solving any equation. Moreover, thanks to its generic form, the lower bound gives a characterization of the target state that is largely influenced by the decoherence. Thereby, as demonstrated in some example, the lower bound provides a useful guide for choosing the target. Importantly, providing deep insight into quantum engineering, the lower bound is used to derive a theoretical limit in quantum metrology; for instance, for a typical large-size atomic ensemble under open-loop control and dephasing noise, the fidelity to the target (the GHZ state or a highly entangled Dicke state) must be less than 0.875, irrespective of the control strategy.

Chapter 4 has studied a limit on the evolution time of a Markovian open quantum system driven by the decoherence in terms of the QSL. The main contribution of this chapter is twofold; First, we have proposed to use the QSL as a measure of robust quantum states; that is, for an undesirable state evolution driven by decoherence, we consider the initial

state ρ_0 with a larger QSL to be robust against a decoherence. Based on this idea, we have formulated the engineering problem of the control Hamiltonian that protect an ideal initial state against a given decoherence. In this engineering problem, it is important for the QSL to be explicitly computable; the QSL derived in Section 4.2 indeed satisfies this condition and further it is tighter than another known QSL in the setup where the decoherence is small and the region $\mathcal{R}_\lambda(\rho_0)$ is small. In addition, the Hamiltonian engineering problem is proven to be a convex quadratic optimization problem. Thanks to this, the problem is efficiently solvable. Some examples have been investigated, in particular showing another view of the fragility of the GHZ state in quantum metrology. Second, we have applied the QSL to the characterization of the reachability for a decohering quantum system; that is to say, we have derived the time-dependent upper bound of the distance from the initial state based on the QSL presented in Section 4.2. The notable points of this approach are the following two: (i) It is possible to take the control time into account for the reachability analysis. (ii) A meaningful bound can be obtained even if the system is closed. A particular interesting example characterizing the gate implementation in a given control time has been given. We believe that the results given in this paper will provide a new perspective of the QSL as a tool in quantum engineering.

5.2 Future work

For the result given in Chapter 3, an important remaining work is to explore an achievable lower bound and develop an efficient strategy for synthesizing the controller (e.g., MBF control input) that achieves it. We have not found the condition to reach the bound. If the amount of energy usable for control $\bar{u}$ increases, we expect that the distance between the state and the target becomes smaller. However, $\mathcal{U}$ increases and as a result the lower bound J_* also becomes smaller. Hence there is no guarantee that the gap between the actual distance and its lower bound J_* becomes exactly zero. A similar result is obtained for the case of decoherence strength, as demonstrated in Fig. 3.4 (c); if the strength of decoherence decreases, then both the actual distance via some control and the lower bound J_* becomes smaller, but we cannot say these values coincide at some point of time.

For the result given in Chapter 4, the derivation of the QSL T_* is based on the assumption that the system operators (H, M) are time-independent. To develop more strategic Hamiltonian engineering, the extension to the case that the system dynamics has a time dependent Hamiltonian H_t is an interesting work. That is, the state ρ_t obeys the master equation

$$\frac{d\rho_t}{dt} = -i[H_t, \rho_t] + \mathcal{D}[M]\rho_t,$$

to have the QSL $T_*(\rho_0)$, from the inequality (4.14)

$$\frac{dV_t}{dt} = \mathcal{K}_t\sqrt{V_t} + \mathcal{C}, \tag{5.1}$$

where $\mathcal{K}_t = \sqrt{2}\|i[H_t, \rho_t] + \mathcal{D}^\dagger[M]\rho_t\|_{\mathrm{F}}$. In this case we can possibly make $\mathcal{K}_t$ smaller than the case time-independent H by suitably designing H_t, instead of not being able to have a general explicit bound. Another important work is the generalization to the case that the system is under the continuous measurement. In fact, the time required for the continuous measurement has not been carefully considered, especially in the MBF scheme. Also, few works of the QSL related to the MBF has been proposed, except for [101]. Therefore, the QSL including the continuous measurement is the important work in the field.

Appendix A: Proof of Some Inequalities

Here we prove the following inequalities used in Chapter 4:

$$\frac{x}{1+x} \leq \ln(1+x) \leq \frac{x(x+2)}{2(x+1)} \quad (x \geq 0), \tag{A.1}$$

and

$$\frac{2(\alpha-\beta)^2}{\alpha+\beta} \leq (\alpha-\beta)\ln\left(\frac{\alpha}{\beta}\right), \quad (\alpha,\beta \geq 0). \tag{A.2}$$

First, we prove the inequality (A.1). The lower bound is simply proved by considering the inequality $\ln(1+x) \leq x$ for $x \geq 0$. By replacing $1+x$ with $1/(1+x)$, we have $x/(1+x) \leq \ln(1+x)$. The upper bound is proved by using the Schwarz inequality for $x \geq 1$ as follows:

$$\ln(x) = \int_1^x \frac{du}{u} \leq \sqrt{\int_1^x du \int_1^x \frac{du}{u^2}} = \sqrt{x} - \frac{1}{\sqrt{x}} \leq \frac{x^2-1}{2x}.$$

Then, by replacing x with $1+x$, we have the upper bound.

Next, to prove the inequality (A.2), we introduce the following relation:

$$\frac{2(x-1)}{x+1} \leq \ln(x) \quad (x \geq 1). \tag{A.3}$$

Now consider the function

$$F(\alpha,\beta) = (\alpha-\beta)\left\{\ln\left(\frac{\alpha}{\beta}\right) - \frac{2(\alpha-\beta)}{\alpha+\beta}\right\}.$$

When $\alpha > \beta$,

$$\begin{aligned} F(\alpha,\beta) &= (\alpha-\beta)\left\{\ln\left(\frac{\alpha}{\beta}\right) - \frac{2(\alpha-\beta)}{\alpha+\beta}\right\} \\ &\geq (\alpha-\beta)\left\{\frac{2(\alpha/\beta-1)}{\alpha/\beta+1} - \frac{2(\alpha-\beta)}{\alpha+\beta}\right\} = 0. \end{aligned}$$

When $\alpha < \beta$,

$$\begin{aligned} F(\alpha,\beta) &= (\beta-\alpha)\left\{\ln\left(\frac{\beta}{\alpha}\right) + \frac{2(\alpha-\beta)}{\alpha+\beta}\right\} \\ &\geq (\beta-\alpha)\left\{\frac{2(\beta/\alpha-1)}{\beta/\alpha+1} - \frac{2(\beta-\alpha)}{\alpha+\beta}\right\} = 0. \end{aligned}$$

Therefore, the inequality (A.2) holds for all $\alpha, \beta \geq 0$.

Figure A.1 (a) and Figure A.1 (b) illustrate the tightness of Eq. (A.1) and Eq. (A.2), respectively. The gap of (A.1) becomes small if x is small [Fig. A.1 (a)]. Figure A.1 (b) shows that the (A.2) is tight over all (α, β), and thus it gives a better estimate on the analysis.

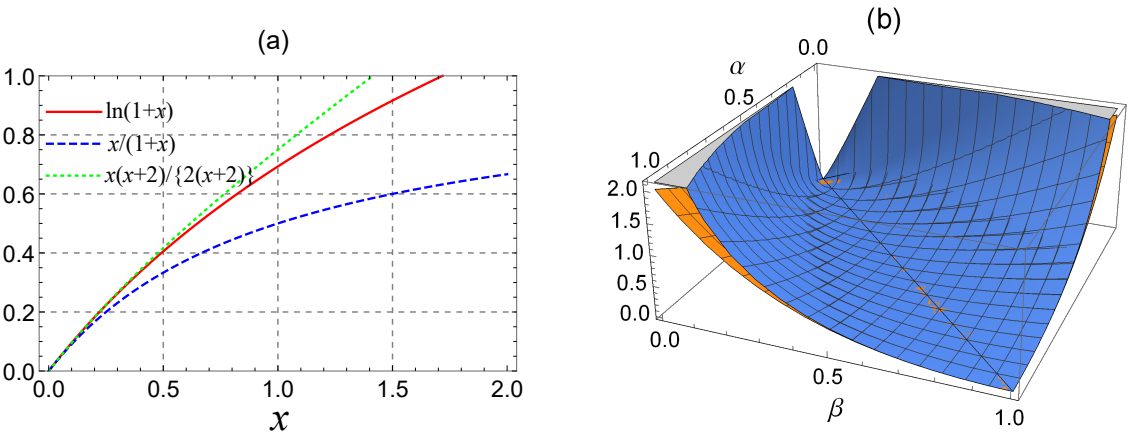

Fig. A.1. Plots of (A.1) and (A.2).

Appendix B: QSL based on J_*

Actually, the lower bound J_* given in Chapter 3 is related to a QSL. We consider the evolution time T such that, for the cost function $J_t = 1 - \mathrm{Tr}(\rho_0\rho_t)$, an initial cost J_0 changes to a final cost J_T; both J_0 and J_T are specified, e.g., $J_0 = 1$ and $J_T = 0.1$. As proven in Chapter 3, the cost function J_t satisfies

$$\frac{dJ_t}{dt} \geq -(\mathcal{A}+\mathcal{U})\sqrt{J_t} + \mathcal{E}. \tag{B.1}$$

Because we are interested in the decrease of the cost, we assume $J_0 > J_T > J_*$ (as J_* is not generally achievable under decoherence). Then, by integrating the above inequality (B.1) from J_T to J_0, we have

$$T \geq T_* := \frac{2}{\mathcal{A}+\mathcal{U}} \left\{ \sqrt{J_0} - \sqrt{J_T} + \sqrt{J_*} \ln \left(\frac{\sqrt{J_0} - \sqrt{J_*}}{\sqrt{J_T} - \sqrt{J_*}} \right) \right\}. \tag{B.2}$$

T_* is the QSL that gives a lower bound of the evolution time of the cost function. Likewise J_*, the lower bound T_* is applicable to several control setting including feedback and reservoir engineering. The lower bound T_* is different from other QSLs for open quantum systems such as Del Campo's bound T_{DC}. Also, for a closed system, (i.e., the case $\mathcal{A} = \mathcal{E} = 0$), the lower bound takes the form $T_* = \{2(\sqrt{J_0} - \sqrt{J_T})\}/\mathcal{U}$, which has the same form of some known QSLs such as the Mandelstam-Tamm bound and Margolus-Levitin bound. Finally, for the case of qubit control problem that aims to change the ground state $|1\rangle$ to the excited state $|0\rangle$ under decoherence $M = \sqrt{\gamma}\sigma_z$ and the driving Hamiltonian $H = u\sigma_x$ with (u, γ) constant, the lower bound T_* is calculated as $T_* = (2 - 2\sqrt{J_T})/(\sqrt{2}\gamma + u)$. For instance when $\gamma = u = 1$ MHz and $J_T = 0.1$, then $T_* \simeq 0.566\mu s$.

Appendix C: Application of QSL to Glover's Problem

The Grover's problem is the database search problem developed in [102]. The purpose here is to find the target state $|M\rangle$ among the N orthonormal state $|0\rangle, |1\rangle, \cdots |M\rangle, \cdots |N-1\rangle$. Classically, the computational time is N steps in average $T \sim O(N)$. On the other hand, the quantum algorithm outperforms the classical one and we find speeding up $T \sim O(\sqrt{N})$. Here we verify that the minimal time for required for the Glover's algorithm is order $O(\sqrt{N})$ by using our QSL T_*. We consider the total Hamiltonian

$$\begin{aligned} H_t &= (1-f_t)H_I + f_t H_P, \\ H_I &= I - |g\rangle\langle g|, \\ H_P &= I - |M\rangle\langle M|, \end{aligned} \tag{C.1}$$

where $0 \leq f_t \leq 1$, $f_0 = g_T = 1$ and $f_T = g_0 = 0$. In the Grover problem, we start from $|g\rangle$ which is the ground state of H_I at $t = 0$, and the state is driven to $|M\rangle$ which is the ground state of H_P at terminal time $t = T$. The relation of $|g\rangle$ and $|M\rangle$ is

$$\langle g|M\rangle = \frac{1}{\sqrt{N}}. \tag{C.2}$$

In this setting

$$\begin{aligned} \langle g|H_t^2|g\rangle &= f_t^2 \left(\langle g| - \frac{1}{\sqrt{N}}\langle M|\right)\left(|g\rangle - \frac{1}{\sqrt{N}}|M\rangle\right) \\ &= f_t^2\left(1 - \frac{1}{N}\right), \end{aligned} \tag{C.3}$$

$$\begin{aligned} \langle g|H_t|g\rangle^2 &= \langle g|f_t\left(|g\rangle - \frac{1}{\sqrt{N}}|M\rangle\right) \\ &= f_t^2\left(1 - \frac{1}{N}\right)^2 \end{aligned} \tag{C.4}$$

Therefore, the lower bound T_* is calculated as

$$\begin{aligned} T_* &= \frac{\sqrt{1-|\langle g|M\rangle|^2}}{\sqrt{\langle g|H_t^2|g\rangle - \langle g|H_t|g\rangle^2}}, \\ &= \frac{\sqrt{1-\frac{1}{N}}}{f_t\sqrt{\frac{1}{N}\left(1-\frac{1}{N}\right)}} \sim O(\sqrt{N}). \end{aligned} \tag{C.5}$$

As a result, we find that the computational time scales with $O(\sqrt{N})$.

Acknowledgements

This thesis would never be completed without the supports around me. I would like to take this opportunity to express my appreciation to them.

First of all, I would like to thank my supervisor Prof. Naoki Yamamoto, for his helpful suggestions and a countless discussion during the entire life from bachelor to doctor research. I was always surprised and encouraged by his extraordinary talent for science and deep kindness. Without his supports, I would not have completed any of my research.

I also would like to thank the following sub-chief examiners of this thesis: Assistant Prof. Tatsuhiko Koike (Department of Physics), Associate Prof. Hiroshi Watanabe (Department of Applied Physics and Physico-Informatics), and Associate Prof. Shu Tanaka (Department of Applied Physics and Physico-Informatics). Their critical comments and suggestions make me reflect upon my poor understanding and carelessness.

I also thank all the members of Yamamoto Lab who have been involved with me for having a good time and presenting some interesting topics.

Finally, I would like to express the gratitude for my parents, brother, and grandmother who passed away, Kazuyuki, Kiyomi, Keisuke, and Hanai Kobayashi, for their support and encouragement. I would also like to express special thanks to my aunt, Miss Keiko Kobayashi, for her deep affection. Sorry for making you worry so much!

Bibliography

[1] W. S. Warren, H. Rabitz, and M. Dahleh, Coherent control of quantum dynamics: The dream is alive, Science **259**, 1581 (1993).

[2] L. Viola, E. Knill, and S. Lloyd, Dynamical decoupling of open quantum systems, Phys. Rev. Lett. **82**, 2417 (1999).

[3] N. Khaneja, T. Reiss, B. Luy, and S. J. Glaser, Optimal control of spin dynamics in the presence of relaxation, J. Magn. Reson. **162**, 311 (2003).

[4] D. D'Alessandro, *Introduction to Quantum Control and Dynamics* (Chapman & Hall/CRC, 2007).

[5] K. Jacobs, Engineering quantum states of a nanoresonator via a simple auxiliary system, Phys. Rev. Lett. **99**, 117203 (2007).

[6] K. Jacobs, L. Tian, and J. Finn, Engineering superposition states and tailored probes for nanoresonators via open-loop control, Phys. Rev. Lett. **102**, 057208 (2009).

[7] P. Doria, T. Calarco, and S. Montangero, Optimal control technique for many-body quantum dynamics Phys. Rev. Lett. **106**, 190501 (2011).

[8] J. Li, D. Lu, Z. Luo, R. Laflamme, X. Peng, and J. Du, Approximation of reachable set for coherently controlled open quantum systems: Application to quantum state engineering, Phys. Rev. A **94**, 012312 (2016).

[9] J. K. Stockton, R. van Handel, and H. Mabuchi, Deterministic Dicke-state preparation with continuous measurement and control, Phys. Rev. A **70**, 022106 (2004).

[10] R. van Handel, J. K. Stockton, and H. Mabuchi, Feedback control of quantum state reduction, IEEE Trans. Automat. Contr. **50**-6, 768/780 (2005).

[11] J. M. Geremia, Deterministic and nondestructively verifiable preparation of photon number states, Phys. Rev. Lett. **97**, 073601 (2006).

[12] M. Yanagisawa, Quantum feedback control for deterministic entangled photon generation, Phys. Rev. Lett. **97**, 190201 (2006).

[13] N. Yamamoto, K. Tsumura, and S. Hara, Feedback control of quantum entanglement in a two-spin system, Automatica **43**, 981/992 (2007).

[14] A. Negretti, U. V. Poulsen, and K. Molmer, Quantum superposition state production by continuous observations and feedback, Phys. Rev. Lett. **99**, 223601 (2007).

[15] M. Mirrahimi and R. van Handel, Stabilizing feedback controls for quantum systems, SIAM J. Control Optim. **46**, 445/467 (2007).

[16] L. Bouten, R. van Handel, and M. R. James, A discrete invitation to quantum filtering and feedback control, SIAM Review **51**, 239/316 (2009).

[17] J. F. Poyatos, J. I. Cirac, and P. Zoller, Quantum reservoir engineering with laser cooled trapped ions, Phys. Rev. Lett. **77**, 4728 (1996).

[18] S. G. Schirmer and X. Wang Stabilizing open quantum systems by Markovian reservoir engineering, Phys. Rev. A **81**, 062306 (2010).

[19] N. Yamamoto, Coherent versus measurement feedback: Linear systems theory for quantum information, Phys. Rev. X **4**, 041029 (2014).

[20] M. Asjad and D. Vitali, Reservoir engineering of a mechanical resonator: generating a macroscopic superposition state and monitoring its decoherence, J. Phys. B: At. Mol. Opt. Phys. **47**, 045502 (2014).

[21] J.-R. Souquet and A. A. Clerk, Fock-state stabilization and emission in superconducting circuits using dc-biased Josephson junctions, Phys. Rev. A **93**, 060301 (2016).

[22] J. Combes, J. Kerckhoff, and M. Sarovar, The SLH framework for modeling quantum input-output networks, Advances in Physics: X **2**, 784/888 (2017).

[23] M. Brunelli, O. Houhou, D. W. Moore, A. Nunnenkamp, M. Paternostro, and A. Ferraro, Unconditional preparation of nonclassical states via linear-and-quadratic optomechanics, arXiv:1804.00014 (2018).

[24] C. Sayrin, I. Dotsenko, X. Zhou, B. Peaudecerf, T. Rybarczyk, S. Gleyzes, P. Rouchon, M. Mirrahimi, H. Amini, M. Brune, J.-M. Raimond, and S. Haroche, Real-time quantum feedback prepares and stabilizes photon number states, Nature (London) **477**, 73 (2011).

[25] R. Vijay, C. Macklin, D. H. Slichter, S. J. Weber, K. W. Murch, R. Naik, A. N. Korotkov, and I. Siddiqi, Stabilizing Rabi oscillations in a superconducting qubit using quantum feedback, Nature (London) **490**, 77 (2012).

[26] D. Riste, M. Dukalski, C. A. Watson, G. de Lange, M. J. Tiggelman, Ya. M. Blanter, K. W. Lehnert, R. N. Schouten, and L. DiCarlo, Deterministic entanglement of superconducting qubits by parity measurement and feedback, Nature (London) **502**, 350 (2013).

[27] S. Hacohen-Gourgy, L. S. Martin, E. Flurin, V. V. Ramasesh, K. B. Whaley, and I. Siddiqi, Quantum dynamics of simultaneously measured non-commuting observables, Nature (London) **538**, 491 (2016).

[28] K. C. Cox, G. P. Greve, J. M. Weiner, and J. K. Thompson, Deterministic Squeezed States with Collective Measurements and Feedback, Phys. Rev. Lett. **116**, 093602 (2016).

[29] Y. Liu, S. Shankar, N. Ofek, M. Hatridge, A. Narla, K. M. Sliwa, L. Frunzio, R. J. Schoelkopf, and M. H. Devoret, Comparing and Combining Measurement-Based and Driven-Dissipative Entanglement Stabilization, Phys. Rev. X **6**, 011022 (2016).

[30] C. P. Koch, Controlling open quantum systems: tools, achievements, and limitations,

J. Phys.: Condens. Matter **28** 213001 (2016).

[31] N. Khaneja, B. Luy, and S. J. Glaser, Boundary of quantum evolution under decoherence, PNAS **100**, 13162/13166 (2003).

[32] B. Qi and L. Guo, Is measurement-based feedback still better for quantum control systems?, System and Control Letters **59**, 333/339 (2010).

[33] B. Qi, H. Pan, and L. Guo, Further results on stabilizing control of quantum systems, IEEE Trans. Automat. Contr. **58**, 1349/1354 (2013).

[34] C. Altafini, Controllability properties for finite dimensional quantum Markovian master equations, J. Math. Phys. **44**, 2357/2372 (2003).

[35] C. Altafini, Coherent control of open quantum dynamical systems, Phys. Rev. A **70**, 062321 (2004).

[36] J. S. Li and N. Khaneja, Ensemble control of Bloch equations, IEEE Trans. Automat. Contr. **54**, 528/536 (2009).

[37] G. Dirr, U. Helmke, I. Kurniawan, and T. Schulte-Herbruggen, Lie-semigroup structures for reachability and control of open quantum systems: Kossakowski-Lindblad generators form Lie-wedge to Markovian channels, Reports Math. Phys. **64**, 93/121 (2009).

[38] C. O'Meara, G. Dirr, and T. Schulte-Herbruggen, Illustrating the geometry of coherently controlled unital open quantum systems, IEEE Trans. Automat. Contr. **57**, 2050/2056 (2012).

[39] H. Yuan, Reachable set of open quantum dynamics for a single spin in Markovian environment, Automatica **49**, 955/959 (2013).

[40] A. Carlini, A. Hosoya, T. Koike, and Y. Okudaira, Quantum Brachistochronem, Phys. Rev. Lett. **96**, 060503 (2006).

[41] A. Carlini, A. Hosoya, T. Koike, and Y. Okudaira, Time Optimal Unitary Operations, Phys. Rev. A **75**, 042308 (2007).

[42] A. Carlini, A. Hosoya, T. Koike, and Y. Okudaira, Quantum Brachistochrone for Mixed States, J. Phys. A: Math. Theor. **41**, 045303 (2008).

[43] A. Carlini, and T. Koike, Time-Optimal Transfer of Coherence, Phys. Rev. A **86**, 054302 (2012).

[44] C. W. Gardiner and M. J. Collett, Input and output in damped quantum systems: Quantum stochastic differential equations and the master equation,Phys. Rev. A **31**, 3761 (1985).

[45] R. L. Hudson and K. R. Parthasarathy,Quantum Ito's formula and stochastic evolutions,Math. Phys. **93**, 301–323 (1984).

[46] H. M. Wiseman and G. J. Milburn, *Quantum Measurement and Control* (Cambridge University Press, 2010).

[47] K. Jacobs, *Quantum Measurement Theory and its Applications* (Cambridge Univ. Press, 2014).

[48] H. I. Nurdin and N. Yamamoto, *Linear Dynamical Quantum Systems: Analysis, Synthesis, and Control* (Springer, 2017).

[49] M. A. Nielsen and I. L. Chuang, *Quantum Computation and Quantum information* (Cambridge University Press, 2010).

[50] R. Bianchetti, et al., Control and tomography of a three level superconducting artificial atom, Phys. Rev. Lett. **105**, 223601 (2010).

[51] L. Mandel and E. Wolf, *Optical Coherence and Quantum Optics* (Cambridge University Press, Cambridge, UK, 1997).

[52] Z. Zhang and L. M. Duan, Quantum metrology with Dicke squeezed states, New J. Phys. **16**, 103037 (2014).

[53] J. J . Bollinger, W. M. Itano, D. J. Wineland, and D. J. Heinzen, Optimal frequency measurements with maximally correlated states, Phys. Rev. A **54**, 4649 (1996).

[54] S. F. Huelga, C. Macchiavello, T. Pellizzari, A. K. Ekert, M. B. Plenio, and J. I. Cirac, Improvement of frequency standards with quantum entanglement, Phys. Rev. Lett. **79**, 3865 (1997).

[55] U. Dorner, Quantum frequency estimation with trapped ions and atoms, New J. Phys. **14**, 043011 (2012).

[56] R. P. Agarwal and D. O'Regan, *An introduction to ordinary differential equations* (Springer, 2008).

[57] L. Mandel and E. Wolf, Optical Coherence and Quantum Optics, Cambridge University Press, Cambridge (1997)

[58] J. J. Bollinger, W. M. Itano, D. J. Wineland, and D. J. Heinzen, Optical frequency measurements with maximally correlated states, Phys. Rev. A **54**, R4649(R) (1996).

[59] S. F. Huelga, C. Macchiavello, T. Pellizari, A. K. Elert, M. B. Plenio, and J. I. Cirac, Improvement of Frequency Standards with Quantum Entanglement, Phys. Rev. Lett. **79**, 3865 (1997).

[60] U. Dorner, Quantum frequency estimate with trapped ions and atoms, New J. Phys, **14**, 043011 (2012).

[61] J. M. Geremia, Deterministic and Nondestructively Verifiable Preparation of Photon Number States, Phys. Rev. Lett. **97**, 073601 (2006).

[62] M. Yanagisawa, Quantum Feedback Control for Deterministic Entangled Photon Generation, Phys. Rev. Lett. **97**, 190201 (2006).

[63] A. Negretti, U. V. Poulsen, and K. Molmer, Quantum Superposition State Production by Continuous Observations and Feedback, Phys. Rev. Lett. **99**, 223601 (2007).

[64] R. P. Agarwal and D. O' Regan, An Introduction to Ordinary Differential Equations, Soringer, Berlin (2008).

[65] M. Brunelli, O. Houhou, D. W. Moore, A. Nunnenkamp, M. Paternostro, A. Ferraro, Unconditional preparation of nonclassical states via linear-and-quadratic optomechanics, Phys. Rev. A **98**, 063801 (2018).

[66] S. Lloyd, Ultimate physical limits to computation, Nature **406**, 1047 (2000).

[67] M. A. Nielsen and I. L. Chuang, *Quantum Computation and Quantum Information* (Cambridge University Press, Cambridge, 2010).

[68] P. J. Jones and P. Kok, Geometric derivation of the quantum speed limit, Phys. Rev. A **82**, 022107 (2010).

[69] F. Frowis, Kind of entanglement that speed up quantum evolution, Phys. Rev. A **85**, 052127 (2012).

[70] T. Caneva, M. Murphy, T. Calarco, R. Fazio, S. Montangero, V. Giovannetti, and G. E. Santoro, Optimal Control at the Quantum Speed Limit, Phys. Rev. Lett. **103**, 240501 (2009).

[71] P. M. Poggi, F. C. Lombardo, and D. A. Wisniacki, Quantum speed limit and optimal evolution time in a two-level system, EPL **104** (2013).

[72] O. Andersson and H. Heydari, Quantum speed limits and optimal Hamiltonians for driven systems in mixed states, J. Phys. A: Math. Theor. **47**, 215301 (2014).

[73] P. M. Poggi, F. C. Lombardo, and D. A. Wisniacki, Enhancement of quantum speed limit time due to cooperative effects in multilevel systems, J. Phys. A: Math. Theor. **48**, 35FT02 (2015).

[74] P. M. Poggi, Geometric quantum speed limits and short-time accessibility to unitary operations, Phys. Rev. A **99**, 042116 (2019).

[75] L. Mandelstam and I. Tamm, The uncertainty relation between energy and time in nonrelativistic quantum mechanics, J. Phys. (USSR) **9**, 249-254 (1945).

[76] N. Margolus and L. B. Levitin, The maximum speed of dynamical evolution, Physica D **120**, 188 (1998).

[77] G.N. Fleming, A unitarity bound on the evolution of nonstationary states, Nuovo Cim. A, **16**, 232-240 (1973).

[78] K. Bhattacharyya, Quantum decay and the Mandelstam-Tamm-energy inequality, J. Phys. A: Math. Gen., **16** (1983).

[79] J. Anandan and Y. Aharanov, Geometry of quantum evolution. Phys. Rev. Lett, **65** 1990.

[80] A. Uhlmann, An energy dispersion estimate, Phys. Lett. A **161**, 329 (1992).

[81] V. Giovannetti, S. Lloyd, and L. Maccone, Quantum limits to dynamical evolution, Phys. Rev. A **67**, 052109 (2003).

[82] P. J. Jones and P. Kok, Geometric derivation of the quantum speed limit, Phys. Rev. A **82**, 022107 (2010).

[83] P. Pfeifer, How Fast Can a Quantum State Change with Time?, Phys. Rev. Lett. **70**, 22, 3365 (1993).

[84] P. Pfeifer and J. Frohlich, Generalized time-energy uncertainty relations and bounds on lifetimes of resonance, Rev. Mod. Phys. **67**, 759 (1995).

[85] S. Luo, How fast can a quantum state evolve into a target state? Physica D **189**, 1

(2004).

[86] S. Deffner and E. Lutz, Energy-time uncertainty relation for driven quantum systems, J. Phys. A **46**, 335302 (2013).

[87] M. M. Taddei, B. M. Escher, L. Davidovich, and R. L. de Matos Filho, Quantum Speed Limit for Physical Processes, Phys. Rev. Lett. **110**, 050402 (2013).

[88] A. del Campo, I. L. Egusquiza, M. B. Plenio, and S. F. Huelga, Quantum Speed Limits in Open System Dynamics, Phys. Rev. Lett. **110**, 050403 (2013).

[89] S. Deffner and E. Lutz, Quantum Speed Limit for Non-Markovian Dynamics, Phys. Rev. Lett. **111**, 010402 (2013).

[90] Z. Sun, J. Liu, J. Ma, and X. Wang, Quantum speed limits in open systems: Non-Markovian dynamics without rotating-wave approximation, Sci. Rep. **5**, 8444 (2015).

[91] X. Meng, C. Wu, and H. Guo, Minimal evolution time and quantum speed limit of non-Markovian open systems, Sci. Rep. **7**, 15046 (2015).

[92] N. Mirkin, F. Toscano, and D. A. Wisniacki, Quantum-speed limit bounds in an open quantum evolution, Phys. Rev. A **94**, 052125 (2016).

[93] Y.-J. Zhang, W. Han, Y.-J. Xia, J.-P Cao, and H. Fan, Quantum speed limit for arbitrary initial states, Sci. Rep. **4**, 27349 (2016).

[94] F. Campaioli, F. A. Pollock, and K. Modi, Tight, robust, and feasible quantum speed limits for open dynamics, Quantum **3**, 168 (2019).

[95] Z.-Y. Xu, S. Luo, W. L. Yang, C. Liu, and S. Zhu, Quantum speedup in a memory environment, Phys. Rev. A **89**, 012307 (2014).

[96] C. Liu, Z.-Y. Xu, and S. Zhu, Quantum-speed-limit for multiqubit open systems, Phys. Rev. A **91**, 022102 (2015).

[97] S.-X. Wu, Y. Zhang, C.-S. Yu, and H.-S. Song, The initial-state dependence of the quantum speed limit, J. Phys. A **48**, 045301 (2015).

[98] Y.-J. Zhang, W. Han, Y.-J. Xia, J.-P. Cao, and H. Fan, Classical-driving-assisted quantum speed-up, Phys. Rev. A **91**, 032112 (2015).

[99] Y.-J. Song, Q.-S. Tan, and L.-M. Kuang, Control quantum evolution speed of a single dephasing qubit for arbitrary initial states via periodic dynamical decoupling pulses, Sci. Rep. **7**, 43654 (2017).

[100] K. B. Petersen and M. S. Pedersen, The Matrix Cookbook, url=http://matrixcookbook.com (2012).

[101] L. P. G.-Pintos and A. del Campo, Quantum speed limits under continuous quantum measurements, New J. Phys. **21**, 033012 (2019).

[102] L. K. Grover, Quantum mechanics helps in searching for a needle in a haystack, Phys. Rev. Lett. **79**, 325 (1997).

[103] C. H. Bennett, E. Bernstein, G. Brassard, and U. Vazirani, Strengths and weaknesses of quantum computing, SIAM J. Comp, **26**, 1510-1523 (1997).

[104] K. Kobayashi and N. Yamamoto, Control limit on quantum state preparation under

decoherence, Phys. Rev. A **99**, 052347 (2019).

[105] K. Kobayashi and N. Yamamoto, Quantum speed limit for robust state characterization and engineering, Phys. Rev. A **102**, 042606 (2020).